Elucidating the signaling roles of CCaMK and IPD3 in early-diverging plant lineages.

by

Anthony Joseph Bortolazzo

A dissertation submitted in partial fulfillment of the requirements for the degree of

Doctor of Philosophy

(Genetics)

at the

University of Wisconsin-Madison

2020

Date of final oral examination: 03/26/2020

The dissertation is approved by the following members of the Final Oral Committee:

Dr. Jean-Michel Ané, Professor, Agronomy and Bacteriology
Dr. Andrew Bent, Professor, Plant Pathology
Dr. Linda Graham, Professor, Botany
Dr. Patrick Masson, Professor, Genetics
Dr. Marisa Otegui, Professor, Botany and Genetics

Abstract

Decades of research into two immensely important plant-microbial symbioses, the arbuscular mycorrhizal symbioses (AMS) and root nodule symbioses, have elucidated a highly conserved plant signal transduction pathway known as the common symbiosis pathway (CSP) which is responsible for perception of arbuscular mycorrhizal fungi (AMF) or rhizobia and subsequent symbiotic root development. Through advances in genomic sequencing throughout land plants and algae, the evolutionary origin of the CSP has been mainly placed within the advanced charophyte algae, predating the origin of AMS and even land plants themselves. Furthermore, CSP genes have been found within the mostly non-mycorrhizal mosses, including the critical nuclear signaling factors, the Calcium/CalModulin-dependent protein Kinase (CCaMK) and Interacting Protein of DMI3 (IPD3), despite a common understanding that these two genes are specific to plants that undergo AMS or RNS and are absent in non-hosts. As such, the presence of these genes in these “non-symbiotic” lineages casts doubt on the idea they are indeed specific to AMS or RNS in mosses or advanced charophyte algae. We sought to characterize the function(s) and biological relevance of these genes in mosses with molecular and physiological experiments, using *Physcomitrella patens* (Physcomitrella) as a model. Through analysis of constitutively active isoforms of CCaMK and IPD3, we have elucidated a novel role of both in abscisic acid (ABA)-mediated developmental stress-responses in Physcomitrella. However, by genetic deletion of either the *CCaMK* or *IPD3* loci, it is clear that neither gene is a necessary component of ABA-mediated stress signaling. Instead, *ipd3* mutant Physcomitrella is impaired in negative gravitropism of caulonemal filaments, surprisingly, and this phenotype was not ablated by modulating ABA signaling. Similar phenotypes were not observed in analogous mutants of

angiosperms, suggesting a specificity to the moss lineage or perhaps a loss of such functions in angiosperms.

Unfortunately, genetic tools in the advanced charophyte algae are severely lacking in order to perform similar studies. We sought to test numerous direct and indirect methods of transformation on a panel of charophyte species. In this work, we describe a new promoter found to be active in two species, as well as a generalizable method of microparticle bombardment that successfully transforms three species. It is our hope that increased use of such techniques and tools within the charophytes will build towards a better community of research and resources with which to study charophytes in the context of the CSP and plant evolution in general.

Acknowledgements

I must thank many for making this journey of mine possible. First, I thank my fiancé, Victoria Martinez, for accompanying me on this journey, and always being there for me through thick and thin. Victoria essentially “went to grad school” with me, and for this I am eternally grateful.

Second, I would like to thank my parents, Richard and Sherri Bortolazzo. I am indebted to them for their constant support throughout my life and giving me the opportunities to explore my education and beyond.

Of course, I would like to thank my graduate advisor, Dr. Jean-Michel Ané, who has spent so much time and effort mentoring and pushing me to be the best version of graduate student I could be. From the get-go, Jean-Michel has always approached me through the lens of my future and my mentorship, and has always been an advocate.

I have to thank my other mentors, including my committee for their critique, recommendations, and for keeping me honest. I would like to thank Dr. Andrew Bent, Dr. Linda Graham, Dr. Patrick Masson, and Dr. Marisa Otegui. My committee has been a pleasure to work with throughout my time in Madison. I also thank Dr. Thomas Kleist who has been a good mentor to me in the study of *Physcomitrella patens* and also as a graduate student in general.

Over the years, I have met many other researchers in the lab whom I owe my thanks; for the advice, the camaraderie, and general support. In particular I would like to thank Dr. Dhileepkumar Jayaramen, Dr. Thomas Irving, Dr. Michelle Keller-Pearson, Dr.

Kevin Garcia, Shane Bernard, and Zackery Keyser. I would also like to thank the undergraduates that have helped me do my research over the years: Min Su Park, Alyssa Lentine, Mitch Wanta, Cali Lunowa, Brandy Koehler, and Stuart Fass.

Lastly, I would like to thank the Genetics graduate program here at UW Madison, in particular Audrey Gasch and Martha Reck.

Table of contents

Abstract…… i

Acknowledgements…… iii

Table of contents…… v

Chapter 1 – Introduction

1.1 - Plant-fungal symbioses…… 1

1.2 - Arbuscular mycorrhizal symbiosis…… 2

1.3 - The Common symbiosis pathway…… 5

1.4 - Host specificity of common symbiosis pathway…… 9

1.5 - Symbiosis genes in mosses and charophytes..... 10

1.6 - Rational for studying mosses and charophytes…… 14

1.7 - References…… 18

Chapter 2 – Conserved components of the common symbiosis pathway regulate ABA levels and stress-associated developmental reprogramming in Physcomitrella. (MANUSCRIPT TO BE SUBMITTED TO CELL REPORTS)

2.1 - Abstract…… 29

2.2 - Introduction…… 31

2.3 - Results…… 35

2.4 - Discussion…… 50

2.5 - Materials and Methods…… 54

2.6 - Acknowledgements…… 61

2.7 - Supplementary Figures…… 62

2.8 - Supplementary Tables…… 68

2.9 - Additional Data…… 69

2.10 - References…… 74

Chapter 3 – IPD3 deletion causes 'wrong-way-response' in gravitropic caulonema in *Physcomitrella patens*. (PREPARING MANUSCRIPT FOR REVIEW)

3.1 - Abstract…… 84

3.2 - Introduction…… 85

3.3 - Results…… 87

3.4 - Discussion…… 92

3.5 - Materials and Methods……96
3.6 - Acknowledgements……98
3.7 - Supplementary Figures……99
3.8 - Supplementary Movie Legends……100
3.9 - References……100

Chapter 4 – Developing a transformation model for late-diverging charophyte algae.

4.1 - Introduction……104
4.2 - General methods and materials……107
4.3 - *Agrobacterium*-mediated transformation……108
4.4 - Protoplast generation and PAG/Ca^{2+} transformation……113
4.5 - Cell-penetrating peptide transformation……116
4.6 - Silicon carbide whisker transformation……120
4.7 - Particle bombardment transformation……122
4.8 - Fluorescence activated cell sorting of transformants……126
4.9 - Discussion and future prospects……128
4.10 - Supplementary Tables……133
4.11 - References……134

Chapter 5 – Summary and Future Directions

5.1 – Summary……142
5.2 - Future directions in CCaMK/IPD3 signaling in mosses……144
5.3 - Further development of charophyte models……145
5.4 - References……146

Chapter 1 – Introduction

1.1 - Symbiotic associations with fungi

Due to their sessile nature, plants by necessity evolved numerous strategies to cope with dynamic environments but also to occupy new niches. Such strategies include interactions with microorganisms that are paramount to plants' ability to gather water and nutrients, cope with reduced access to water and nutrients, and to defend against pathogens that are detrimental to growth and development. Despite the sheer complexity of the microbiomes of plants, there are reproducible effects of microbiomes on important plant developmental traits, such as flowering time (Panke-Buisse *et al.*, 2015). Adding to the complexity of plant-microbe interactions, the simultaneous interplay of symbionts and pathogens on the plant host influences the development and evolutionary history of plant lineages (Metcalf & Koskella, 2019). The algal ancestor of land plants, similarly, must have evolved numerous critical innovations necessary to cope with drastic environmental challenges, including desiccation and lack of nutrients. Such ancient critical innovations in plant lineages not only led to the diverse group of extant land plants we see today, but also had drastic effects upon the geochemistry and atmosphere of the earth (Wallace *et al.*, 2017). Early terrestrial lineages leveraged symbiotic interactions with early mycorrhizal fungi to mitigate drought and nutrient stress, among other stressors. One of the major and most prevalent symbioses that occur within land plants are the arbuscular mycorrhizas (AM) and AM symbioses are some of the most prevalent and consequential beneficial interactions present in extant plants (Parniske, 2008).

1.2 - Arbuscular mycorrhizal symbiosis

AM symbiosis is a very characteristic plant-fungal interaction seen in land plants. Arbuscular mycorrhizal fungi (AMF) are filamentous fungi of the phylum Mucoromycota, subgroup Glomeromycota and are obligate symbionts with their plant hosts (Naranjo-Ortiz & Gabaldón, 2019; Smith & Read, 2010). In an estimated 71% of land plants, AMF colonize the roots and develop highly branched fungal structures, known as “arbuscules”, inside the cells of the host plant (Wang & Qiu, 2006; Brundrett & Tedersoo, 2018). The infection process is preceded by plant-to-fungal and fungal-to-plant signaling in the rhizosphere (**Figure 1**). Strigolactones, present in root exudates are perceived by AMF and promote hyphal germination, hyphal branching, and stimulate mitochondrial activity (Besserer *et al.*, 2006, 2008). Hyphae infect the host root epidermis through use of hyphopodia (Chabaud *et al.*, 2011). Intraradical hyphae proceed through the epidermis and subsequently penetrate individual cortical cells and develop highly branched structures known as “arbuscules”. Arbuscules serve as the site of nutrient exchange between the host plant and the resident AMF; through its expansive mycelial network, the fungus provides the host with greater access to water and nutrients, most notably phosphate, and in return the host provides the fungus with photosynthate and fatty acids (Parniske, 2008; Smith & Read, 2010; Luginbuehl *et al.*, 2017). In addition to alleviating water and nutrient stress, AMF also limit the colonization of soil-borne pathogens (Harrier & Watson, 2004). In later developmental stages of the symbiosis, AMF sporulate from inside colonized plants to give rise to more spores in the rhizosphere, completing their life-cycle.

Given the near ubiquitous nature of AM symbioses in land plants, AMF are near omnipresent in environments dominated by land plants and have far reaching implications

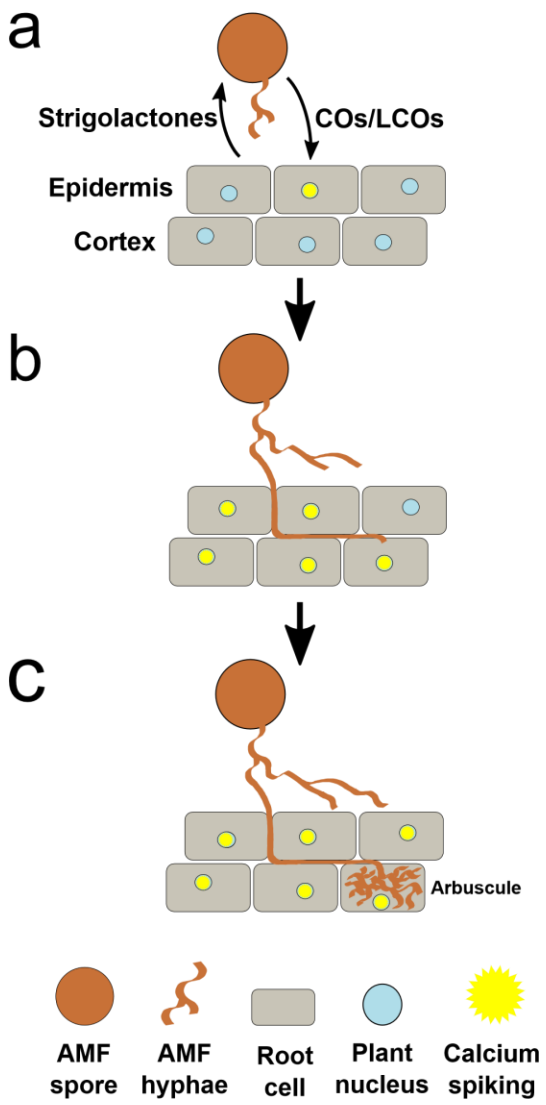

Figure 1: Overview of arbuscular mycorrhizal development

a) Reciprocal signaling between AMF and host plant roots occurs within the rhizosphere. Root exudates include strigolactones and cause AMF to increase respiration, hyphal germination, and hyphal branching. Conversely, AMF exude complex mixtures of COs and LCOs which are perceived by the host plant, induce nuclear calcium spiking, activating the symbiotic repertoire of the plant.
b) With the aid of hyphopodia, AMF hyphae enter through the epidermis of the host plant. Intraradical hyphae grow between root cells. **(legend continued on next page)**.

c) Intraradical hyphae enter root cells of the cortex and undergo high levels of branching to form intracellular arbuscules. Arbuscules serve as the interface of nutrient exchange between the symbionts.

on nutrient transfer that occurs in the soil, most notably of phosphorus, nitrogen, and carbon (van der Heijden *et al.*, 2015). In certain plant species, the percent of their acquired phosphorus and nitrogen from AM partners has been estimated to be up to 90% and 20%, respectively (van der Heijden *et al.*, 2015). Due to host plants' integration with the fungal partner's mycelial network, roots have access to a greater proportion of water and nutrients within their vicinity. There is ample evidence that AM helps plants acquire and retain water, by symbiotic transfer but also the modulation of stomatal activity (Augé, 2001; Augé *et al.*, 2014).

Although the causes and consequences of arbuscular mycorrhizal symbiosis (AM) are mostly studied in angiosperms, similar, AM-like symbiotic interactions also occur in early-diverging lineages of land plants, including liverworts and hornworts, where fungi develop intricate coils of hyphae in the cells of the thallus or rhizoids (Humphreys *et al.*, 2010; Desiro *et al.*, 2013; Field *et al.*, 2015; Rimington *et al.*, 2019). Fossil evidence is consistent with an early origin of arbuscular mycorrhizal interactions; examples of intracellular arbuscule-like structures exist in both ancient tracheophyte and bryophyte-like plants of the Early Devonian, developed roughly 400 million years ago (MYA) (Remy *et al.*, 1994a). Aseptate Glomalean-like spores are also present in the fossil record of the Ordovician dated back to 460 MYA (Redecker *et al.*, 2000). Taken together, the evidence seen in the fossil record, and the known influence of AM symbiosis on plant acquisition of water and nutrients, ancient AM-like symbiotic associations may represent a critical innovation aiding plants' conquest of land. As one might expect with such an ancient

plant-fungal association, both partners have evolved complex regulatory mechanisms to influence themselves and their partners. Currently, due to the genetic intractability of AMF species, the regulatory aspects of AM symbiosis and its effects are better understood on the plant side of the interaction.

1.3 - The Common symbiosis pathway

The initial infection and development of arbuscular mycorrhizal interactions is controlled through the action of a conserved plant signal transduction pathway, referred to as the common symbiosis pathway (CSP) **(Figure 2)** (Oldroyd, 2013). The CSP has acquired its “common” epithet due to its facilitation of other, non-AMF interactions. Rhizobia, nitrogen-fixing bacteria that infect legume roots through root-hairs and lead to nodule development, rely on the very same pathway for root nodule symbiosis (RNS). Despite the stark differences between RNS and AM symbiosis, in both cases the microbe partner exudes signaling molecules that are required for proper symbiotic development and to activate the CSP in the plant host. It is important to distinguish the evolutionary timelines that underscore RNS, AM symbiosis, and the CSP itself. RNS is much less prevalent in land plants, restricted to a subset of Rosids – the Fabales, Rosales, Fagales, and Cucurbitales, referred to as the “nitrogen-fixing clade”. Accordingly, RNS is estimated to have evolved 90 MYA, hundreds of millions of years after AM symbiosis or the CSP itself (Remy *et al.*, 1994b; Doyle, 2011; Delaux *et al.*, 2015a). Given these evolutionary timelines and the common necessity for the CSP for RNS signal transduction and development, it’s widely accepted that rhizobia have coopted the CSP from its putatively original role in mediating AM symbiosis.

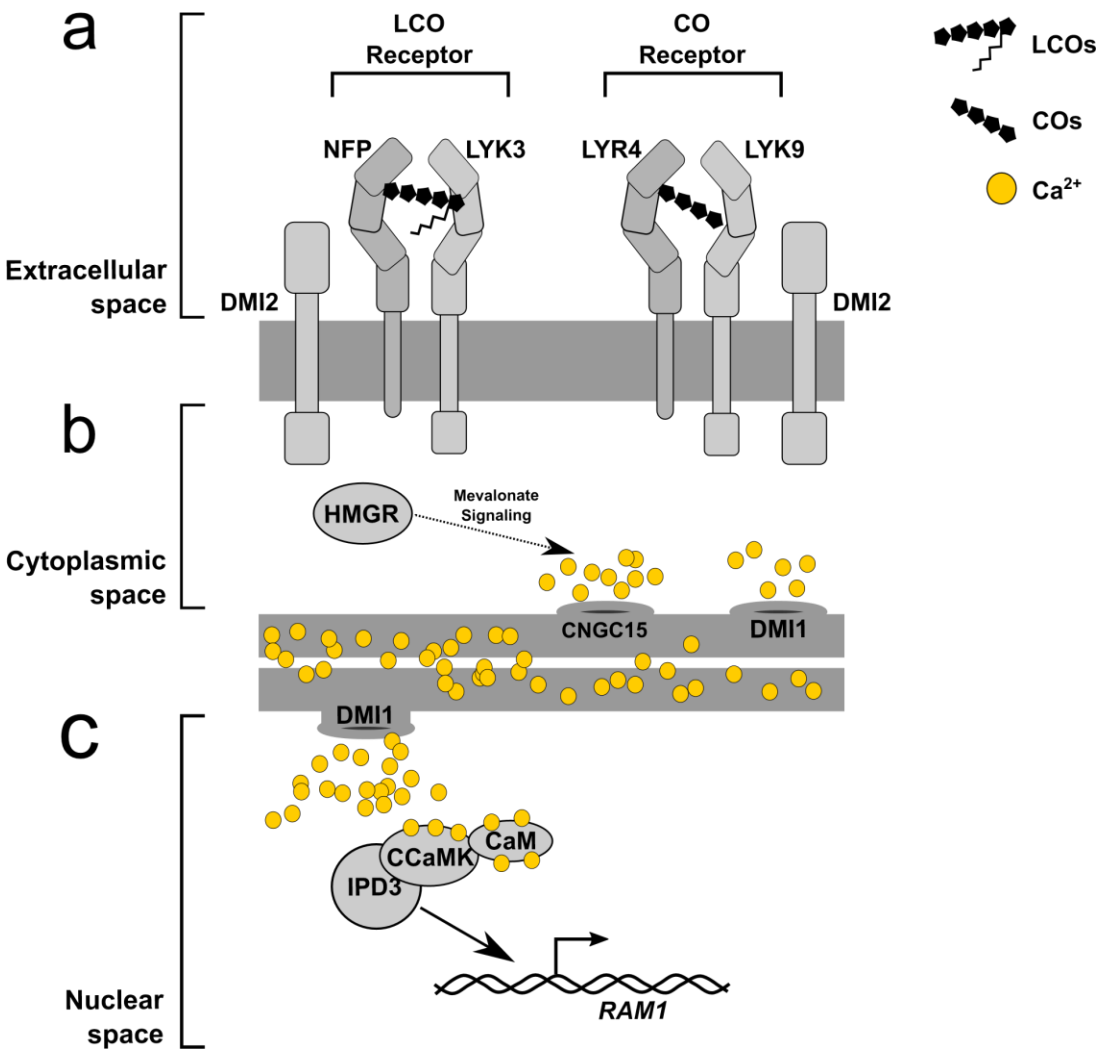

Figure 2: Overview of early fungal-to-plant signaling in the common symbiosis pathway

a) In the extracellular space, combinations of LysM-RLKs cooperatively perceive COs and LCOs from AMF exudates by direct binding to lysin motifs. Some LysM-RLKs contain a functional intracellular kinase domain and others do not. A co-receptor, DMI2, interacts with LysM-RLK complexes and transduces the signal from the plasma membrane.
b) DMI2 interacts with the enzyme HMGR, an enzyme directly upstream of the mevalonate synthetic pathway. Through an as-of-yet unknown mechanism, mevalonate-derived signaling induces nuclear and perinuclear calcium spiking by activation of calcium channel CNGC15.
c) Release of calcium stores triggers the calcium channel DMI1, which is responsible for the oscillatory nature of calcium spikes. Calcium stores for nuclear spiking are within the nuclear envelope/endoplasmic reticulum and are replenished by calcium pumps.
In the nucleus, the calcium sensor CCaMK is activated by high levels of calcium/Calmodulin (CaM) and transphosphorylates the transcription factor IPD3 (or IPD3-LIKE). Once activated, a CCaMK-IPD3 complex acts upon specific cis-elements to induce transcription, namely of the GRAS transcription factor *REDUCED ARBUSCULAR MYCORRHIZA1 (RAM1)*.

AMF exude diffusible signals known as lipo-chitooligosaccharides (LCOs), short lipidated chitin chains, and chitooligosaccharides (COs), short naked chitin chains into the rhizosphere (Maillet *et al.*, 2011b). At the plasma membrane of host plants, COs and LCOs are perceived by assemblages of LysM-Receptor Like Kinases (LysM-RLKs) (Zipfel & Oldroyd, 2017; Feng *et al.*, 2019). The LysM domains found in extracellular portions of LysM-RLKs are responsible for direct binding to COs and LCOs. Through the cooperative action of a transmembrane coreceptor, Doesnt Make Infections2 (DMI2/NORK/SYMRK), a signal is transduced from the plasma membrane to the nuclear envelope through a mechanism involving mevalonate (Gherbi *et al.*, 2008; Venkateshwaran *et al.*, 2015). In response a cyclic nucleotide-gated calcium channel, CNGC15, initiates calcium fluxes that activate the oscillatory behavior of yet another calcium channel, Doesnt Make Infections1 (DMI1). The activity of calcium pumps and calcium channels in the nuclear envelope are required for the induction of repetitive, high amplitude, calcium fluxes in the nucleus, referred to as “calcium spikes” (Ané *et al.*, 2004a; Capoen *et al.*, 2011; Charpentier *et al.*, 2016; Kim *et al.*, 2019).

Nuclear calcium spikes are decoded by a nuclear calcium/calmodulin-dependent protein kinase (CCaMK), which in response activates a transcriptional cascade by phosphorylation of transcription factors (Lévy *et al.*, 2004; Miller *et al.*, 2013). The regulation of CCaMK activity and its downstream consequences are complex. Calcium binding to the C-terminal EF-hand domains of CCaMK alone has negative regulatory effects upon its transphosphorylation activity. This is accomplished in part by autophosphorylation of the kinase in its activation loop domain, causing a “closed”, inactive state. In contrast, the combined activity of calcium and calmodulin reverses the

inactive state of the kinase, permitting its downstream transphosphorylation function (Miller *et al.*, 2013). In other words, calcium at low concentration negatively regulates CCaMK and calcium at high concentration activates the kinase relative to its target. Through molecular modeling incorporating calcium concentration and frequency of calcium spikes, it has been proposed that the frequency of nuclear calcium spikes is responsible for the rate of CCaMK activation (Miller *et al.*, 2013). The negative autoregulatory activity of CCaMK is necessary for proper infection of host roots by AMF (Liao *et al.*, 2012). Expression of truncated, constitutively active forms of CCaMK initiates developmental aspects of AM and RNS in roots, however, in the absence of either symbiont. Relative to RNS, expression of constitutively active variants of CCaMK is sufficient to induce root nodule development (Gleason *et al.*, 2006a; Tirichine *et al.*, 2006). A similar variant of CCaMK induces spontaneous development of the prepenetration apparatus, a novel cellular structure that facilitates AMF entry into the root epidermis (Takeda *et al.*, 2012).

Upon activation of CCaMK phosphorylates two transcription factors, Interacting Protein of DMI3 (IPD3) and a homolog, IPD3-like (IPD3L) (Messinese *et al.*, 2007; Horváth *et al.*, 2011; Singh *et al.*, 2014; Jin *et al.*, 2018). IPD3 phosphorylation permits DNA binding activity of the transcription factor. Once active, IPD3 binds specific cis-elements and promotes the transcription of downstream genes, such as the GRAS transcription factor *REDUCED ARBUSCULAR MYCORRHIZA1* (*RAM1*), in cooperative action with other GRAS transcription factors (Xue *et al.*, 2015; Pimprikar *et al.*, 2016). As is the case concerning CCaMK, specific mutagenic strategies can be used to express constitutively active variants of IPD3. Through phosphomimetic mutation as important

phosphosites, constitutively active IPD3 is also sufficient to induce nodule development (Singh *et al.*, 2014). These mutagenesis strategies allow the study of processes downstream of CCaMK or IPD3 activation.

1.4 - Host specificity of common symbiosis pathway

Many of the genes that function within the CSP are specific to mediating interactions with AMF and rhizobial bacteria and are therefore absent in the genomes of non-host plant species, heretofore referred to as “symbiosis-specific” genes. This relationship between CSP gene presence and AMF-host status is seen from angiosperms to the early diverging hornworts and liverworts of the bryophytes. Examples of significant CSP gene loss concomitant with loss of host-status are seen within the angiosperm and gymnosperm lineages. Both the Pinaceae (pine family) and Brassicaceae (mustard family) are unable to form *bona fide* AMS and show family-wide losses of CSP genes, including the symbiosis-specific nuclear signaling proteins CCaMK and IPD3 (Delaux *et al.*, 2014a; Garcia *et al.*, 2015). In less frequent cases, species that have lost the ability to host AMF have still retained symbiosis-specific genes likely to maintain the ability to form RNS, as seen in the genus *Lupinus* of the legume family (Delaux *et al.*, 2014b).

In contrast, some genes of the CSP that are functionally involved with AMF or RNS interactions are not specific to them alone, such as the calcium channel DMI1 or the two nucleoporins NUP85 and NUP133 (Delaux *et al.*, 2014b; Delaux, 2017). A notable example of dual functionality is the chitin receptor CERK1. CERK1 is not only involved in AM signaling, but is also a major player in chitin signaling in general, including plant-pathogenic interactions; CERK1 is present in non-mycorrhizal plants such as *Arabidopsis thaliana* or the moss *Physcomitrella patens* (Miya *et al.*, 2007; Petutschnig *et al.*, 2014;

Miyata *et al.*, 2014; Zhang *et al.*, 2015; Bressendorff *et al.*, 2016). The cross-talk between innate immunity and symbiosis signaling is not confined to interactions at the plasma membrane. The GRAS transcription factor DELLA has also been shown to be important for both symbiotic and pathogenic interactions (Navarro *et al.*, 2008; Floss *et al.*, 2013; Pimprikar *et al.*, 2016).

Aside from the issue of specificity or multiple roles of CSP genes, some genes that are necessary for AM development in certain linages are notably absent in other lineages that still form AM symbioses. In particular, a number of GRAS transcription factors important for AM development in angiosperms are absent in mycorrhizal liverworts (Xue *et al.*, 2015; Pimprikar *et al.*, 2016; Grosche *et al.*, 2018). This pattern is consistent with the recent hypothesis that critically important players in the CSP, such as CCaMK or DMI1, evolved early in land plant evolution, however numerous CSP genes evolved later in land plant evolution where AM interactions were refined (Delaux *et al.*, 2015a).

1.5 - Conspicuous presence of symbiosis genes in algae and mosses

The cytological and physiological study of broad lineages of land plants in combination with comparative genomics has proven fruitful in elucidating and predicting genes to be involved in or necessary for AM (Delaux *et al.*, 2014b; Bravo *et al.*, 2016). However, this methodology can only go so far to determine the evolutionary history of the function(s) of the CSP in green plants. The two most notable examples that break the mold of symbiosis-specific genes of the CSP are the mosses of the bryophytes and the advanced charophyte algae, the latter of whom diverged prior to the emergence of either AM or land plants (**Figure 3**). The mosses show conservation of the symbiosis-specific nuclear calcium signaling genes *CCaMK* and *IPD3* (Wang *et al.*, 2010a; Delaux *et al.*,

2015b). Lineages of the zygnematalean algae show conservation of *CCaMK*. One could imagine that the presence of these genes in these lineages belies the very notion that they are symbiosis-specific. On the other hand, one could hypothesize that CCaMK/IPD3 mediate as-of-yet unknown symbiotic or other microbial associations in these lineages.

Mosses belong to the early-diverging bryophytes along with liverworts and hornworts. The bryophytes in general form many interactions with diverse fungi, including endophytic interactions (Knack *et al.*, 2015; Graham *et al.*, 2017; Graham *et al.*, 2019; Nelson & Shaw, 2019). Abundant AM and AM-like associations are found in both liverworts and hornworts, however it is clear that most mosses, with the exception of the earliest diverging lineage of genus *Takakia*, are not *bona fide* hosts of AMF (Boullard, 1988). Experimental studies have shown mycorrhization of mosses, however all of these studies have been done in the presence of “nurse plants” which are AMF hosts used in coculture to increase the activity of AMF in an artificial way; other studies have used similar techniques to force mycorrhization in *Arabidopsis thaliana*, which is widely known to not form AM (Hanke & Rensing, 2010; Veiga *et al.*, 2013). To our knowledge, there have been no reports of healthy mycorrhized moss samples collected from nature outside of *Takakia*. The phylogenetic relationships of the bryophytes to themselves as well as to vascular plants has long been in question. Recent phylotranscriptomic analyses based upon the 1,000 Plant Genomes consortium consistently place the mosses and liverworts as sister lineages to one another (Wickett *et al.*, 2014; Leebens-Mack *et al.*, 2019). The branching

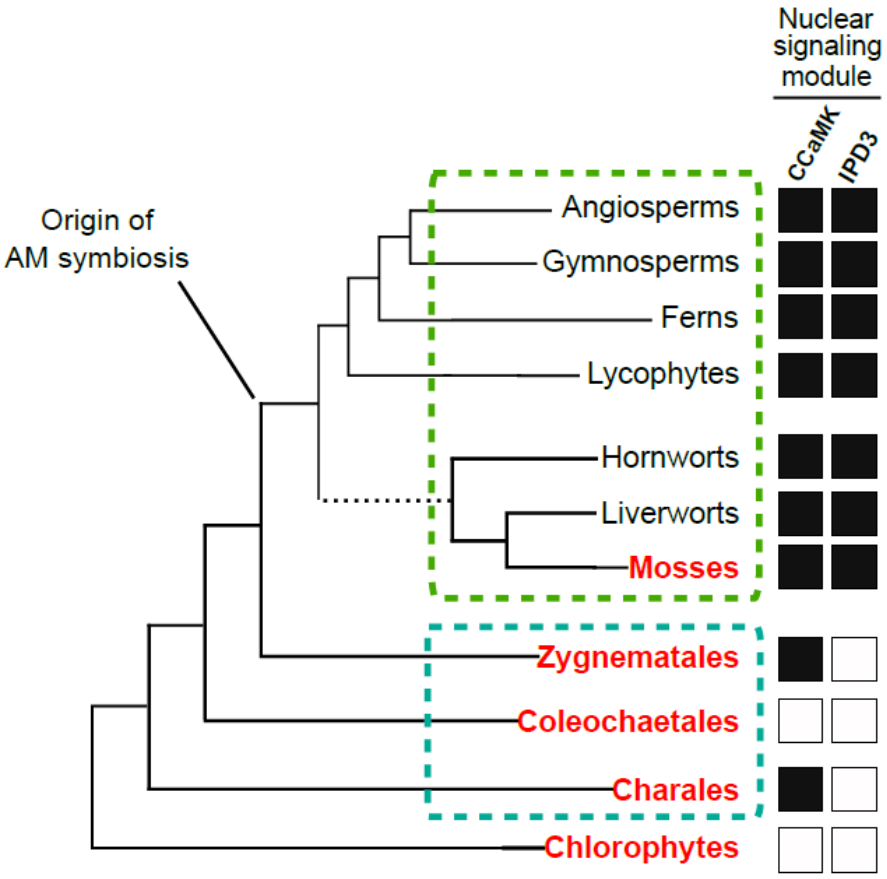

Figure 3: Conspicuous presence of the symbiosis-specific nuclear signaling module, *CCaMK/IPD3*, in the mostly non-mycorrhizal moss lineage and advanced charophyte algae.

AM-compatible host plants are found in every lineage of land plants, however there are notable examples of lineage-specific loss of AM symbiosis, exemplified by the lack of arbuscular mycorrhizas in the Brassicaceae (angiosperms) and the Pinaceae (gymnosperms). A highly conserved genomic trait of hosts is the presence of *CCaMK* and *IPD3*, the symbiosis specific nuclear signaling genes. *CCaMK* and *IPD3* are consistently absent in non-host genomes. The most inconsistent examples of *CCaMK* and *IPD3* conservation are in the mosses and advanced charophyte algae, neither of whom form AM- or AM-like symbiotic interactions. Lineages without AM- or AM-like interactions are highlighted red. Land plants are circled in green. Advanced charophyte algae are circled in blue. The dotted line indicates the putative monophyly of bryophytes. This phylogeny is based upon the recent 1,000 Plant Genomes consortium and is currently based upon mostly transcriptomic evidence; this phylogeny may be subject to change as more genomes become available (Wickett *et al.*, 2014; Leebens-Mack *et al.*, 2019)

relationship between hornworts and the monophyletic group of liverworts+mosses is less certain, however. Despite some contention due to the use of transcriptomics, the currently

proposed scenarios are that hornworts are basal to liverworts+mosses and that bryophytes are monophyletic, or that hornworts are basal to liverworts+mosses and the latter lineage is sister to all other land plants. These branching scenarios of the bryophytes are likely to be reassessed as genomic data becomes more available. In these hypothetical branching scenarios of the bryophytes, it appears that mosses have lost the ability to form AM as opposed to diverging from land plants prior to the emergence of AM. One should not discount the possibility that mosses form a sister lineage to all land plants, however. These scenarios are parsimonious with a single origin of AM interactions at the base of the land plants. As such, the presence of *CCaMK* and *IPD3* in mosses calls into question the role(s) of these genes in mosses. In theory these genes may have retained functions that fall outside of our understanding of fungal interactions in mosses, or perhaps have neofunctionalized for moss-specific functions.

Even more enigmatic is the evolution of *CCaMK* in advanced charophyte algae, which as a group of lineages are more ancient than land plants or AM (Delaux *et al.*, 2015a; Nishiyama *et al.*, 2018; Cheng *et al.*, 2019). Specifically, *CCaMK* homologs are found in the later-diverging clades of the charophytes, Charales and Zygnematales (advanced charophyte algae). The *CCaMK* homolog of *Closterium peracerosum–strigosum–littorale* complex was furthermore shown to possess the molecular determinants necessary to fully rescue the symbiotic defects of *ccamk-1* mutant *Medicago truncatula* (Medicago). The advanced charophyte algae are known to form epiphytic associations with diverse groups of fungi, however apparently not with AMF (Knack *et al.*, 2015). These revelations obfuscate the role(s) of *CCaMK* in extant charophyte algae, but also the ancestral role(s) of symbiotic signaling genes. Similar to

the case of mosses, there is a lacking of genomic data to settle the question of the branching order of advanced charophyte algae and which lineage is sister to land plants. Again, care must be taken when making conclusions concerning these algae as the majority of the currently used data is confined to transcriptomics (Wickett *et al.*, 2014). Despite simple appearances in the lab, the growth stages, culture conditions, and environment of these cultures likely have consequential effects upon the calling of "absence" of certain genes.

Although AM symbiosis may be seen as unique to particular lineages of land plants, mosses and charophyte algae certainly form abundant and complex interactions with microorganisms, including diverse fungi (Pressel *et al.*, 2010; Knack *et al.*, 2015; Graham *et al.*, 2017). As such, although it appears that mosses and charophytes may be using the CSP for as-of-yet unknown function(s), that is not to say that this ancient signaling pathway may be involved in other plant-fungal interactions.

1.6 - Rationale for studying symbiotic genes in mosses and charophyte algae

The biological relevance of CSP genes in mosses and charophytes is completely unanswered, although there are hints that at least *CCaMK* serves a similar cellular signaling role (Wang *et al.*, 2010b; Delaux *et al.*, 2015a). We hypothesize that the CSP indeed serves some relevant biological function in these ancient lineages, perhaps other uncharacterized plant-fungal interactions. Have these genes influenced the evolutionary history of mosses and algae, as they have with other land plants? Determining the biological function(s) of CSP genes is key to tackling this question. Leveraging what has been learned about *CCaMK* and *IPD3* in angiosperms, in combination with recent advances in the genomics of bryophytes and charophyte algae provides a unique vantage

point with which to study the unknown function(s) of symbiosis genes in mosses and charophyte algae.

In the case of mosses, conveniently the moss *Physcomitrella patens* (Physcomitrella) has been robustly developed as a genetic and molecular model for mosses. Physcomitrella has a complete, well annotated genome which has benefited from updates and an active research community (Rensing *et al.*, 2008; Lang *et al.*, 2018). Of all the bryophytes, Physcomitrella is currently the easiest model to transform (Genet *et al.*, 1991; Hohe *et al.*, 2004). The Physcomitrella research community has also kept up with recent "-omics" techniques, including small RNA sequencing and proteomics, but also with state-of-the-art multiplex genome editing techniques using CRISPR technology (Sarnighausen *et al.*, 2004; Coruh *et al.*, 2015; Mallett *et al.*, 2019). Physcomitrella has a very simple developmental cycle and body plan, one can argue even simpler than hornworts or liverworts. Nearly all tissues of Physcomitrella are one cell-layer in thickness, benefiting morphological observation, including through the use of microfluidics tools (Prigge & Bezanilla, 2010; Bascom *et al.*, 2016). Like other bryophytes, mosses, including Physcomitrella, are gametophyte-dominant plants, meaning the majority of their life cycle is spent in a haploid state. This is primarily useful in generating loss-of-function mutants and negates the need of performing crosses to obtain homozygous lines. Given these qualities of Physcomitrella as a model, it is the best suited model moss with which to study the function(s) of *CCaMK* and *IPD3* in mosses.

Charophyte algae as comparative genomics systems have recently benefitted from the 1,000 Plant Genomes consortium, although to date the majority of available data is transcriptomic (Leebens-Mack *et al.*, 2019). Genome assemblies are also being

published more commonly (Hori *et al.*, 2014; Nishiyama *et al.*, 2018; Cheng *et al.*, 2019; Wang *et al.*, 2019a). Unfortunately, reliable and reproducible methods for charophyte transformation are currently lacking, which severely restricts our ability to study the genetics and physiology of these organisms. In the last decade, examples of *Agrobacterium*-mediated and microparticle bombardment transformation have been reported, however these methods have not caught on with a broad research community studying charophyte algae (Vannerum *et al.*, 2010; Abe *et al.*, 2011; Sørensen *et al.*, 2014). There are multiple culture resources, such as the UTEX culture collection at University of Texas at Austin, from which to purchase diverse species of charophyte algae, including axenic cultures critical for any future charophyte-microbe interaction studies. Given the simplicity of growing and maintaining unicellular, unialgal cultures such as desmids, which belong to a putative sister lineage of land plants, Zygnematales, there are innumerable evolutionary questions that can be answered by developing a reliable transformation model. As such, we sought to first develop a reliable methodology for transformation, focusing on a panel of unicellular and filamentous species of the Zygnematales.

In **Chapter 2** of this work, we report that Physcomitrella CCaMK possesses the molecular determinants required for symbiotic function in Medicago, despite the inability of Physcomitrella to associate with AM fungi. Furthermore, we report that drought stress-like developmental programs are activated in Physcomitrella in response to CCaMK or IPD3 activation, however abscisic acid signaling remains functional in Physcomitrella upon genetic deletion of *CCaMK* or *IPD3.* This indicates that although CCaMK/IPD3 signaling is sufficient to induce drought stress signaling in Physcomitrella, CCaMK or

IPD3 do not constitute a necessary component of drought stress signaling pathways in mosses. This was unexpected, because although it is known that water status is intimately tied to the interaction between host plants and AMF, there is to date no known function in angiosperms of CSP components directly influencing drought stress-related signaling.

Initially, it appeared we were without any observable phenotype of the *ccamk* or *ipd3* mutant of Physcomitrella. In **Chapter 3**, we describe that through close microfluidic examination of tip-growing cells in *ipd3* mutant Physcomitrella, we serendipitously uncovered a striking gravitropic defect of filamentous cells. The *ipd3* mutant was not affected by modulating ABA signaling. This was also unexpected because no previous reports have ever tied CSP signaling to gravitropisms. Analogous mutants in Medicago presented no observable defects in root gravitropism. These studies suggest we have stumbled upon two novel, uncoupled functions of CSP in mosses.

In **Chapter 4**, we describe our tested methods of charophyte transformation, including indirect methods utilizing *Agrobacterium*, but also direct mechanisms such as microparticle bombardment. In all cases, these methods were tested with varying parameters on a panel of unicellular and filamentous zygnematalean species. We describe a generalizable method for microparticle bombardment for transient transformation of three zygnematalean species, *Mesotaenium caldariorum*, *Zygnema sp*, and *Mougeotia transeaui*.

1.7 - References

Abe J, Hori S, Tsuchikane Y, Kitao N, Kato M, Sekimoto H. **2011**. Stable nuclear transformation of the *Closterium peracerosum-strigosum- littorale* complex. *Plant and Cell Physiology* **52**: 1676–1685.

Ané J-M, Kiss GB, Riely BK, Penmetsa RV, Oldroyd GED, Ayax C, Lévy J, Debellé F, Baek J-M, Kalo P. **2004**. *Medicago truncatula DMI1* required for bacterial and fungal symbioses in legumes. *Science* **303**: 1364–1367.

Augé RM. **2001**. Water relations, drought and vesicular-arbuscular mycorrhizal symbiosis. *Mycorrhiza* **11**: 3–42.

Augé RM, Toler HD, Saxton AM. **2014**. Arbuscular mycorrhizal symbiosis alters stomatal conductance of host plants more under drought than under amply watered conditions: a meta-analysis. *Mycorrhiza* **25**: 13–24.

Bascom CS, Wu SZ, Nelson K, Oakey J, Bezanilla M. **2016**. Long-term growth of moss in microfluidic devices enables subcellular studies in development. *Plant Physiology* **172**: 28–37.

Besserer A, Bécard G, Jauneau A, Roux C, Séjalon-Delmas N. **2008**. GR24, a synthetic analog of strigolactones, stimulates the mitosis and growth of the arbuscular mycorrhizal fungus *Gigaspora rosea* by boosting its energy metabolism. *Plant Physiology* **148**: 402–413.

Besserer A, Puech-Pagès V, Kiefer P, Gomez-Roldan V, Jauneau A, Roy S, Portais JC, Roux C, Bécard G, Séjalon-Delmas N. **2006**. Strigolactones stimulate arbuscular mycorrhizal fungi by activating mitochondria. *PLoS Biology* **4**: 1239–1247.

Bravo A, York T, Pumplin N, Mueller LA, Harrison MJ. **2016**. Genes conserved for arbuscular mycorrhizal symbiosis identified through phylogenomics. *Nature Plants* **2**: 1–6.

Bressendorff S, Azevedo R, Kenchappa CS, Ponce de Leon I, Olsen J V, Rasmussen MW, Erbs G, Newman M-A, Petersen M, Mundy J. **2016**. An innate

immunity pathway in the moss *Physcomitrella patens*. *The Plant Cell* **28**: tpc.00774.2015.

Brundrett MC, Tedersoo L. **2018**. Evolutionary history of mycorrhizal symbioses and global host plant diversity. *New Phytologist* **220**: 1108–1115.

Boullard, B. 1988. Observations on the coevolution of fungi with hepatics. *Coevolution of Fungi with Plants and Animals*, eds K. A. Pirozynski and D. L.Hawksworth. Cambridge, MA: Academic Press

Capoen W, Sun J, Wysham D, Otegui MS, Venkateshwaran M, Hirsch S, Miwa H, Downie JA, Morris RJ, Ané J-M. **2011**. Nuclear membranes control symbiotic calcium signaling of legumes. *Proceedings of the National Academy of Sciences* **108**: 14348–14353.

Chabaud M, Genre A, Sieberer BJ, Faccio A, Fournier J, Novero M, Barker DG, Bonfante P. **2011**. Arbuscular mycorrhizal hyphopodia and germinated spore exudates trigger Ca2+ spiking in the legume and nonlegume root epidermis. *New Phytologist* **189**: 347–355.

Charpentier M, Sun J, Martins TV, Radhakrishnan G V, Findlay K, Soumpourou E, Thouin J, Véry A-A, Sanders D, Morris RJ. **2016**. Nuclear-localized cyclic nucleotide–gated channels mediate symbiotic calcium oscillations. *Science* **352**: 1102–1105.

Cheng S, Xian W, Fu Y, Marin B, Keller J, Wu T, Sun W, Li X, Xu Y, Zhang Y, *et al.* 2019. Genomes of subaerial *Zygnematophyceae* provide insights into land plant evolution. *Cell* **179**: 1057-1067.e14.

Coruh C, Cho SH, Shahida S, Liu Q, Wierzbicki A, Axtell MJ. **2015**. Comprehensive annotation of *Physcomitrella patens* small RNA loci reveals that the heterochromatic short interfering rna pathway is largely conserved in land plants. *Plant Cell* **27**: 2148–2162.

Delaux P. **2017**. Comparative phylogenomics of symbiotic associations. *New Phytologist* **213**: 89–94.

Delaux P-M, Radhakrishnan G V., Jayaraman D, Cheema J, Malbreil M, Volkening JD, Sekimoto H, Nishiyama T, Melkonian M, Pokorny L, *et al.* 2015. Algal ancestor of land plants was preadapted for symbiosis. *Proceedings of the National Academy of*

Sciences **112**: 201515426.

Delaux P-M, Varala K, Edger PP, Coruzzi GM, Pires JC, Ané J-M. **2014**. Comparative phylogenomics uncovers the impact of symbiotic associations on host genome evolution. *PLoS Genet* **10**: e1004487.

Desiro A, Duckett JG, Pressel S, Villarreal JC, Bidartondo MI, Desirò A, Duckett JG, Pressel S, Villarreal JC, Bidartondo MI. **2013**. Fungal symbioses in hornworts: a chequered history. *Proceedings of the Royal Society B-Biological Sciences* **280**: 20130207.

Doyle JJ. **2011**. Phylogenetic perspectives on the origins of nodulation. *Molecular Plant-Microbe Interactions* **24**: 1289–1295.

Feng F, Sun J, Radhakrishnan G V., Lee T, Bozsóki Z, Fort S, Gavrin A, Gysel K, Thygesen MB, Andersen KR, *et al.* 2019. A combination of chitooligosaccharide and lipochitooligosaccharide recognition promotes arbuscular mycorrhizal associations in *Medicago truncatula*. *Nature Communications* **10**.

Field KJ, Rimington WR, Bidartondo MI, Allinson KE, Beerling DJ, Cameron DD, Duckett JG, Leake JR, Pressel S. **2015**. First evidence of mutualism between ancient plant lineages (*Haplomitriopsida liverworts*) and Mucoromycotina fungi and its response to simulated Palaeozoic changes in atmospheric CO2. *New Phytologist* **205**: 743–756.

Floss DS, Levy JG, Lévesque-Tremblay V, Pumplin N, Harrison MJ. **2013**. DELLA proteins regulate arbuscule formation in arbuscular mycorrhizal symbiosis. *Proceedings of the National Academy of Sciences* **110**: E5025–E5034.

Garcia K, Delaux P, Cope KR, Ané J. **2015**. Molecular signals required for the establishment and maintenance of ectomycorrhizal symbioses. *New Phytologist* **208**: 79–87.

Genet MG, Schaefer D, Zryd P, Cove J, October UKR. **1991**. Stable transformation of the moss *Physcomitrella patens*. *Molecular and Genetical Genetics*: 418–424.

Gherbi H, Markmann K, Svistoonoff S, Estevan J, Autran D, Giczey G, Auguy F, Péret B, Laplaze L, Franche C. **2008**. SymRK defines a common genetic basis for plant

root endosymbioses with arbuscular mycorrhiza fungi, rhizobia, and Frankiabacteria. *Proceedings of the National Academy of Sciences* **105**: 4928–4932.

Gleason C, Chaudhuri S, Yang T, Mun A, Muñoz A, Poovaiah BW, Oldroyd GED. **2006**. Nodulation independent of rhizobia induced by a calcium-activated kinase lacking autoinhibition. *Nature* **441**: 1149–1152.

Graham LE, Graham JM, Knack JJ, Trest MT, Piotrowski MJ, Arancibia-Avila P. **2017**. A Sub-Antarctic peat moss metagenome indicates microbiome resilience to stress and biogeochemical functions of early paleozoic terrestrial ecosystems. *International Journal of Plant Sciences* **178**: 618–628.

Graham LE, Graham JM, Wilcox LW, Cook ME, Arancibia-Avila P, Knack JJ. 2018. Evolutionary roots of plant microbiomes and biogeochemical impacts of nonvascular autotroph-microbiome systems over deep time. *International Journal of Plant Sciences.* **7**: 505-522

Grosche C, Genau AC, Rensing SA. **2018**. Evolution of the symbiosis-specific gras regulatory network in bryophytes. *Frontiers in Plant Science* **871**: 1–13.

Hanke ST, Rensing SA. **2010**. In vitro association of non-seed plant gametophytes with arbuscular mycorrhiza fungi. *Journal of endocytobiosis and cell research*: 95–101.

Harrier LA, Watson CA. **2004**. The potential role of arbuscular mycorrhizal (AM) fungi in the bioprotection of plants against soil-borne pathogens in organic and/or other sustainable farming systems. *Pest Management Science* **60**: 149–157.

van der Heijden MGA, Martin FM, Selosse MA, Sanders IR. **2015**. Mycorrhizal ecology and evolution: The past, the present, and the future. *New Phytologist* **205**: 1406–1423.

Hohe A, Egener T, Lucht JM, Holtorf H, Reinhard C, Schween G, Reski R. **2004**. An improved and highly standardised transformation procedure allows efficient production of single and multiple targeted gene-knockouts in a moss, *Physcomitrella patens*. *Current Genetics* **44**: 339–347.

Hori K, Maruyama F, Fujisawa T, Togashi T, Yamamoto N, Seo M, Sato S, Yamada T, Mori H, Tajima N. **2014**. *Klebsormidium flaccidum* genome reveals primary factors for

plant terrestrial adaptation. *Nature communications* **5**.

Horváth B, Yeun LH, Domonkos Á, Halász G, Gobbato E, Ayaydin F, Miró K, Hirsch S, Sun J, Tadege M, *et al.* 2011. *Medicago truncatula IPD3* is a member of the common symbiotic signaling pathway required for rhizobial and mycorrhizal symbioses. *Molecular Plant-Microbe Interactions* **24**: 1345–1358.

Humphreys CP, Franks PJ, Rees M, Bidartondo MI, Leake JR, Beerling DJ. **2010**. Mutualistic mycorrhiza-like symbiosis in the most ancient group of land plants. *Nature Communications* **1**.

Jin Y, Chen Z, Yang J, Mysore KS, Wen J, Huang J, Yu N, Wang E. **2018**. *IPD3* and *IPD3L* function redundantly in rhizobial and mycorrhizal symbioses. *Frontiers in Plant Science* **9**: 1–12.

Kim S, Zeng W, Bernard S, Liao J, Venkateshwaran M, Ane JM, Jiang Y. **2019**. Ca2+-regulated Ca2+ channels with an RCK gating ring control plant symbiotic associations. *Nature Communications* **10**: 1–12.

Knack JJ, Wilcox LW, Delaux P-M, Ané J-M, Piotrowski MJ, Cook ME, Graham JM, Graham LE, Knoll AH. **2015**. Microbiomes of stephtophyte algae and bryophytes suggest that a functional suite of microbiota fostered plant colonization of land. *Int. J. Plant Sci.* **176**: 405–420.

Lang D, Ullrich KK, Murat F, Fuchs J, Jenkins J, Haas FB, Piednoel M, Gundlach H, Van Bel M, Meyberg R, *et al.* 2018. The *Physcomitrella patens* chromosome-scale assembly reveals moss genome structure and evolution. *Plant Journal* **93**: 515–533.

Leebens-Mack JH, Barker MS, Carpenter EJ, Deyholos MK, Gitzendanner MA, Graham SW, Grosse I, Li Z, Melkonian M, Mirarab S, *et al.* 2019. One thousand plant transcriptomes and the phylogenomics of green plants. *Nature* **574**: 679–685.

Lévy J, Bres C, Geurts R, Chalhoub B, Kulikova O, Duc G, Journet E-PP, Ané J-M, Lauber E, Bisseling T, *et al.* 2004. A putative Ca2+ and calmodulin-dependent protein kinase required for bacterial and fungal symbioses. *Science* **303**: 1361–4.

Liao J, Singh S, Hossain MS, Andersen SU, Ross L, Bonetta D, Zhou Y, Sato S,

Tabata S, Stougaard J, *et al.* 2012. Negative regulation of CCaMK is essential for symbiotic infection. *Plant Journal* **72**: 572–584.

Luginbuehl LH, Menard GN, Kurup S, Van Erp H, Radhakrishnan G V., Breakspear A, Oldroyd GED, Eastmond PJ. **2017**. Fatty acids in arbuscular mycorrhizal fungi are synthesized by the host plant. *Science* **356**: 1175–1178.

Maillet F, Poinsot V, André O, Puech-Pagés V, Haouy A, Gueunier M, Cromer L, Giraudet D, Formey D, Niebel A, *et al.* 2011. Fungal lipochitooligosaccharide symbiotic signals in arbuscular mycorrhiza. *Nature* **469**: 58–64.

Mallett DR, Chang M, Cheng X, Bezanilla M. **2019**. Efficient and modular CRISPR-Cas9 vector system for *Physcomitrella patens*. *Plant Direct* **3**: 1–15.

Messinese E, Mun J-H, Yeun LH, Jayaraman D, Rougé P, Barre A, Lougnon G, Schornack S, Bono J-J, Cook DR. **2007**. A novel nuclear protein interacts with the symbiotic DMI3 calcium-and calmodulin-dependent protein kinase of *Medicago truncatula*. *Molecular Plant-Microbe Interactions* **20**: 912–921.

Metcalf CJE, Koskella B. **2019**. Protective microbiomes can limit the evolution of host pathogen defense. *Evolution Letters* **3**: 534–543.

Miller JB, Pratap A, Miyahara A, Zhou L, Bornemann S, Morris RJ, Oldroyd GED. **2013**. Calcium/Calmodulin-dependent protein kinase is negatively and positively regulated by calcium, providing a mechanism for decoding calcium responses during symbiosis signaling. *The Plant Cell* **25**: 5053–5066.

Miya A, Albert P, Shinya T, Desaki Y, Ichimura K, Shirasu K, Narusaka Y, Kawakami N, Kaku H, Shibuya N. **2007**. CERK1, a LysM receptor kinase, is essential for chitin elicitor signaling in Arabidopsis. *Proceedings of the National Academy of Sciences of the United States of America* **104**: 19613–19618.

Miyata K, Kozaki T, Kouzai Y, Ozawa K, Ishii K, Asamizu E, Okabe Y, Umehara Y, Miyamoto A, Kobae Y, *et al.* 2014. Bifunctional plant receptor, OsCERK1, regulates both chitin-triggered immunity and arbuscular mycorrhizal symbiosis in rice. *Plant & cell physiology* **55**: 1864–1872.

Naranjo-Ortiz MA, Gabaldon T. 2019. Fungal evolution: diversity, taxonomy and phylogeny of the Fungi. *Biological Reviews.* **94:** 2101–2137.

Navarro L, Bari R, Achard P, Lisón P, Nemri A, Harberd NP, Jones JDG. **2008**. DELLAs control plant immune responses by modulating the balance of jasmonic acid and salicylic acid signaling. *Current Biology* **18**: 650–655.

Nelson J, Shaw AJ. **2019**. Exploring the natural microbiome of the model liverwort: fungal endophyte diversity in *Marchantia polymorpha L*. *Symbiosis* **78**: 45–59.

Nishiyama T, Sakayama H, de Vries J, Buschmann H, Saint-Marcoux D, Ullrich KK, Haas FB, Vanderstraeten L, Becker D, Lang D, *et al.* 2018. The *Chara* genome: Secondary complexity and implications for plant terrestrialization. *Cell* **174**: 448-464.e24.

Oldroyd GED. **2013**. Speak, friend, and enter: signalling systems that promote beneficial symbiotic associations in plants. *Nature Reviews Microbiology* **11**: 252–263.

Panke-Buisse K, Poole AC, Goodrich JK, Ley RE, Kao-Kniffin J. **2015**. Selection on soil microbiomes reveals reproducible impacts on plant function. *ISME Journal* **9**: 980–989.

Parniske M. **2008**. Arbuscular mycorrhiza: the mother of plant root endosymbioses. *Nature reviews. Microbiology* **6**: 763–75.

Petutschnig EK, Stolze M, Lipka U, Kopischke M, Horlacher J, Valerius O, Rozhon W, Gust AA, Kemmerling B, Poppenberger B, *et al.* 2014. A novel *Arabidopsis CHITIN ELICITOR RECEPTOR KINASE 1 (CERK1)* mutant with enhanced pathogen-induced cell death and altered receptor processing. *New Phytologist* **204**: 955–967.

Pimprikar P, Carbonnel S, Paries M, Katzer K, Klingl V, Bohmer MJ, Karl L, Floss DS, Harrison MJ, Parniske M. **2016**. A CCaMK-CYCLOPS-DELLA complex activates transcription of *RAM1* to regulate arbuscule branching. *Current Biology* **26**: 987–998.

Pressel S, Bidartondo MI, Ligrone R, Duckett JG. **2010**. Fungal symbioses in bryophytes: New insights in the Twenty First Century. *Phytotaxa* **9**: 238.

Prigge MJ, Bezanilla M. **2010**. Evolutionary crossroads in developmental biology:

Physcomitrella patens. *Development* **137**: 3535–3543.

Read DJ, Ducket JG, Francis R, Ligron R, Russell a. **2000**. Symbiotic fungal associations in 'lower' land plants. *Philosophical transactions of the Royal Society of London. Series B, Biological sciences* **355**: 815–830; discussion 830-831.

Redecker D, Kodner R, Graham LE. **2000**. Glomalean fungi from the Ordovician. *Science* **289**: 1920–1921.

Remy W, Taylor TN, Hass H, Kerp H. **1994a**. Four hundred-million-year-old vesicular arbuscular mycorrhizae. *Proceedings of the National Academy of Sciences* **91**: 11841–11843.

Remy W, Taylor TN, Hass H, Kerp H. **1994b**. Four hundred-million-year-old vesicular arbuscular mycorrhizae. *Proceedings of the National Academy of Sciences of the United States of America* **91**: 11841–11843.

Rensing SA, Lang D, Zimmer AD, Terry A, Salamov A, Shapiro H, Nishiyama T, Perroud P-F, Lindquist EA, Kamisugi Y. **2008**. The *Physcomitrella* genome reveals evolutionary insights into the conquest of land by plants. *Science* **319**: 64–69.

Rimington WR, Pressel S, Duckett JG, Field KJ, Bidartondo MI. **2019**. Evolution and networks in ancient and widespread symbioses between Mucoromycotina and liverworts. *Mycorrhiza* **29**: 551–565.

Sarnighausen E, Wurtz V, Heintz D, Van Dorsselaer A, Reski R. **2004**. Mapping of the *Physcomitrella patens* proteome. *Phytochemistry* **65**: 1589–1607.

Singh S, Katzer K, Lambert J, Cerri M, Parniske M. **2014**. CYCLOPS, A DNA-binding transcriptional activator, orchestrates symbiotic root nodule development. *Cell Host and Microbe* **15**: 139–152.

Smith SE, Read DJ. **2010**. *Mycorrhizal symbiosis*. Academic press.

Sørensen I, Fei Z, Andreas A, Willats WGT, Domozych DS, Rose JKC. **2014**. Stable transformation and reverse genetic analysis of *Penium margaritaceum*: A platform for studies of charophyte green algae, the immediate ancestors of land plants. *Plant Journal*

77: 339–351.

Takeda N, Maekawa T, Hayashi M. **2012**. Nuclear-localized and deregulated calcium- and calmodulin-dependent protein kinase activates rhizobial and mycorrhizal responses in *Lotus japonicus*. *The Plant cell* **24**: 810–22.

Tirichine L, Imaizumi-Anraku H, Yoshida S, Murakami Y, Madsen LH, Miwa H, Nakagawa T, Sandal N, Albrektsen AS, Kawaguchi M, *et al.* 2006. Deregulation of a Ca2+/calmodulin-dependent kinase leads to spontaneous nodule development. *Nature* **441**: 1153–6.

Vannerum K, Abe J, Sekimoto H, Inzé D, Vyverman W. **2010**. Intracellular localization of an endogenous cellulose synthase of micrasterias denticulata (desmidiales, chlorophyta) by means of transient genetic transformation. *Journal of Phycology* **46**: 839–845.

Veiga RSL, Faccio A, Genre A, Pieterse CMJ, Bonfante P, Van der Heijden MGA. **2013**. Arbuscular mycorrhizal fungi reduce growth and infect roots of the non-host plant *Arabidopsis thaliana*. *Plant, Cell and Environment* **36**: 1926–1937.

Venkateshwaran M, Jayaraman D, Chabaud M, Genre A, Balloon AJ, Maeda J, Forshey K, den Os D, Kwiecien NW, Coon JJ. **2015**. A role for the mevalonate pathway in early plant symbiotic signaling. *Proceedings of the National Academy of Sciences* **112**: 9781–9786.

Wallace MW, Hood A, Shuster A, Greig A, Planavsky NJ, Reed CP. **2017**. Oxygenation history of the Neoproterozoic to early Phanerozoic and the rise of land plants. *Earth and Planetary Science Letters* **466**: 12–19.

Wang S, Li L, Li H, Sahu SK, Wang H, Xu Y, Xian W, Song B, Liang H, Cheng S, *et al.* 2019. Genomes of early-diverging streptophyte algae shed light on plant terrestrialization. *Nature Plants*.

Wang B, Qiu Y-LYL. **2006**. Phylogenetic distribution and evolution of mycorrhizas in land plants. *Mycorrhiza* **16**: 299–363.

Wang B, Yeun LH, Xue J, Liu Y, Ané J, Qiu Y. **2010a**. Presence of three mycorrhizal

genes in the common ancestor of land plants suggests a key role of mycorrhizas in the colonization of land by plants. *New Phytologist* **186**: 514–525.

Wang B, Yeun LH, Xue JY, Liu Y, Ané JM, Qiu YL. **2010b**. Presence of three mycorrhizal genes in the common ancestor of land plants suggests a key role of mycorrhizas in the colonization of land by plants. *New Phytologist* **186**: 514–525.

Wickett NJ, Mirarab S, Nguyen N, Warnow T, Carpenter E, Matasci N, Ayyampalayam S, Barker MS, Burleigh JG, Gitzendanner MA. **2014**. Phylotranscriptomic analysis of the origin and early diversification of land plants. *Proceedings of the National Academy of Sciences* **111**: E4859–E4868.

Xue L, Cui H, Buer B, Vijayakumar V, Delaux P-M, Junkermann S, Bucher M. **2015**. Network of GRAS transcription factors involved in the control of arbuscule development in Lotus japonicus. *Plant physiology* **167**: 854–871.

Zhang X, Dong W, Sun J, Feng F, Deng Y, He Z, Oldroyd GED, Wang E. **2015**. The receptor kinase CERK1 has dual functions in symbiosis and immunity signalling. *The Plant Journal* **81**: 258–267.

Zipfel C, Oldroyd GED. **2017**. Plant signalling in symbiosis and immunity. *Nature* **543**: 328–336.

Chapter 2 - (MANUSCRIPT SUBMITTED TO iSCIENCE (CELL PRESS) FOR REVIEW)

Conserved components of the common symbiosis pathway regulate ABA levels and stress-associated developmental reprogramming in Physcomitrella

Thomas J. Kleist[1,2,3,*,#], Anthony Bortolazzo[4,5*], Adele M. Perera[1], Thomas B. Irving[5], Muthusubramanian Venkateshwaran[6,7], Fatiha Atanjaoui[3], Ren-Jie Tang[1], Heather N. Cartwright[2], Michael L. Christianson[1], Peggy G. Lemaux[1], Sheng Luan[1], and Jean-Michel Ané[5,6,#]

[1] Department of Plant & Microbial Biology, University of California-Berkeley, Berkeley, CA 94720, USA

[2] Department of Plant Biology, Carnegie Institute for Science, Stanford, CA 94305, USA

[3] Department of Biology, Heinrich Heine University, Düsseldorf 40225, Germany (current affiliation)

[4] Laboratory of Genetics, University of Wisconsin-Madison, Madison, WI 53706, USA

[5] Department of Bacteriology, University of Wisconsin-Madison, Madison, WI 53706, USA

[6] Department of Agronomy, University of Wisconsin-Madison, Madison, WI 53706, USA

[7] School of Agriculture, University of Wisconsin-Platteville, Platteville, WI 53818, USA (current affiliation)

* These authors contributed equally to this work.

[#] Corresponding authors: Thomas J. Kleist, Phone: +49 211 81-14826, Email: kleistt@hhu.de , Jean-Michel Ané, Phone: 608-262-6457, Email: jeanmichel.ane@wisc.edu

A.Bortolazzo's contributions to manuscript/Ch. 2

AB performed the protein sequence alignment homolog tabulation. AB performed all protein biochemistry work, including protein purification, with the exception of yeast two-hybrid assays. AB cloned the visual reporters of PpCCaMK and PpIPD3 and localized them in transgenic tobacco pavement cells. AB performed the mutant rescue experiments done in *Medicago truncatula*. Concerning work done in *Physcomitrella patens*, AB designed and generated the *Ppccamk* deletion mutant, performed lipid-staining in gain-of-function lines, and performed stress-treatments in the mutants as well as abscisic acid measurements in the gain-of-function mutants. AB illustrated the following figures: Figures 1a,b,c,e,f,g,h (with input from TK on b and c), 3e, 4a,b, S4, S5a, S6a,b,c, Stable 2, AD1a,b, AD2, and AD3. AB shared half of the writing with the co-first author as each author wrote one iteration of the manuscript. Input on writing was regularly provided by J.-M.A. and T.I.

2.1 - Abstract

Symbioses between angiosperms and rhizobia or arbuscular mycorrhizal fungi are controlled through a conserved signaling pathway wherein microbe-derived, chitin-based elicitors activate plant cell-surface receptors and trigger oscillatory nuclear calcium signals, which are decoded by a calcium/calmodulin-dependent protein kinase (CCaMK) and its target transcription factor Interacting Protein of DMI3 (IPD3). Genes encoding CCaMK and IPD3 have been lost in multiple non-mycorrhizal plant lineages yet retained among non-mycorrhizal mosses. Here, we demonstrated that the moss *Physcomitrella* is equipped with a bona fide CCaMK that can functionally complement a *Medicago* loss-of-function mutant. Conservation of regulatory phosphosites allowed us to generate predicted hyperactive forms of *Physcomitrella* CCaMK and IPD3. Expression of synthetically activated CCaMK or IPD3 in *Physcomitrella* led to abscisic acid (ABA)

accumulation and ectopic development of brood cells, which are asexual propagules that facilitate escape from local abiotic stresses. We therefore propose a functional role for *Physcomitrella* CCaMK-IPD3 in stress-associated developmental reprogramming.

2.2 - Introduction

During their early evolution, plants faced numerous challenges in the shift from freshwater to terrestrial environments. These problems would have included decreased availability of water, the sparsity of nutrients, and increased levels of ultraviolet radiation. The shared ancestor of extant land plants evolved several strategies to surmount these stressors. For example, arbuscular mycorrhizal fungi (AMF) and AMF-like interactions with fungal mutualists likely aided early land plants in the acquisition of water and nutrients (Pirozynski & Malloch, 1975; Read *et al.*, 2000; Bonfante & Genre, 2008). Arbuscular mycorrhizae are controlled infections of plant roots by fungi of the Glomeromycotina (Parniske, 2008; Spatafora *et al.*, 2016). Establishment of intracellular arbuscules within cortical root cells enables the fungus to provide the plant host with greater access to resources such as phosphate, nitrogen, potassium, and water in exchange for host photosynthates (Parniske, 2008; Smith & Read, 2010; Garcia *et al.*, 2017). Endomycorrhizal, AMF-like interactions also occur in early-diverging plant lineages, including some liverworts. Moreover, fossil samples provide evidence for ancient AMF-like associations. Endophytic structures with a striking similarity to arbuscules are present in the Early Devonian fossil record of the Rhynie chert (Remy *et al.*, 1994b; Strullu-Derrien *et al.*, 2014, 2015). Fossilized fungal spores with similar morphology to extant AMF have been found in the Ordovician (Redecker *et al.*, 2000). The broad phylogenetic distribution of AMF and AMF-like host lineages among land plants and the available fossil evidence point towards the establishment of plant-fungal symbioses early in land plant evolution (Wang & Qiu, 2006). Mosses are one of the earliest diverging and most diverse lineages of extant land plants. Whereas numerous pathogenic, saprotrophic, and commensal

fungal interactions have been described in mosses (Davey & Currah, 2006), no convincing evidence has been published to date for *bona fide* mutualistic interactions among mosses and AMF with the possible exception of *Takakia*, which is distantly related to other extant mosses (Newton *et al.*, 2000; Liu *et al.*, 2019). A few reports describing observations of AMF within moss samples (e.g., Rabatin, 1980; Carleton & Read, 1991) were likely due to misinterpretation of fungal growth present in senescent or dead plant tissues.

Perception and accommodation of AMF are achieved through a conserved signal transduction pathway in plants, often referred to as the “common symbiosis pathway” (Delaux *et al.*, 2013; Oldroyd, 2013). AM fungi exude chitooligosaccharides and lipo-chitooligosaccharides (LCOs) into the rhizosphere. LysM-receptor-like kinases (RLKs) at the plasma membrane of plant cells directly bind to these chitin-derived molecules and are required for colonization (Maillet *et al.*, 2011a; Sun *et al.*, 2015; Buendia *et al.*, 2015). Activation of RLKs upon ligand binding ultimately leads to repetitive oscillations of calcium concentrations, often referred to as “calcium spikes”, in plant nuclei (Ané *et al.*, 2004b; Capoen *et al.*, 2011). These oscillatory calcium signals are decoded by a calcium/calmodulin-dependent protein kinase (CCaMK, also known as DOESN’T MAKE INFECTIONS 3 or DMI3 in *Medicago truncatula*) (J. Levy et al. 2004; Miller et al., 2013). Activated CCaMK phosphorylates the transcription factor Interacting Protein of DMI3 (IPD3, also known as CYCLOPS in *Lotus japonicus*) at two serine residues required for infection (Messinese *et al.*, 2007; Chen *et al.*, 2008; Horváth *et al.*, 2011; Singh *et al.*, 2014). CCaMK and IPD3 initiate transcriptional cascades required for developmental reprogramming and AMF colonization by working in concert with numerous GRAS

transcription factors (Gobbato *et al.*, 2012; Xue *et al.*, 2015). Endosymbiotic interactions with nitrogen-fixing rhizobial bacteria arose roughly 90 million years ago in select land plant lineages, most notably the “nitrogen-fixing clade” of the Rosids (Doyle, 2011). Similarly to AMF, rhizobia communicate with their host-plant in the rhizosphere through LCO exudates. Indeed, many of the core symbiosis signaling components are also required for rhizobial colonization of legume roots and nitrogen fixation (Venkateshwaran *et al.*, 2013).

Nearly all AMF-host plants that have been studied possess the full complement of this core signaling pathway, from angiosperms to liverworts (Delaux et al., 2015; Wang et al., 2010). In several instances, plant lineages that have lost the ability to host AMF have also lost several symbiosis pathway genes. This correlation is exemplified by the Brassicaceae, including the model plant *Arabidopsis thaliana* (**Figure 1A**, **Supplemental Table 1**), in which many species are unable to host AMF and have concomitantly lost many of the core common signaling components (Delaux *et al.*, 2014a; Garcia *et al.*, 2015). The retention of symbiosis signaling genes in non-mycorrhizal mosses, including the model organism *Physcomitrella patens* (Physcomitrella), provides a striking counter-example (Delaux et al., 2015; Wang et al., 2010). Given that mosses have retained the vertically inherited symbiosis signaling pathway yet are unable to form AMF or AMF-like interactions, we pursued an investigation of the biochemical properties and physiological function(s) of these proteins in mosses using Physcomitrella as a model.

CCaMK and *IPD3* are two of the genes whose presence or absence most strongly correlates with AMF host compatibility or incompatibility, respectively, in studied plant lineages (Wang *et al.*, 2010b; Delaux *et al.*, 2014a; Garcia *et al.*, 2015). Moreover, genetic

studies in legumes have elucidated mutational strategies to produce gain-of-function variants of either of these two proteins that can auto-activate root nodule development in the absence of symbionts or symbiont-derived signals, a phenomenon termed spontaneous nodulation. Expression of a constitutively active CCaMK, lacking the C-terminal autoinhibitory domain, in *Medicago truncatula* (Medicago) or *Lotus japonicus* (Lotus) is sufficient to cause the development of root nodules in the absence of rhizobia or rhizobial exudates (Gleason *et al.*, 2006b; Tirichine *et al.*, 2006). Spontaneous nodule development can also be achieved by substituting an aspartate for a threonine residue in the kinase auto-activation loop of Medicago CCaMK. In Lotus, nuclear-localized and constitutively active CCaMK induced the partial development of the pre-penetration apparatus, a structure that facilitates hyphal entry of AMF into host roots (Genre *et al.*, 2008; Takeda *et al.*, 2012). A pair of phosphomimetic substitutions in the IPD3 ortholog, CYCLOPS, in Lotus is likewise sufficient to induce the development of root nodules (Singh *et al.*, 2014). These legume gain-of-function mutants revealed the pivotal role of the CCaMK-IPD3 module in this signaling pathway. We hypothesized that similar molecular genetic manipulations in Physcomitrella might lead to phenotypes that could provide clues to the possible biological relevance of these genes in mosses.

In this study, we investigated the evolutionary conservation, biochemical activities, and physiological function(s) of the two CCaMK and sole IPD3 homologs present in the Physcomitrella genome. We cloned the coding sequence of each homolog from cDNA and used yeast two-hybrid and biochemical assays to demonstrate that one of two CCaMKs and the sole IPD3 homolog from Physcomitrella have retained many of the biochemical properties required for CCaMK and IPD3 functionality in angiosperms. We

further demonstrated that the Physcomitrella CCaMK, which shared biochemical properties with angiosperm CCaMKs, could restore both nodulation and mycorrhization when expressed in a Medicago *ccamk-1* mutant background defective for both symbioses. Transgenic expression of modified forms of CCaMK and IPD3 predicted to show constitutive activation in Physcomitrella (but not the unmodified forms driven by the same promoter) promoted ectopic development of brood cells, a well-characterized developmental program of mosses in response to drought or osmotic stress. Brood cell development was accompanied by changes in abiotic stress-responsive *LEA* gene transcript levels and elevated amounts of abscisic acid (ABA). Whereas activation of PpCCaMK or PpIPD3 promoted brood cell development, genetic deletion of either the CCaMK or IPD3 loci from Physcomitrella was insufficient to block brood cell development in response to osmotic stress treatment, suggesting alternative pathways for activation of brood cell development. Collectively, our results indicate that the Physcomitrella CCaMK-IPD3 signaling module has retained many of the biochemical properties that typify these components in symbiont host plants and that the CCaMK-IPD3 module regulates ABA levels and associated developmental reprogramming to promote escape from adverse environmental conditions.

2.3 - Results

Conservation of the CCaMK-IPD3 Signaling Module in Physcomitrella

Homologs of CCaMK encoded in the *Physcomitrella patens* genome sequence version 3.3 were identified by BLASTp homology searches (Altschul *et al.*, 1990) of the predicted proteome using Medicago CCaMK/DMI3 (MtCCAMK, Medtr8g043970) and

Lotus CCaMK (LjCCaMK, Lj3g3v1739280) as queries. The top five hits were used for reciprocal BLAST against the predicted Medicago or Lotus proteomes (**Supplemental Figure 1A,B**). The two most significant BLAST hits in Physcomitrella, *Pp3c21_15330* (expectation or E-value = 0, hereafter PpCCaMK) and *Pp3c19_20580* ($E = 6 \times 10^{-171}$, hereafter PpCCaMKb), each returned MtCCAMK or LjCCaMK as the top reciprocal BLAST hit with highly significant E-values ($E \leq 6 \times 10^{-176}$). The top reciprocal BLAST hits for other loci were identified as calcium-dependent protein kinases (CDPKs), which lack the distinctive CaM-binding site found in CCaMKs. Thus, it appears that up to two loci in the Physcomitrella genome may encode functional CCaMKs. To confirm expression and validate gene models for candidate CCaMKs, we extracted RNA from Physcomitrella protonema and cloned the full-length coding sequence (CDS) for each locus. Protein sequences were aligned using MUSCLE (Edgar, 2004), and the resulting sequence alignment corroborated that the protein kinase domain, auto-activation loop, predicted CaM-binding site, and three calcium-binding EF-hand domains were each conserved in candidate PpCCaMKs (**Supplemental Figure 1C**). Closer inspection of the auto-activation loop, which is required for MtCCaMK function, revealed that PpCCaMK and PpCCaMKb each have a serine residue at the position orthologous to the auto-phosphorylated threonine residue (T271) in MtCCaMK (**Figure 1B**), which suggests that PpCCaMK and/or PpCCaMKb may likewise be subject to regulatory autophosphorylation.

To identify potential IPD3 homologs encoded in the Physcomitrella genome, we employed a similar strategy. The protein sequences of Medicago IPD3 (MtIPD3, Medtr5g026850) or Lotus IPD3/CYCLOPS (LjIPD3, Lj2g3v1549600) were used as queries; and, in each search, only a single locus (*Pp3c23_22500V3*) yielded a subzero

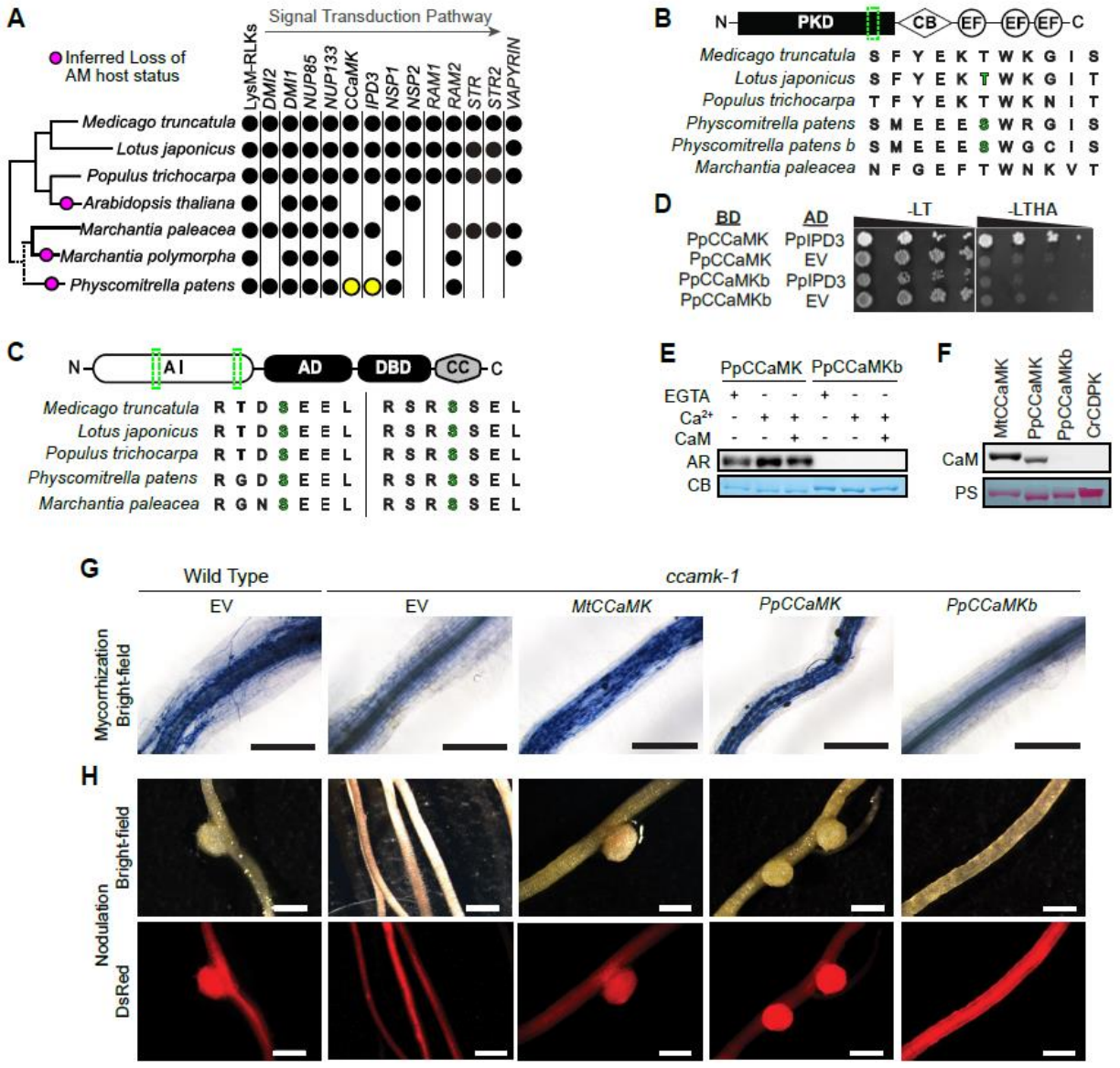

Figure 1: Functional conservation of CCaMK and IPD3 in Physcomitrella.

a) Species cladogram (left) showing the presence or absence of symbiotic signaling genes in corresponding lineages (right). Physcomitrella CCaMK and IPD3 are highlighted in yellow. See **Supplemental Table 1** for details.

b) Domain architecture diagram of CCaMK and multiple sequence alignment of the region (green) surrounding the regulatory autophosphorylation site (green). CB: CaM-binding domain, PKD: protein-kinase domain, EF: EF-hand.

c) Domain architecture diagram of IPD3 and multiple sequence alignments of regions (green) surrounding two regulatory phospho-sites (green) that are **(Legend continued onto next page)**

necessary and sufficient for activation LjIPD3/CYCLOPS. AI: autoinhibitory domain, AD: activation domain, DBD: DNA-binding domain, CC: coiled coil.
d) PpCCaMK interacted with PpIPD3 in yeast two-hybrid assay, whereas PpCCaMKb or empty vector (EV) controls did not. Left panel shows growth on control (-LT) media; right panel shows growth on test (-LTHA) media to screen for physical interactions. AD: activating-domain, BD: DNA-binding-domain.
e) Kinase assays using purified recombinant proteins showed that PpCCaMK but not PpCCaMKb exhibited kinase activity and that kinase activity is responsive to calcium (Ca2+) and CaM. AR: autoradiogram, CB: Coomassie Brilliant Blue stain.
f) Calmodulin-binding assays show that PpCCaMK or positive control (MtCCaMK) binds calmodulin, whereas PpCCaMKb or negative control from Chlamydomonas reinhardtii (CrCDPK) does not. PS: Ponceau S staining.
g) PpCCaMK rescues the arbuscular mycorrhizal defects of the *Medicago truncatula ccamk-1* mutant. Roots transformed with MtCCaMK or PpCCaMK developed intracellular hyphae, arbuscules, and vesicles after inoculation with Rhizophagus irregularis.
h) *PpCCaMK* rescues the nodulation defects of the Medicago truncatula ccamk-1 mutant. Roots transformed with *MtCCaMK* or *PpCCaMK* developed root nodules after inoculation with *Sinorhizobium meliloti.*

E-value ($E = 1 \times 10^{-21}$ or $E = 1 \times 10^{-22}$, respectively). Results of reciprocal BLAST searches of the predicted proteomes of Medicago or Lotus corroborated that *Pp3c23_22500V3* is the sole locus in the Physcomitrella genome encoding a homolog of IPD3, returning Medicago or Lotus IPD3, respectively, as the unambiguous top BLAST hit ($E < 1 \times 10^{-16}$, **Supplemental Figure 2A,B**). We cloned and confirmed the CDS of this putative Physcomitrella *IPD3* homolog, henceforth referred to as *PpIPD3*, from cDNA synthesized protonemal RNA. Using MUSCLE (Edgar, 2004), the PpIPD3 protein sequence was aligned to MtIPD3, LjIPD3, and a recently identified paralog of MtIPD3 from Medicago named IPD3L (Jin *et al.*, 2018). The multiple sequence alignment revealed that each of the functionally important regions described for Medicago or Lotus IPD3, including CCaMK-targeted phospho-motifs and a C-terminal coiled-coil domain, are also present in PpIPD3 (**Supplemental Figure 2C**). In particular, two sequence motifs surrounding

CCaMK-targeted phosphosites that are necessary and sufficient for activation of LjIPD3 are strongly conserved in PpIPD3 (**Figure 1C**), suggesting that CCaMK-mediated phosphoregulation of IPD3 may be conserved in Physcomitrella.

If identified CCaMK and IPD3 homologs constitute a functional signaling module in Physcomitrella, then the respective genes should be co-expressed in the same cell types. To determine and compare the relative expression patterns of *PpCCaMK*, *PpCCaMKb*, and *PpIPD3*, we mined their expression profiles from two Physcomitrella transcriptome atlas studies (Frank & Scanlon, 2015; Ortiz-Ramírez *et al.*, 2016). Data from both studies confirmed that *PpCCaMK*, *PpCCaMKb*, and *PpIPD3* show strongly overlapping expression patterns and that each is expressed in protonema, which we had expected based on our ability to clone each CDS from protonemal cDNA. Moreover, *PpCCaMK* showed greater transcript abundance than *PpCCaMKb* in all tested tissues (**Supplemental Figure 3**). Physical interaction between CCaMK and IPD3 has been demonstrated in multiple legume models (Messinese *et al.*, 2007; Yano *et al.*, 2008). We tested whether PpCCaMK or PpCCaMKb could interact with PpIPD3 in yeast two-hybrid (Y2H) assays. PpIPD3 was fused to the GAL4 split-transcription factor activation domain (AD) and tested in pairwise combination with PpCCaMK or PpCCaMKb, which were each fused to the GAL4 DNA-binding domain (BD). Co-transformation of PpIPD3-AD with PpCCaMK-BD confirmed robust growth on selective media, indicative of strong interaction. However, no growth or evidence for interaction was detected between PpIPD3-AD and PpCCaMKb-BD (**Figure 1D**). The lower expression levels of *PpCCaMKb* compared to *PpCCaMK*, along with the apparent inability of its gene product to bind PpIPD3 suggest that *PpCCaMKb* may encode a non-functional protein.

Legume CCaMKs have been characterized biochemically, and their autophosphorylation activity is known to be stimulated by elevated levels of calcium and inhibited by calmodulin (CaM) in the presence of high calcium levels (e.g., *Miller et al.*, 2013). Based on the conservation of the autoactivation loop shown in Figure 1B, we predicted that PpCCaMK and/or PpCCaMKb would show similar activities *in vitro*. To test if either Physcomitrella CCaMK homolog showed calcium/CaM-dependent protein kinase activity that could be by in Physcomitrella, we purified recombinant PpCCaMK and PpCCaMKb, along with positive and negative controls, and assayed autophosphorylation activity using radiolabeled adenosine triphosphate. Autophosphorylation of purified PpCCaMK was detectable and was enhanced in buffer containing free calcium ions, as compared to the EGTA control (**Figure 1E**). The autophosphorylation of PpCCaMK was suppressed in the presence of calcium and calmodulin, as described for Medicago CCaMK (Miller *et al.*, 2013). No detectable kinase activity was observed for PpCCaMKb under the same conditions. These results demonstrate that PpCCaMK has retained similar calcium- and calmodulin-regulated kinase activity and suggest that PpCCaMKb may not be enzymatically active. To further assess whether PpCCaMK and/or PpCCaMKb are *bona fide* CCaMKs, we tested whether either could bind calmodulin (CaM) *in vitro*. Biotin-labeled CaM was applied to immobilized recombinant PpCCaMK and PpCCaMKb and detected by chemiluminescence to check for evidence of binding (**Figure 1F**). PpCCaMK showed similar levels of CaM-binding activity to MtCCaMK, the positive control; however, PpCCaMKb showed nearly undetectable CaM-binding activity under the same conditions. Thus, consistent with gene expression and Y2H data, biochemical data supported a model wherein PpCCaMK but not PpCCaMKb comprises

a functional signaling module with PpIPD3. Given the presence of this symbiosis signaling module in Physcomitrella, co-culture of wild-type moss with the model mycorrhizal fungus *Rhizophagus irregularis* was attempted. Still, no evidence of intracellular infection was obtained after six months of co-culture (**Supplemental Figure 4**), which is consistent with the prevailing interpretation that Physcomitrella is not an AMF host plant.

Complementation of symbiosis-defective phenotypes of Medicago *ccamk* loss-of-function mutants by heterologous expression of *PpCCaMK*

To interrogate the functionality of PpCCaMK or PpCCaMKb *in vivo*, within the functional context of the symbiotic signaling pathway, we tested their ability to rescue the phenotype of Medicago *ccamk-1* mutants, which are defective for both nodulation and mycorrhization. 'Hairy root' genetic transformations mediated by *Agrobacterium rhizogenes* were used to introduce expression vectors containing the CDS from *MtCCaMK* (positive control), *PpCCaMK*, *PpCCaMKb*, or the empty vector (EV) negative control into roots of Medicago *ccamk-1* plants. A red fluorescent protein (RFP) visual marker was used to confirm that transformations were successful. To test for the ability to nodulate, transformed roots were inoculated with *Sinorhizobium meliloti* and co-cultured for two weeks. Whereas roots transformed with EV or PpCCaMKb did not form any nodules, roots transformed with PpCCaMK formed nodules similarly to roots transformed with MtCCaMK (**Figure 1G**). To test for AMF colonization, transformed roots were inoculated with *Rhizophagus irregularis* and grown in co-culture for six weeks. Trypan blue staining was used to visualize arbuscules and revealed that, similarly to the results of nodulation assays, roots transformed with vectors containing PpCCaMK or the

MtCCaMK formed arbuscules indicative of colonization. In contrast, roots transformed with PpCCaMKb or EV did not show any instances of arbuscule formation (**Figure 1H**). These data powerfully corroborate the conservation of key functional features of CCaMK between legumes and mosses and demonstrate that PpCCaMK can decode symbiotic signals when expressed heterologously in legumes.

Developmental reprogramming and brood cell formation associated with synthetic activation of CCaMK-IPD3 in Physcomitrella

Previous studies in legumes have shown that mutated forms of CCaMK or IPD3 are sufficient to cause striking gain-of-function phenotypes: the development of nodules or the prepenetration apparatus in the absence of rhizobial or mycorrhizal symbionts (Gleason *et al.*, 2006b; Tirichine *et al.*, 2006; Takeda *et al.*, 2012; Singh *et al.*, 2014). We introduced equivalent amino acid substitutions or deletions into PpCCaMK or PpIPD3 to engineer predicted gain-of-function variants and native or modified forms (hereafter referred to as PpCCaMK^{K}, PpCCaMK^{D}, and PpIPD3^{DD}) were transgenically expressed in Physcomitrella under the control of a maize ubiquitin (ZmUBI1) promoter (**Supplemental Table 2**). Expression of unmodified PpIPD3 in this manner did not yield any noticeable effects on the development or morphology of protonemata or gametophores, as these lines closely resembled wild-type Physcomitrella or empty vector controls (**Figure 2A,B, Supplemental Figure 5A**). Under the same conditions, lines expressing the predicted constitutively active variant, PpIPD3^{DD}, driven by the same promoter, developed branched chains of slowly growing, nearly isodiametric cells with dense chloroplasts and prominent cell wall thickenings (**Figure 2C**, **Supplemental Figure 5B,C**). These features

are diagnostic of brood cells, which are stress-resistant asexual propagules found in mosses (Correns, 1899; Duckett & Ligrone, 1992; Schnepf & Reinhard, 1997; Pressel & Duckett, 2010). Lines expressing PpIPD3^{DD} failed to form normal chloronema or caulonema and did not develop gametophores (**Supplemental Figure 5D**). Transformants expressing unmodified PpCCaMK displayed typical protonemal morphology and were able to develop gametophores, albeit with reduced frequency and size (**Figure 2D**). Importantly, brood cell formation was not observed in lines expressing unmodified PpCCaMK under standard growth conditions. Transformants expressing a phosphomimetic variant, PpCCaMK^{D}, developed mixed populations of phenotypically normal protonema and brood cells under standard growth conditions (**Figure 2E**, **Supplemental Figure 5E**). Gametophores were rarely observed and, if present, were stunted and malformed (**Supplemental Figure 5F**). Lines expressing PpCCaMK^{K} showed similar but more severe phenotypes, with frequent brood cell development and scarce instances of gametophore formation (**Figure 2F**). The developmental phenotypes that we observed in CCaMK and IPD3 gain-of-function lines, in particular, the constitutive development of brood cells, which generally only occurs in response to stress, led us to hypothesize that the Physcomitrella CCaMK-IPD3 module functions in developmental reprogramming to mediate resistance to or escape from stress conditions.

Elevated levels of ABA and *LATE EMBRYOGENESIS ABUNDANT* transcripts in Physcomitrella expressing synthetically activated forms of CCaMK or IPD3

The stress-associated phytohormone abscisic acid (ABA) has long been linked to the induction of brood cells (Schnepf & Reinhard, 1997; Bopp, 2000). As expected,

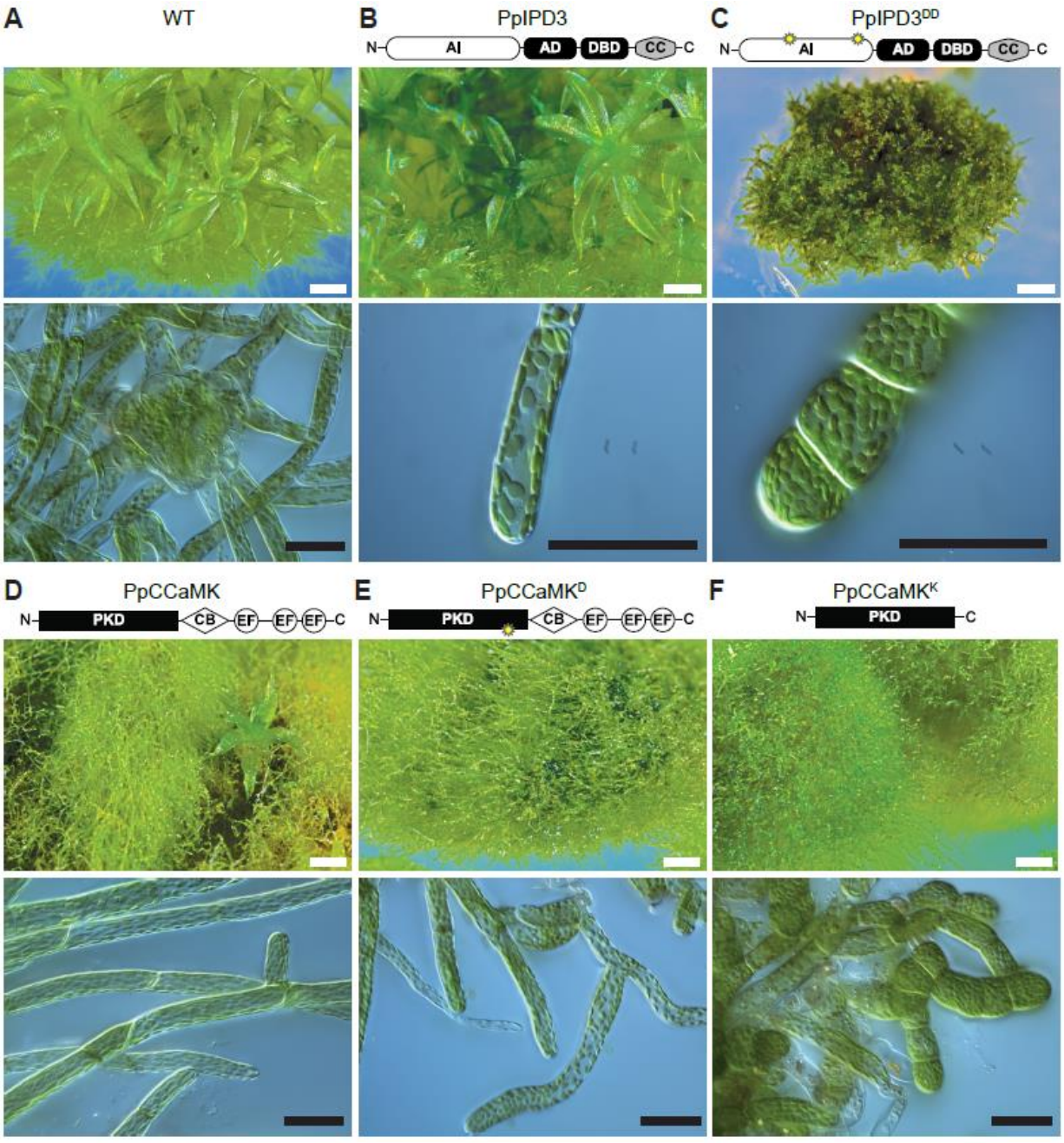

Figure 2: Ectopic development of brood cells in Physcomitrella expressing synthetically activated, engineered forms of *PpCCaMK* or *PpIPD3.*

a) Example of protonema and gametophores in wild-type Physcomitrella under standard in vitro growth conditions.
b) Lines transformed with unmodified *PpIPD3* driven by a *Zea mays UBIQUITIN1* (*ZmUBI1*) promoter did not display abnormal gametophore or protonemal morphology.
c) Lines transformed with a modified *PpIPD3* (*PpIPD3DD*) carrying two phosphomimetic substitutions in the autoinhibitory domain, driven by the same promoter, constitutively formed brood cells and failed to develop gametophores. (**legend continued on next page**)

d) Lines transformed with the native form of *PpCCaMK* developed excess protonema and fewer gametophores compared to WT controls, but protonemal morphology was not strongly affected.
e) Lines transformed with a modified *PpCCaMK* containing a phosphomimetic substitution in the regulatory domain (*PpCCaMKD*) typically did not develop any gametophores, and gametophores that did develop were stunted (see **Supplemental Figure 5B**). Brood cells were commonly found among protonema under unstressed conditions (see **Supplemental Figure 5B-C**)
f) Lines transformed with a modified *PpCCaMK* with the C-terminal regulatory region deleted (*PpCCaMKK*) constitutively developed brood cells under standard growth conditions. Constructs were driven by the same promoter. Samples were grown in BCDAT medium under the same conditions. Images are representatives of 4-week- (top) or 2-week-old (bottom) subcultured lines. White scale bars = 500 μm. Black scale bars = 50 μm.

treatment of wild-type protonema with ABA phenocopied the gain-of-function effects of PpCCaMK^{K} or PpIPD3^{DD} and stimulated the development of brood cells (**Figure 3A**). Quantitative RT-PCR was used to test whether stress-associated, ABA-inducible marker genes were likewise upregulated in CCaMK-IPD3 gain-of-function lines. We selected two previously described marker genes, *LEA3-1* and *LEA3-2*, which encode LATE EMBRYOGENESIS ABUNDANT (LEA) proteins (Shinde *et al.*, 2012, 2013) and confirmed that transcript levels were elevated in wild-type protonema treated with exogenously supplied ABA (**Figure 3B**). Initially characterized in seeds, LEA proteins serve as osmoprotective molecules and are thought to confer abiotic stress resistance in brood cells and thereby enhance their dispersal ability (**Figure 3C**). Transgenic lines that constitutively developed brood under standard growth conditions similarly accumulated elevated levels of *LEA3-1* and *LEA3-2* relative to wild type (**Figure 3D**). Transcript levels were more strongly elevated in gain-of-function lines compared to lines expressing unmodified PpCCaMK or PpIPD3. For example, expression of PpCCaMK^{K} was associated with significantly higher levels of *LEA3-1* transcript compared to lines expressing native PpCCaMK form the same promoter ($p < .05$). As observed for

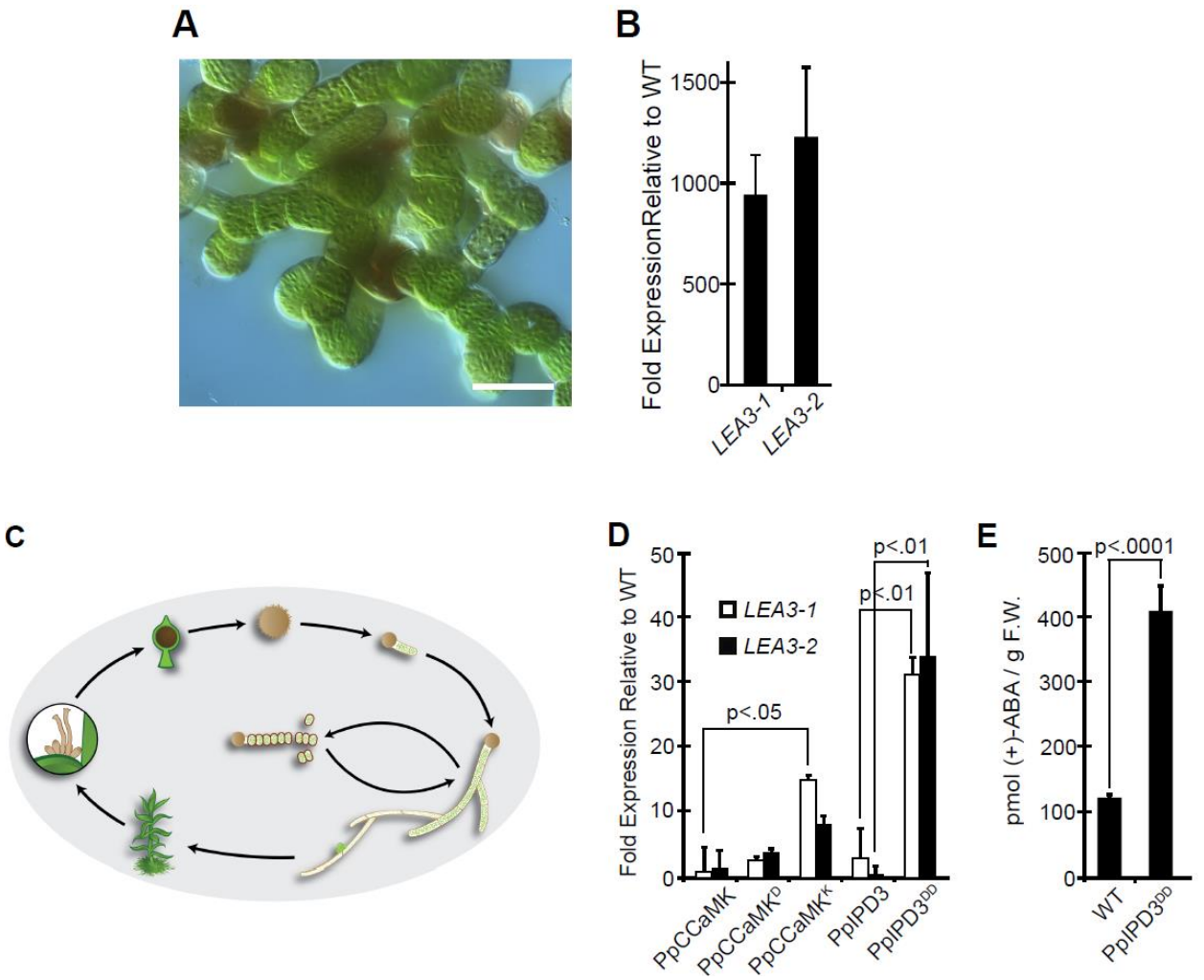

Figure 3: Phenotypic comparison of Physcomitrella CCaMK-IPD3 gain-of-function lines to ABA-treated WT protonema.

a) WT protonema developed brood cells under unstressed conditions in BCDAT growth medium within two weeks of treatment with 100 µM ABA. Scale bar = 50 µm.
b) Quantitative reverse transcription PCR (RT-qPCR) demonstrated that WT protonemal tissues treated with ABA contain elevated transcript levels for the ABA response marker genes *LEA3-1* and *LEA3-2*. Error bars indicate standard error of the mean (SEM) among treatments.
c) Illustrated life cycle of Physcomitrella. Spores (top) germinate and give rise to chloronema, which give rise to caulonema and gametophores. Gametangia develop in leaf axils of gametophores, and motile sperm swim through the environment to achieve fertilization. The mature zygote forms a spore capsule. From germination until fertilization, the moss is dependent on locally available water. Under stress conditions (e.g., drought), brood cells serve as stress-resistant 'vegetative spores' that fragment to facilitate dispersal. Brood cells germinate upon relief from stress; the life cycle resumes with development of chloronema. (**legend continued on next page**)

d) RT-qPCR analyses indicated that activation of the CCaMK-IPD3 signaling module is associated with elevated transcript levels for the ABA response marker genes *LEA3-1* and *LEA3-2*. Error bars indicate SEM among biological replicates.
Results were statistically evaluated using the Tukey honestly significant difference (HSD) test. The p-values that yielded statistical significance below a threshold of .05 are annotated.
e) Enzyme-linked immunosorbent assays (ELISAs) revealed substantially elevated levels of (+)-ABA in protonemal tissues of lines expressing *PpIPD3^{DD}* compared to wild-type controls under standard in vitro growth conditions. A minimum of two independently transformed lines were tested. Error bars indicate SEM among three biological replicates. The p-value was obtained using a two-sample Student's t-test

developmental phenotypes, expression of PpIPD3^{DD} had the most substantial effect on *LEA* transcript abundance, and accumulation of *LEA3-1* and *LEA3-2* transcripts was significantly higher in lines expressing PpIPD3^{DD} compared to lines expressing PpIPD3 ($p < .01$), providing further evidence for a functional link between activation of the Physcomitrella CCaMK-IPD3 module and ABA signaling.

The observed phenotypic similarities between ABA-treated wild-type Physcomitrella and PpCCaMK-IPD3 gain-of-function lines may, in theory, be caused by an increase in ABA accumulation, an increase in ABA sensitivity, activation of a different pathway with similar effects, or a combination of these scenarios. To further investigate the mechanism whereby the CCaMK-IPD3 module elicited these responses, we quantified the levels of ABA in tissues overexpressing IPD3^{DD} compared to wild type by ELISA (enzyme-linked immunosorbent assays). Three independently transformed lines were analyzed, and all three IPD3^{DD} lines contained significantly higher levels of ABA compared to wild type (**Figure 3E**), suggesting that the ABA-like responses we observed are likely due, at least in part, to increased ABA accumulation.

Brood cell formation in Physcomitrella *ccamk* and *ipd3* loss-of-function mutants

To investigate if the CCaMK-IPD3 module is required for the development of brood cells, we assayed responses to stress treatments in deletion lines lacking either the *CCaMK* or *IPD3* genomic locus. Each locus was deleted by homologous recombination with antibiotic selective markers. Disruption of the respective locus was confirmed by PCR genotyping using genomic DNA and by RT-PCR (**Supplemental Figure 6**). These lines displayed stereotypical protonemal and gametophore morphology when grown under standard conditions (**Figure 4A, B**). When treated with ABA or hyperosmotic media supplemented with mannitol, multiple independently generated *ccamk* and *ipd3* knockout lines responded similarly to wild-type controls by developing brood cells, which do not develop in wild-type moss under standard laboratory growth conditions (**Figure 4B**). These results suggest that, while sufficient to stimulate ABA accumulation and brood cell formation, the CCaMK-IPD3 module is not required for brood cell development in response to ABA or osmotic stress treatments. We did not observe any noticeable differences in levels of brood cell formation between mutant and wild-type on both treatments, indicating that genetic perturbation of the CCaMK-IPD3 module does not substantially alter the sensitivity of Physcomitrella to ABA. These data imply functional redundancy in stress-induced developmental programming. Collectively, our results are consistent with the hypothesis that the CCaMK-IPD3 module operates in the context of a broader signaling network that mediates stress-responsive developmental reprogramming in Physcomitrella (**Figure 4C**).

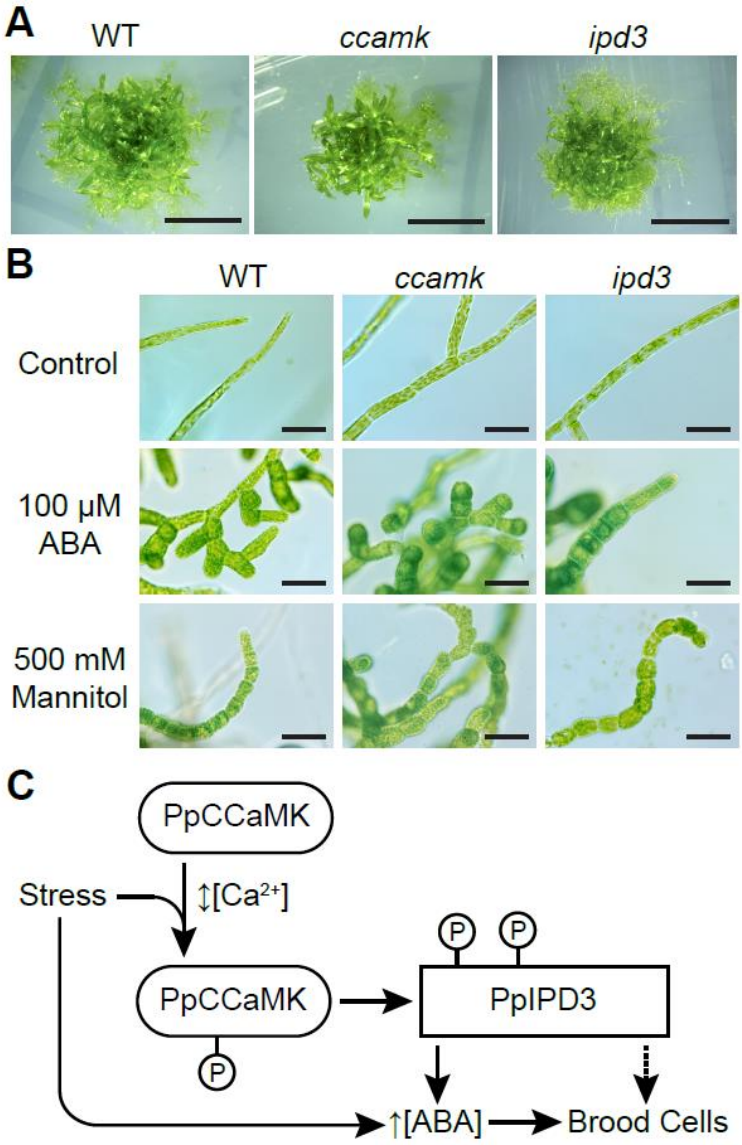

Figure 4: Neither *CCaMK* nor *IPD3* are required for brood cell formation under ABA treatment or osmotic stress conditions.

a) Physcomitrella *ccamk* and *ipd3* deletion mutants did not show any obvious phenotypic aberrations relative to WT under standard in vitro growth conditions in BCDAT medium. Scale bar = 500 mm

b) Physcomitrella *ccamk* and *ipd3* deletion mutants were able to develop brood cells when 100 µM ABA was added to BCDAT medium under standard growth conditions or when hyperosmotic stress was applied by addition of 500 mM mannitol to the growth medium. Treatments were performed for two weeks before images were taken. Two independently generated deletion mutant lines each were tested for *IPD3* and *CCaMK*. Scale bar = 50 µm.

c) Diagram showing hypothetical model for PpCCaMK-IPD3 function during stress signaling in relation to ABA accumulation and brood cell formation. In this model, stress conditions provoke changes in nucleocytoplasmic Ca^{2+} levels, leading to activation of PpCCaMK. Trans-phosphorylation of PpIPD3 renders it active and leads to elevated levels of ABA and development of brood cells. The ability of *ccamk* and *ipd3* deletion lines to develop brood cells in response to tested stress treatments indicates that there are likely other pathways that trigger stress-induced ABA accumulation. Dotted line indicates uncertainty whether or not PpIPD3 acts exclusively through ABA signaling to promote brood cell development.

2.4 - Discussion

Many of the critical components of the symbiosis pathway were present in the algal ancestors of land plants, indicating that they have been vertically inherited across land plants (Delaux et al., 2015). Across evolutionary time, spanning from the divergence of bryophytes to the emergence of angiosperms, AMF-like interactions have remained morphologically similar (Remy *et al.*, 1994b; Strullu-Derrien *et al.*, 2014). In light of plant comparative genomics of AMF-host versus non-host lineages, the symbiosis pathway in the earliest land plants likely contributed to recognition and intracellular infection of AMF, as the presence/absence of the symbiosis pathway is strongly correlated with host/non-host status, respectively (Delaux *et al.*, 2014a; Garcia *et al.*, 2015; Kamel *et al.*, 2016; Delaux, 2017). Among embryophytes, the moss clade is a striking exception to this genomic signature. To date, there has been no demonstration of the mutualistic transfer of nutrients between mosses and AMF. On the contrary, endophytic fungal interactions described in mosses have appeared to be restricted to dead or senescing tissues (Pressel *et al.*, 2010). This peculiarity piqued our interest in the conserved components of the common symbiosis pathway in mosses.

In the present study, we investigated the functional reason for the retention of the CCaMK-IPD3 signaling module in non-mycorrhizal mosses, which stands in stark contrast to multiple independent losses of these genes in non-mycorrhizal angiosperm and liverwort lineages. Biochemical and mutant-rescue assays demonstrate that the biochemical activities of CCaMK and IPD3 are conserved broadly throughout land plants, which suggests that CCaMK may decode similar oscillatory calcium signals in bryophytes. We used a gain-of-function strategy in Physcomitrella to shed light on the physiological

consequences of CCaMK-IPD3 activation. The developmental phenotypes observed in Physcomitrella cells expressing CCaMK and IPD3 carrying predicted gain-of-function mutations imply a functional link between the CCaMK-IPD3 module and ABA signaling in mosses. The most striking finding in this study is the developmental phenotype of $IPD3^{DD}$-expressing lines: $IPD3^{DD}$ transgenics displayed prolific, nearly constitutive formation of brood cells largely to the exclusion of other cell types. The effect does not appear to be attributable to transcript or protein abundance, as controls transformed with the same vectors differing only by two codon changes to introduce putatively phosphomimetic substitutions. The observation that gain-of-function lines expressing modified forms of CCaMK showed a less severe phenotype than lines expressing modified may simply reflect a signaling bottleneck of natively expressed IPD3 upon the activities of expressed CCaMK. Comparative genomics across green plants have shown that core ABA signaling components are conserved in bryophytes (Wang *et al.*, 2015). Although ABA biosynthesis and downstream signal transduction have been studied in the context of Physcomitrella protonemal development (Schnepf & Reinhard, 1997; Shinde *et al.*, 2012; Komatsu *et al.*, 2013; Yotsui *et al.*, 2013; Takezawa *et al.*, 2015; Vesty *et al.*, 2016), our data provide a first link between CCaMK-IPD3 and ABA signaling in Physcomitrella.

We propose a model wherein calcium-dependent activation of CCaMK and trans-phosphorylation of IPD3 in Physcomitrella leads to ABA accumulation and brood cell formation. The rescue of Medicago *ccamk-1* mutants by *PpCCaMK* seemingly suggests that PpCCaMK may be activated by similar oscillatory calcium signals, as seen in legumes in response to symbionts. Nonetheless, nuclear calcium oscillations and potential elicitors have not been described in Physcomitrella. Hyperosmotic stress has

been shown to elicit a pronounced transient elevation of cytosolic calcium levels. However, this response was neither found to be oscillatory nor predominantly restricted to the nuclear region (Kleist *et al.*, 2017). Given these discrepancies and the abundance of predicted calcium-binding proteins encoded in the Physcomitrella genome, further work is needed to identify factors involved in decoding osmotic stress-induced cytosolic calcium transients. The regular elicitation and development of brood cells in Physcomitrella *ccamk* or *ipd3* deletion lines in response to ABA or osmotic stress implies there are other signaling components capable of triggering brood cell formation in response to abiotic stressors. In addition to identifying putatively functionally redundant signaling components, other interesting topics for future work include whether parallel pathways are calcium-dependent or -independent and whether ABA hyperaccumulation, which we observed, is required for the developmental phenotypes of CCaMK-IPD3 gain-of-function lines.

The established physiological function of brood cells is to serve as stress-resistant asexual propagules that break away from parent plants and enable mosses to escape osmotic stress and dehydration. For this reason, they have also been referred to as ‘vegetative spores.’ The phenotypes of Physcomitrella CCaMK and IPD3 gain-of-function lines suggest that these components may also be linked to osmotic stress and dehydration responses. Because osmotic stress and dehydration are closely related to oxidative stress, it is worth noting that CCaMK has been associated with oxidative stress responses in other plants. CCaMK expression is induced by ABA or oxidative stress in rice; CCaMK was also required for ABA-mediated antioxidant responses (Shi *et al.*, 2012, 2014). Similarly, CCaMK has been reported to be activated by nitric oxide and required

for ABA-mediated antioxidant activity in maize (Ma *et al.*, 2012; Yan *et al.*, 2015). In wheat (*Triticum aestivum*), CCaMK expression is modulated by ABA and osmotic stress, likely through the activity of numerous predicted ABA-response elements in its promoter region (Yang *et al.*, 2011). In light of these observations, the CCaMK-IPD3 may play a role in abiotic stress acclimation not only in Physcomitrella but also in other plants. This possibility may explain its retention in non-mycorrhizal mosses.

The cell wall thickenings, lipid reserves, and enhanced dispersal ability of brood cells could conceivably be useful in evading pathogenesis, although this idea is presently unsubstantiated. Fungal pathogens, as well as oomycetes, have been shown to induce reactive oxygen species (ROS) production, cell-wall depositions (including callose depositions mediated in part through ABA signaling), and altered fatty acid metabolism (Oliver *et al.*, 2009; Ponce de León, 2011; de León *et al.*, 2015). There are also mechanistic links between pathogen perception and the symbiosis pathway in angiosperms. In rice, chitin-receptor *cerk1* mutants were impaired in both mycorrhizal and blast fungus infections (Miyata *et al.*, 2014), and CERK1 is conserved as a chitin-induced immunity signaling receptor in Physcomitrella, possibly hinting at a further link between the common symbiosis pathway and immunity signaling (Bressendorff *et al.*, 2016). These observations may warrant further investigation into the possibility that brood cells, as well as the CCaMK-IPD3 pathway, could also serve a heretofore unnoticed function in moss acclimation to biotic stresses.

In summary, activation of CCaMK or its downstream target transcriptional activator IPD3 in Physcomitrella induces ABA signaling and constitutive formation of brood cells, which serve as asexual propagules that enable escape from abiotic stresses. Our

observations are consistent with a model wherein PpCCaMK-IPD3 functions in the decoding of stress-associated calcium signatures and developmental reprogramming. Further work is needed to identify upstream elicitors that lead to CCaMK activation and direct transcriptional targets of IPD3 in Physcomitrella. Functional inquiries into CCaMK and IPD3 homologs in other early-diverging embryophytes such as the mycorrhizal host plant *Marchantia paleacea* and charophyte green algae are expected to complement these efforts and provide a fuller perspective of the evolutionary establishment of the molecular mechanisms underpinning the plant-microbe common symbiosis pathway.

2.5 - Materials and Methods

Bioinformatic analyses. To identify CCaMK and IPD3 homologs encoded in the Physcomitrella genome, the full-length protein sequences of CCaMK and IPD3 from *Lotus japonicus* (LjCCaMK, UniProt: A0AAR7, loci: Lj3g3v1739280; LjIPD3, UniProt: A9XMT3, locus ID: Lj2g3v1549600) and *Medicago truncatula* (MtCCaMK, UniProt: Q6RET7, locus ID: Medtr8g043970; MtIPD3, UniProt: A7TUE1, locus ID: Medtr5g026850) were retrieved from UniProt and used as BLASTp queries against the predicted *Physcomitrella patens* version 3.3 predicted proteome (Lang *et al.*, 2018) using Phytozome 12 (https://phytozome.jgi.doe.gov/pz/portal.html). The BLOSUM62 scoring matrix was used. E-value thresholds were set to -1 for CCaMK searches and $1x10^4$ for IPD3 searches. Other parameters followed default settings. Data were downloaded and analyzed from December 11 to 17, 2019. The top five hits were used as queries for reciprocal BLASTp searches against either the *Lotus japonicus* MG20 v3.0 protein database (https://lotus.au.dk/blast/#database-protein) using default settings, or the *Medicago*

truncatula Mt4.0 predicted proteome, accessed through Phytozome 12 and performed using default settings (Mun *et al.*, 2016; Tang *et al.*, 2014). For each reciprocal BLASTp search, the top hit was displayed. Multiple sequence alignments were made using MUSCLE (Edgar, 2004) version 3.8.425 plugin for Geneious Prime under default settings and were annotated manually or using the InterProScan feature in Geneious Prime (Biomatters). Accession numbers for putative orthologs referred to in Figure 1A can be found in **Supplemental Table 1**.

***Biological material and growth conditions*.** For moss growth and phenotypic assays, *Physcomitrella patens*, ecotype Gransden 2004, was used (Rensing *et al.*, 2008). Tissue was grown on BCD medium supplemented with 5 mM diammonium tartrate (BCDAT medium), pH 6.0, supplemented with 0.8% high gel strength agar (Sigma) or 1% Phytoblend (Caisson Labs). The medium was supplemented with (+/-)-abscisic acid (Sigma) or mannitol, as indicated. Moss cultures were grown in a growth chamber at 22°C under 50-100 µmol m^{-2} s^{-1} light with a 16-hour photoperiod. *Medicago truncatula* mutant-rescue assays were performed as previously described (Delaux *et al.*, 2015).

Co-culture of Physcomitrella and Rhizophagus irregularis. Three-week-old gametophores were collected from cellophane-overlaid Knop agar plates. Gametophores were transferred to half-strength Knop semi-liquid medium (0.15% Phytagel) in 24-well plates. In each well, 2 ml of semi-liquid Knop medium was poured in which 50 spores of *R. irregularis* IRBV'95 were added. One gametophore was placed gently over the medium such that the rhizoids were immersed within the semi-liquid medium. This experimental setup was incubated at 25°C with a light intensity of 55 µmol m^{-2} s^{-1}, with a 16hr photoperiod, for six months. Starting from one month after co-culturing, AMF colonization

was analyzed every week for up to six months using brightfield or confocal microscopy. Trypan blue staining of *R. irregularis* was performed as described (Koske & Gemma, 1989). For confocal microscopy, the fungal hyphae were stained using Wheat Germ Agglutinin Alexa Fluor® 488 (Excitation: 488 nm; Emission: 520 nm), and the rhizoids and the gametophores were observed by chlorophyll autofluorescence (Excitation: 488 nm, Emission: 670 nm).

Plant transformations. Biolistic transformation of Physcomitrella protonema was carried out as previously described (Kleist *et al.*, 2017). Antibiotic selection with Hygromycin B (Thermo Fisher) was performed at 50 µg/mL concentration, and transformants were verified by RFP signal. Protoplasts were obtained from one-week-old protonemal cultures using 2% Driselase (Sigma, D8037) in an 8% mannitol solution for cell wall digestion. Protoplast transformations to produce *ccamk* or *ipd3* deletion mutants were performed as previously with minor modifications (Hohe *et al.*, 2004). Briefly, an 8% mannitol solution was made using 1/10 BCDAT medium set to pH 5.8 to improve protoplast survival. Antibiotic selection was performed using 50 µg/mL Hygromycin B or 40 µg/mL G418. For *ipd3* deletion lines, stable transformants were identified by RFP signal using a Zeiss Lumar epifluorescence stereoscope. *Medicago truncatula* root transformations were carried out using *Agrobacterium rhizogenes* strain MSU440, harboring the pK7FWG2 binary vector as previously described (Delaux *et al.*, 2015).

Molecular cloning and plasmid construction. DNA and RNA were extracted from protonemal tissue following previously described protocols (Kleist *et al.*, 2014). The Quantitect (Qiagen) reverse transcription kit was used to synthesize cDNA for cloning and qPCR. PCR reactions were performed using Phusion (Thermo Fisher) or Primestar GXL

DNA Polymerase (Clontech). The sequences of oligonucleotide primers used in this study are given in **Supplemental Table 3**. Single- and multi-site Gateway (Thermo Fisher) cloning reactions were performed per manufacturer's recommendations. The coding sequences (CDSs) of *PpCCaMK, PpCCaMKb,* and *PpIPD3* were cloned into pDONR/Zeo and modified, as described, by site-directed mutagenesis using whole-plasmid amplification with anticomplementary primers followed by digestion with FastDigest *Dpn*I (Thermo Fisher). Native or modified CDSs were subcloned into pANIC5A for plant expression (Mann *et al.*, 2012), pVP16 for N-terminal fusion to maltose-binding protein (MBP), pK7FWG2 for expression in *Medicago truncatula* roots, and pGBT9-BS-GW (*PpCCaMK* and *PpCCaMKb*) or pGAD-GH-GW (*PpIPD3*) for yeast two-hybrid assays. Multisite Gateway recombination was used to generate the deletion construct for *IPD3*. Approximately one kilobase regions located at the N-terminal or C-terminal end of the gene were cloned into pENTRY attB1-attB4 or attB3-attB2 vectors, respectively. *Porites* sp. red fluorescent protein (RFP), driven by a *Panicum virgatum UBIQUITIN* promoter (Mann *et al.*, 2012), was cloned into a pENTRY attB4r-attB5r vector. An antibiotic resistance construct containing the *NPTII* gene driven by a cauliflower mosaic virus 35S promoter was cloned into a pENTRY attB5-attB3r vector. The four fragments were assembled by LR reaction using LR clonase plus enzyme (Thermo Fisher) using a Gateway-compatible destination vector with attL1 and attL2 sites. After sequence confirmation, the linear deletion construct was amplified by PCR using Primestar GXL DNA Polymerase (Takara). The PCR product was purified and concentrated to 1 µg/µL using the PureLink PCR purification kit (Invitrogen).

Yeast two-hybrid assays. The coding sequences of *PpCCaMK*, *PpCCaMKb*, and *PpIPD3* were subcloned into pGAD-GH-GW or pGBT9-GW for yeast two-hybrid analysis. Vectors were co-transformed into *Saccharomyces cerevisiae* strain AH109 using the lithium acetate method and interactions were assayed by growth on synthetic defined media lacking leucine and tryptophan (-LT) or lacking leucine, tryptophan, histidine, and adenine (-LTHA, MP Biomedicals) at 30° C, as previously described (Kleist *et al.*, 2014).

Protein expression and purification. Maltose-binding protein (MBP) fused to PpCCaMK, PpCCaMKb, and CrCDPK1 fusion constructs were transformed into *E. coli* strain Rosetta2, whereas the MBP-MtCCaMK fusion construct was transformed into *E. coli* strain B834-pRARE2 for protein expression. Protein expression and purification were carried out as previously described (Delaux *et al.*, 2015a).

Kinase activity and calmodulin-binding assays. Kinase assays were performed as previously described with slight modifications (Miller *et al.*, 2013). 1 µg of MBP-PpCCaMK or MBP-PpCCaMKb protein was incubated in ATP-containing buffer (50 mM HEPES, pH 7.5, 1 mM DTT, 200 µM ATP, 5 µCi [g-^{32}P]ATP, and 10 mM $MgCl_2$). 20 µL reactions were incubated at 30°C for five minutes with 0.2 mM $CaCl_2$ (+Ca^{2+}) or 2.5 mM EGTA (+EGTA). Where stated, 0.5 µM bovine Calmodulin (Millipore) was added. Reactions were terminated by incubation at 95°C for 5 min. Subsequently, samples were separated on 10% SDS-PAGE gels prior to imaging. Radioactivity was quantified by Molecular Dynamics Storm® 860 phosphorimager (Sunnyvale, CA) and data were analyzed using the Molecular Dynamics ImageQuant® software. Calmodulin-binding assays using recombinant CCaMKs were performed similarly to previous reports (e.g., Routray *et al.*, 2013) with slight modifications. Bovine brain calmodulin (EMD Millipore)

was biotinylated using the ECL Protein Biotinylation Module (GE Healthcare Life Sciences). Proteins were immobilized on a polyvinylidene difluoride (PVDF) membrane followed by incubation in Tris-buffered saline, 0.1% Tween 20 (TBS-T) supplemented with 1 mM $CaCl_2$ and 3 µg/mL biotinylated calmodulin for one hour. Subsequently, the membrane was incubated in TBS-T supplemented with 1 : 6,000 streptavidin-horseradish peroxidase conjugate (GE Healthcare Life Sciences) for 1 hour. Bound calmodulin was detected using ECL Prime (GE Healthcare Life Sciences).

Extraction and quantification of ABA. ABA extraction and quantitation was done was previously described with slight modifications (Ondzighi-Assoume *et al.*, 2016). For each sample, 100 mg of starting tissue was used. Tissue was lyophilized, ground 3 mm glass beads, and then ABA extracted using the referenced methanol-based method. Resulting aqueous ABA extracts were then quantitated using the Phytodetek ABA ELISA assay (Agdia).

Quantitative RT-PCR. Total mRNA was extracted from abscisic acid (ABA)-treated and untreated wild-type samples, as well as from gain-of-function lines. 3 µg RNA samples were reverse transcribed using the Quantitect Reverse Transcription kit (Qiagen), per manufacturer's recommendations, and the resulting 60 µL cDNA samples were diluted by the addition of 90 µL nuclease-free water. The iTaq Universal SYBR Green Supermix (Bio-Rad) was used for qPCR reactions following the manufacturer's recommendations, and reactions were run on a DNA Engine Opticon™ continuous fluorescence detector. Ubiquitin-conjugating enzyme E2 (Pp1s34_302V6) was used throughout as a reference gene (Le Bail *et al.*, 2013). After baseline subtraction, results were analyzed using the ΔΔC(t) method, wherein fold change is taken as 2^[(reference

gene – query gene)$_{\text{transgenic/treated line}}$ – (reference gene – query gene)$_{\text{wildtype/untreated line}}$]. For each line, 3 to 4 biological replicates were used, with a minimum of 2 technical replicates (i.e., each qPCR run was performed multiple times). Statistical tests are described below.

Statistical analyses. For quantitative measurements of ABA content, 7 biological replicates were analyzed for wild-type and 3 biological replicates of three independently transformed lines were analyzed for IPD3^{DD}. Every biological replicate was tested in triplicate for the ABA ELISA. Data were analyzed and tested using a Student's T-Test using the R statistical programming language (R Core Team, 2014). For RT-qPCR analyses, samples were compared via one-way ANOVA analysis using R (R Core Team, 2014). Levene's Test confirmed equality of variance for both sets of data (Levene, 1960). The Tukey honest significant difference (HSD) was used for posthoc analysis of ANOVA results (Tukey, 1949), and the p-values that were reported were calculated using this method.

Microscopy, photography, and image processing. Differential interference contrast (DIC) micrographs were acquired using a Zeiss AxioImager M1 microscope with a 40X, 1.4 numerical aperture (NA) or 100X, 1.3 NA objective and a QImaging 5 MPix MicroPublisher color camera or an Olympus BX60 microscope using a 20X, 0.5 NA and an Olympus DP 72 color camera. Macrophotography images were acquired using a Canon EOS 6D 20.2 Megapixel CMOS Digital SLR camera in conjunction equipped with a Canon MP-E 65 mm f/2.8 1-5x macro lens and Canon MT-24EX macro twin-light flash. Manually acquired z-stacks were focus-stacked using Helicon Focus (HeliconSoft).

Physcomitrella stress assays. Freshly blended protonema from either wild-type, *ccamk-1* or *ipd3-1* lines were plated onto cellophane-overlaid BCDAT medium plates,

supplemented with ABA or mannitol, at concentrations indicated. Stress treatments were grown under standard temperature and photoperiod conditions unless stated otherwise.

Author Contributions

T.J.K., A.B., R.-J.T., M.L.C., P.G.L., S.L., and J.-M.A. designed the research. T.J.K., A.B., A.M.P., M.V., F.A., and H.N.C. performed the experiments. T.J.K., A.B., T.B.I., M.V., R.-J.T., M.L.C., S.L., and J.-M.A analyzed the data. T.J.K, A.B., and J.-M.A. wrote the paper with assistance and input from all authors.

2.6 - Acknowledgements

The authors would like to thank Tony Chour, Min Su Park, Mitch Wanta, and Cali Lunowa for technical assistance and Prof. Brett Mishler (University of California, Berkeley) for helpful discussions. Microscopy was performed at the Newcomb Imaging Center, Department of Botany, University of Wisconsin – Madison or at the Biological Imaging Facility at the University of California, Berkeley. This work was supported in part by grants from the NSF to S.L. (grant # MCB-0723931 and # ISO-1339239). T.J.K. was funded in part by the NSF Graduate Research Fellowship Program (grant # DGE-1106400). This work was supported in part by the Vilas Faculty Young/Mid-Career Award to J.M.A. AB was funded through an NIH Training Grant to the Laboratory of Genetics (grant # 5T32GM007133-40) and by the NSF Graduate Research Fellowship Program (grant # DGE-1256259).

2.7 - Supplementary Figures

A

			Reciprocal		
Locus ID	**E-Value**	**Description**	**Locus ID**	**Description**	**E-Value**
Pp3c21_15330V3	0	CCaMK	Medtr8g043970	CCaMK / DMI3	0
Pp3c19_20580V3	2×10^{-169}	CCaMKb	Medtr8g043970	CCaMK / DMI3	8×10^{-159}
Pp3c4_7390V3	3×10^{-71}	CDPK	Medtr5g089320	CDPK17-Like	0
Pp3c8_690V3	1×10^{-70}	CDPK	Medtr5g089320	CDPK17-Like	0
Pp3c3_37890V3	9×10^{-69}	MAPK-activated CDPK	Medtr8g099095	CDPK3-Like	0

B

			Reciprocal		
Locus ID	**E-Value**	**Description**	**Locus ID**	**Description**	**E-Value**
Pp3c21_15330V3	0	CCaMK	Lj3g3v1739280	CCaMK	0
Pp3c19_20580V3	6×10^{-171}	CCaMKb	Lj3g3v1739280	CCaMK	6×10^{-176}
Pp3c8_690V3	1×10^{-69}	CDPK	Lj4g3v3002290	CDPK3-Like	0
Pp3c9_21410V3	2×10^{-69}	CDPK	Lj4g3v3002290	CDPK3-Like	0
Pp3c4_7390V3	5×10^{-69}	CDPK	Lj4g3v3002290	CDPK3-Like	0

C

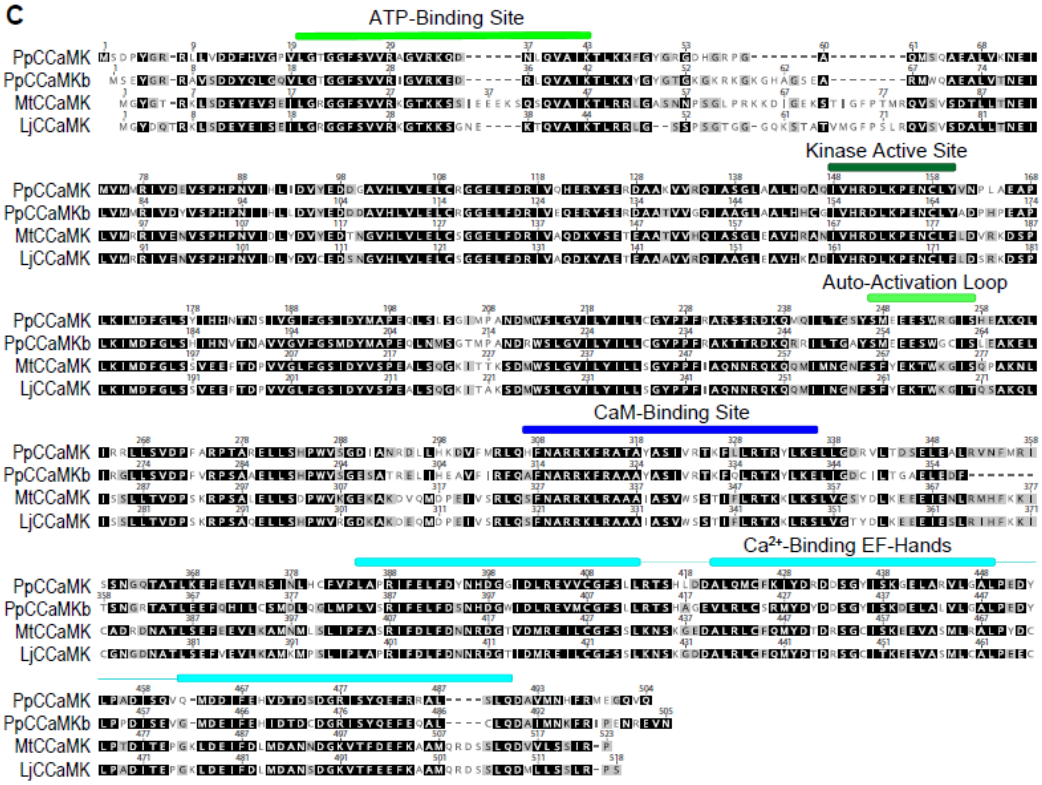

Supplemental Figure 1: Bioinformatic analysis of Physcomitrella CCaMK/CCaMKb compared to characterized homologs.
a) Results of BLASTp search of Physcomitrella predicted proteome using Medicago CCaMK/DMI3 as query. Genomic locus ID, expectation (E)-values, and gene descriptions are provided. (Shaded) Reciprocal BLASTp with E-values for each reciprocal best hit against the Medicago predicted proteome. CDPK: Ca2+-dependent protein kinase, MAPK: Mitogen-activated PK.
b) Results of BLASTp search of Physcomitrella predicted proteome using Lotus CCaMK as query, and reciprocal BLAST for each against the Lotus predicted proteome. Table format is identical to A.
c) Alignment of CCaMK protein sequences made using MUSCLE. Functional predictions are annotated above the alignment. Detailed descriptions are provided in Materials and Methods.

A

			Reciprocal		
Locus ID	**E-Value**	**Description**	**Locus ID**	**Description**	**E-Value**
Pp3c23_22500V3	1 x 10^{-21}	IPD3	Medtr5g026850	IPD3	1 x 10^{-16}
Pp3c24_11410V3	2	Galactan 1,3-β-Galactosidase	Medtr5g015460	Glycosyl Hydrolase	8 x 10^{-153}
Pp3c16_24380V3	3	CCHC-Type Zinc Finger Protein	Medtr8g468600	CCHC-Type Zinc Finger Protein	2 x 10^{-59}
Pp3c1_2420V3	20	Xyloglucan Endotransglycosylase	Medtr4g045853	Xyloglucan Endotransglycosylase	4 x 10^{-55}
Pp3c25_860V3	30	Alkaline Ceramidase-Related	Medtr1g096320	Alkaline Ceramidase-Related	2 x 10^{-170}

B

			Reciprocal		
Locus ID	**E-Value**	**Description**	**Locus ID**	**Description**	**E-Value**
Pp3c23_22500V3	1 x 10^{-22}	IPD3	Lj2g3v1549600	IPD3 / CYCLOPS	5 x 10^{-24}
Pp3c5_28790V3	4	Clathrin Assembly Protein	Lj4g3v1881980	ENTH/ANTH/VHS Family	3 x 10^{-6}
Pp3c24_11410V3	7	Galactan 1,3-β-Galactosidase	Lj2g3v1968430	Glycosyl Hydrolase	9 x 10^{-153}
Pp3c22_12090V3	10	Protein Kinase Superfamily	Lj4g3v0462390	Protein Kinase Superfamily	6 x 10^{-113}
Pp3c14_4840V3	10	Small Acidic Protein Family	Lj0g3v0243989	Arg/Ser-Rich Coiled Coil Protein	5 x 10^{-34}

C

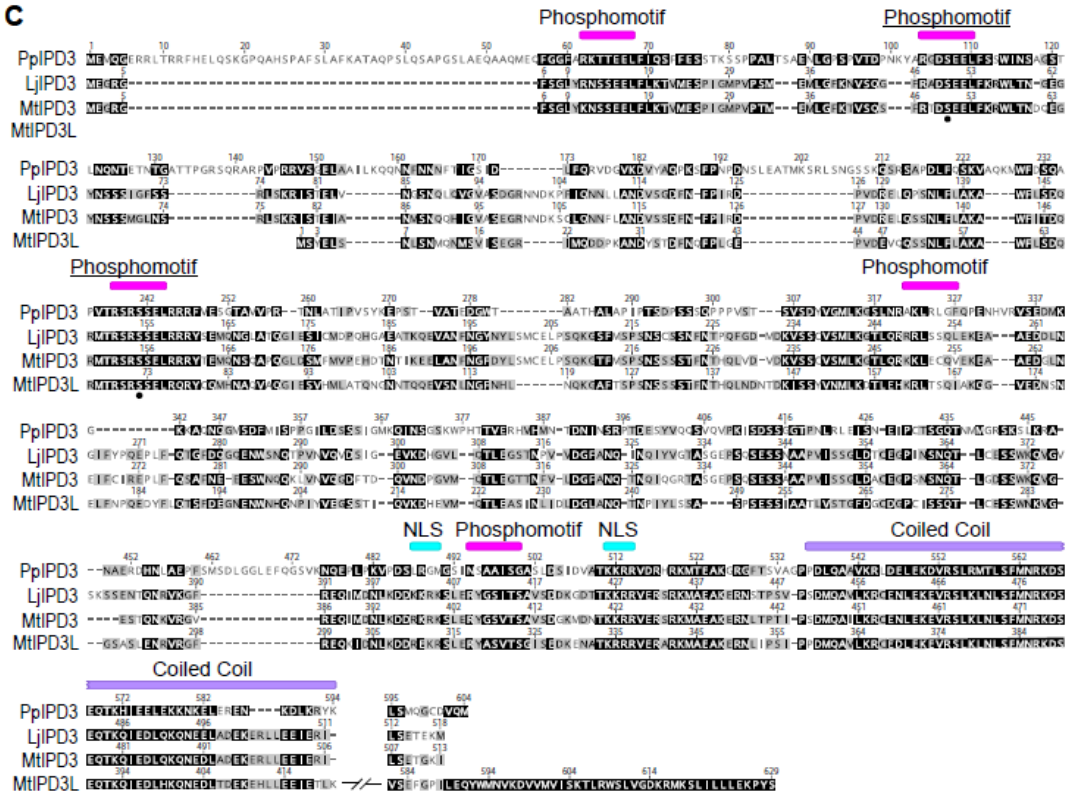

Supplemental Figure 2: Bioinformatic analysis of Physcomitrella IPD3 compared to characterized homologs.

a) Results of BLASTp search of Physcomitrella predicted proteome using Medicago IPD3 as query. Genomic locus ID, expectation (E)-values, and gene descriptions are provided. (Shaded) Reciprocal BLASTp with E-values for each reciprocal best hit against the Medicago predicted proteome.

b) Results of BLASTp search of Physcomitrella predicted proteome using Lotus IPD3/CYCLOPS as query, and reciprocal BLAST for each against the Lotus predicted proteome. Table format is identical to A.

c) Alignment of CCaMK protein sequences made using MUSCLE. Functional predictions are annotated above the alignment. Underlined phosphomotifs are critical for regulation of LjIPD3/CYCLOPS. NLS: Nuclear localization sequence. Detailed descriptions are provided in Materials and Methods.

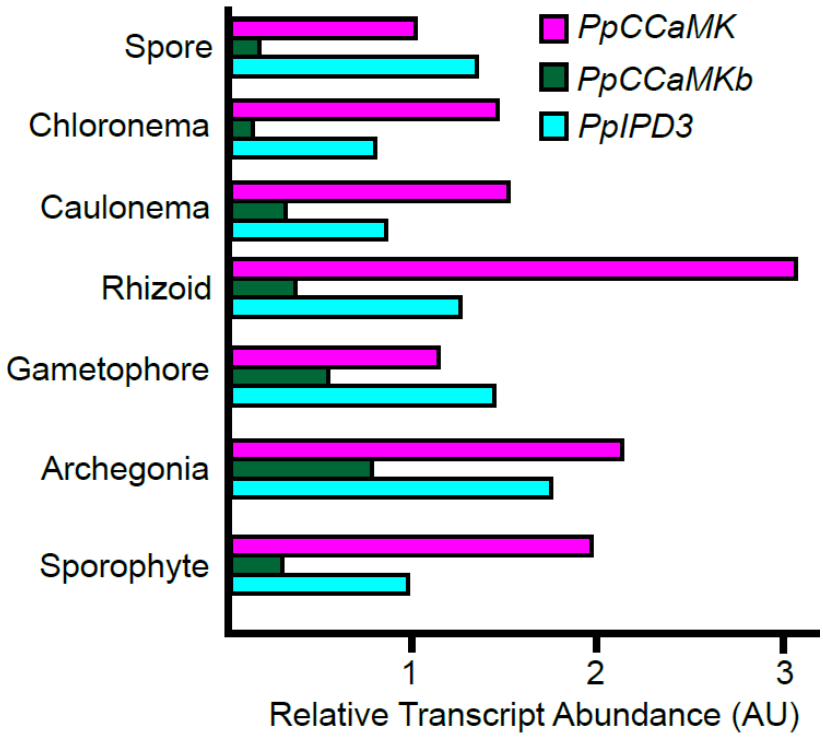

Supplemental Figure 3: Transcript abundance profiles for *PpCCaMK, PpCCaMKb*, and *PpIPD3*.

Inferred relative transcript abundance, expressed in arbitrary units (AU) for *PpIPD3, PpCCaMKb,* and *PpIPD3* from a published transcriptome atlas based on RNA-seq data (Ortiz-Ramírez et al., 2016).

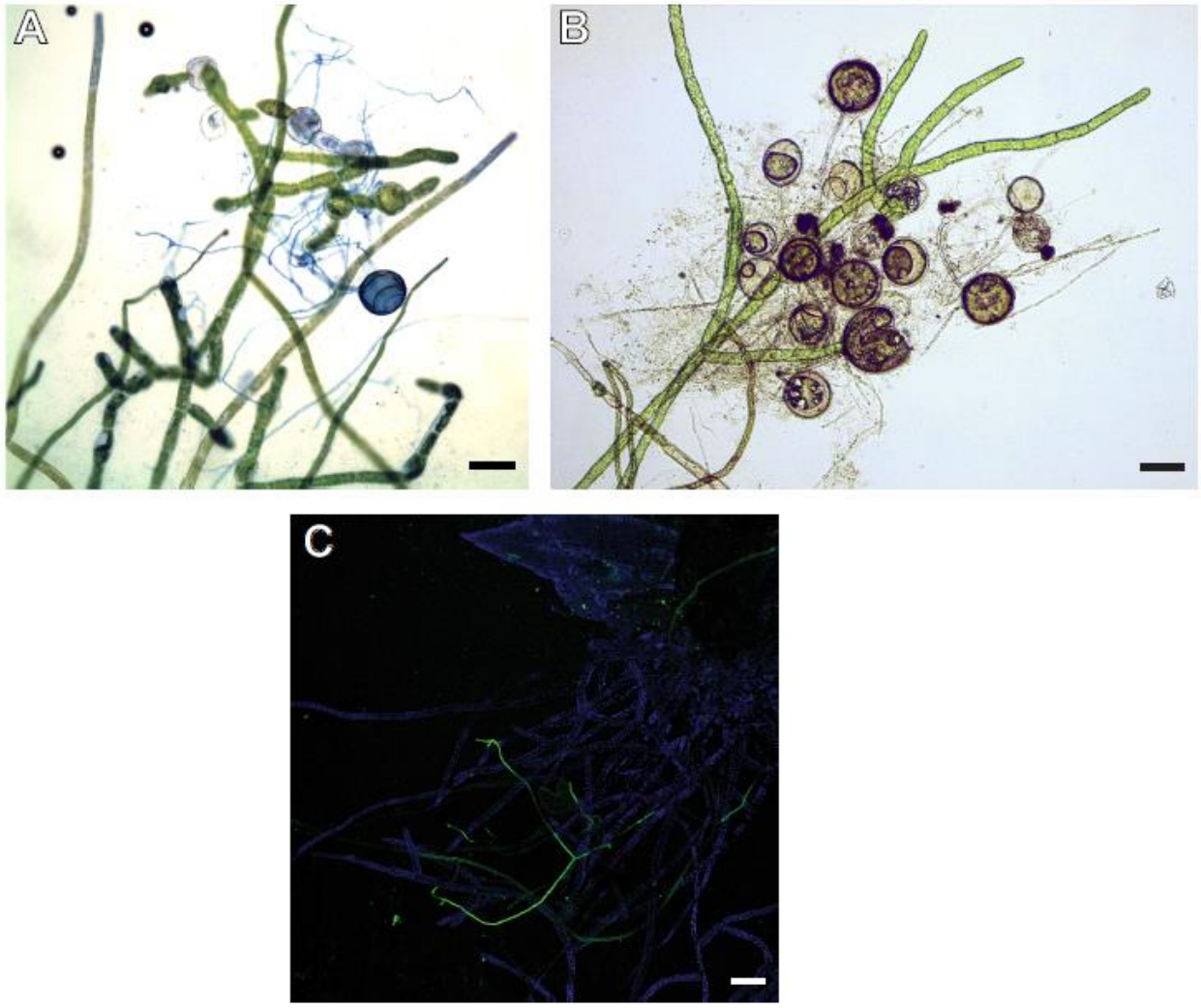

Supplemental Figure 4: Co-culture of the arbuscular mycorrhizal fungus *Rhizophagus irregularis* with Physcomitrella.

a) Bright-field micrograph showing Physcomitrella cells from a sample that was co-cultured with *Rhizophagus irregularis* for three months. Fungal hyphae were stained with trypan blue. No evidence for intracellular colonization was observed. Scale bar = 50 µm.

b) Bright-field micrograph showing Physcomitrella cells from a sample that was co-cultured with *Rhizophagus irregularis* for six months. Note that, despite extensive contact between fungal hyphae and Physcomitrella cells, no hyphal penetration was observed. Scale bar = 50 µm.

c) Confocal micrograph showing Physcomitrella cells from a sample that was co-cultured with *Rhizophagus irregularis* for three months. Chlorophyll autofluorescence (blue) and fungal hyphae stained with AlexaFluor 488 (green) conjugated to wheat germ agglutinin (WGA) are shown in pseudocolor. Scale bar = 100 µm.

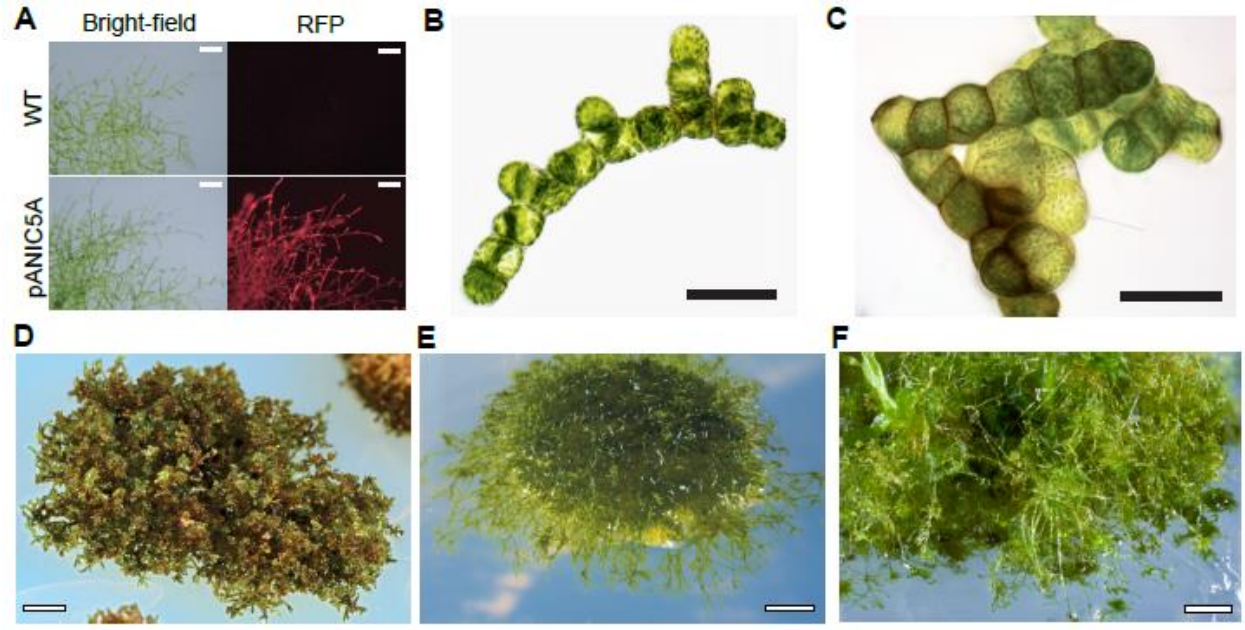

Supplemental Figure 5: Growth phenotypes of *PpCCaMK* or *PpIPD3* gain-of-function lines.

a) Physcomitrella genetically transformed with the empty pANIC5A vector, which was used to drive expression of each of native or modified forms of *PpCCaMK* or *PpIPD3* in this study, did not show any growth defects or phenotypic aberrations compared to WT. Fluorescence from a red fluorescent protein (RFP) visual marker was used to validate transformation. Scale bars = 200 µm.

b) Example of Physcomitrella expressing $PpCCaMK^{D}$. Note the abundant presence of brood cells and the absence of gametophores. Scale bar = 500 µm.

c) Example of Physcomitrella expressing $PpCCaM^{KD}$. Note the presence of brood cells and that gametophores are stunted and malformed. Scale bar = 500 µm.

d) Example of juvenile cluster of cells expressing $PpIPD3^{DD}$. Sample was subcultured less than two weeks before imaging. Scale bar = 50 µm.

e) Example of cluster of cells expressing $PpIPD3^{DD}$ approximately three weeks after subculture. Note the prominent reddish cell wall thickenings. Scale bar = 50 µm.

f) Example of Physcomitrella line expressing $PpIPD3^{DD}$ more than 5 weeks after subculture. Note the dark pigmentation and that the entire visible population of cells are brood cells. Scale bar = 500 µm. All samples were grown in BCDAT medium with 16-hour days and approximately 50 mol m-2 s-1 light intensity and 22 degrees Celsius.

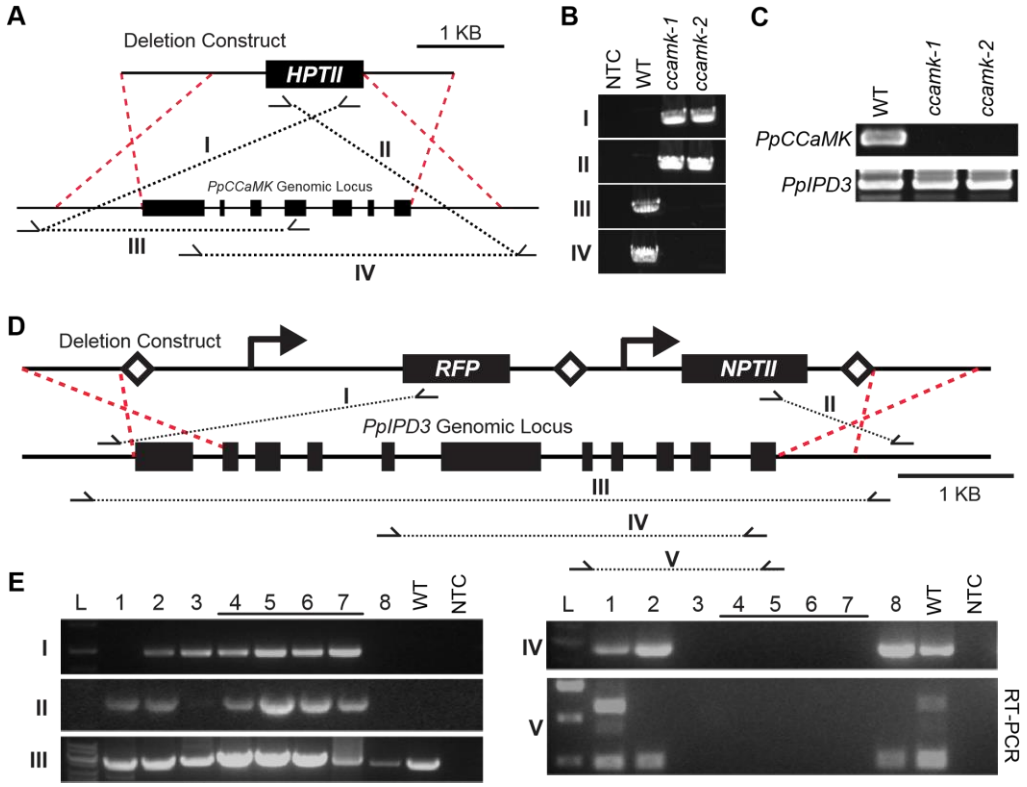

Supplemental Figure 6: Genotypic characterization of transformants and identification of Physcomitrella *ccamk* and *ipd3* deletion lines generated by homologous recombination-mediated gene targeting.

a) Diagram summarizing strategy for genetic deletion of *IPD3*. Roughly 1 kilobase (KB) of genomic DNA was cloned upstream or downstream of the first and last exons of *IPD3*. The two fragments were used to sandwich a hygromycin B selectable marker gene (HPTII) construct. Primers specific to the flanking regions of the native and recombined locus were used to test for recombination events at the targeted locus.

b) Results of PCR reactions using genomic DNA extracted from two independent *ccamk* (*ccamk-1* and *ccamk-2*) deletion mutants, WT, and no template control (NTC). PCR amplicon indicated in A by roman numerals (I-IV).

c) RT-PCR analysis of *ccamk-1* and *ccamk-2* using oligonucleotide primers specific to the coding sequence (CDS) of *PpCCaMK*. Amplification of the *PpIPD3* from the same cDNA samples was used to validate cDNA quality.

d) Diagram illustrating strategy for deletion of *IPD3* and identification of knockout mutants. Deletion construct containing a red fluorescent protein (RFP) visible marker gene expression construct and neomycin resistance selectable marker gene (NPTII) expression construct is shown above the exon-intron structure of the *IPD3*. Expected homologous recombination events are depicted in red dashed lines. PCR reactions with five different primer pairs (I-V) were used to identify *ipd3* deletion mutants. Expected PCR products are represented by arrows and dotted lines.

e) Results of PCR genotyping and RT-PCR. Panels I-IV show PCR results using genomic DNA samples. Panel V shows RT-PCR results. In each case, samples from eight lines stably transformed with *ipd3* deletion constructs (1-8) were analyzed alongside DNA ladder (L), WT sample, and NTC.

2.8 - Supplementary Tables

	Medicago truncatula	*Lotus japonicus*	*Arabidopsis thaliana*	*Populus trichocarpa*	*Marchantia paleacea*	*Marchantia polymorpha*	*Physcomitrella patens*
DMI2	Medtr5g030920	Lj2g3v1467920	-	Potri.007G004700	1KP: LFVP_12404	-	Pp3c3_28930
DMI1	Medtr7g117580	Lj6g3v2275020 Lj1g3v5061360	AT5G49960	Potri.003G008800 Potri.004G223400	1KP: LFVP_10987	1KP: JPYU_1254	Pp3c6_21060
NUP85	Medtr1g006690	Lj1g3v0318210	AT4G32910	Potri.018G044300	1KP: IHWO_2064309	Mapoly0014s0066	Pp3c16_3750
NUP133	Medtr5g097260	Lj2g3v3337540	AT2G05120	Potri.002G221300	1KP: IHWO_2012039	Mapoly0061s0124	Pp3c21_14430
CCaMK	Medtr8g043970	Lj3g3v1739280	-	Potri.008G011400 Potri.010G247400	1KP: IHWO_2068101	-	Pp3c21_15330 Pp3c19_20580
IPD3	Medtr5g026850 NCBI: MG788323	Lj2g3v1549600	-	Potri.001G130800 Potri.003G103100	1KP: LFVP_585	-	Pp3c23_22500
NSP1	Medtr8g020840	Lj3g3v2579340.1	AT3G13840	Potri.001G168800 Potri.003G065400	-	1KP: JPYU_8216	Pp3c2_9730
NSP2	Medtr3g072710	Lj1g3v0785930	AT4G08250	Potri.002G086100 Potri.005G175300	-	-	-
RAM1	Medtr7g027190	NCBI: KU557503	-	Potri.001G326000	-	-	-
RAM2	Medtr1g040500	Lj1g3v2301880	-	Potri.006G198100 Potri.016G063900	1KP: LFVP_13817_3 1KP: LFVP_85930_3 1KP: LFVP_15570_2	1KP: JPYU_7323 1KP: JPYU_5852	Pp3c5_1510 Pp3c6_29200 Pp3c6_29290
STR	Medtr8g107450	Lj4g3v3115140	-	Potri.012G045100 Potri.015G036100	1KP: LFPV_2015253	-	-
STR2	Medtr5g030910	Lj0g3v0104499	-	Potri.007G004800	1KP: LFPV_2012505	-	-
VAPYRIN	Medtr6g027840	Lj0g3v0049599 Lj1g3v3975850	-	Potri.013G062000 Potri.010G185200	1KP: HMHL_4710	1KP: JPYU_2960	-

Supplemental Table 1: Database accession numbers for genes referenced in Figure 1A.

Accessions from the National Center for Biotechnology Information (NCBI, accessible at https://ncbi.nlm.nih.gov) or the 1,000 Plants Initiative (1KP, accessible at https://www.onekp.com) are marked. Other accessions follow standard genomic locus identified for each species. The Lotus japonicus genome is accessible at https://lotus.au.dk. All other data are accessible through Phytozome 12 (https://phytozome.jgi.doe.gov). Dashes indicate inferred ortholog losses.

Name	Mutation(s)	Predicted Effect	# Transformants	Reference(s)
PpCCaMK	None	-	12	-
PpCCaMK^{D}	S252D	Constitutive Activation	8	Banba *et al.*, 2008; Takeda *et al.*, 2012
PpCCaMK^{K}	None	Constitutive Activation	14	Gleason *et al.*, 2006
PpIPD3	None	-	18	-
PpIPD3^{DD}	S107D, S241D	Constitutive Activation	>36	Singh *et al.*, 2014

Supplemental Table 2: Modified forms of *PpCCaMK* and *PpIPD3* used in this study.

The name, introduced mutations (if applicable), and predicted effects of introduced mutations are listed. For each construct, the number (#) of independent transformants that were generated and analyzed is provided. The reference for each study that guided our directed mutagenesis are provided and cited in the main text.

Supplemental Table 3: Primers used in this study. (SUBMITTED AS EXCEL FILE)

2.9 - Additional Data

CCaMK is localized in the cytoplasm and nucleus of Physcomitrella

In legumes, CCaMK is consistently localized to the nucleus. To determine if this trait is conserved in mosses, we tagged the N-terminus of native PpCCaMK and PpCCaMKb with eGFP and transformed tobacco pavement cells via *Agrobacterium rhizogenes* (**Additional Data 1a**). PpCCaMK consistently showed nuclear and cytoplasmic localization, whereas PpCCaMKb could not be expressed under the conditions we used. eGFP alone is known to have nuclear and cytoplasmic localization. To determine if the cytoplasmic localization of PpCCaMK was an artifact of protein degradation or cleavage of the eGFP tag, we also extracted total protein from transformed leaves and performed a western blot. eGFP-PpCCaMK-transformed leaves contained no degradation products of the expressed protein, reaffirming the cytoplasmic localization of

PpCCaMK (**Additional Data 1b**). Total protein extracted from leaves transformed with eGFP-PpCCaMKb showed no signal of protein expression. Interestingly, others have reported *in planta* that kinase activity of CCaMK in Lotus was necessary for protein stability. The absence of kinase activity in PpCCaMKb in our kinase assays could explain our inability to express it *in planta*.

IPD3 is localized in the nucleus of Physcomitrella

IPD3 is nuclear localized in legumes. To determine if this was conserved in Physcomitrella, we also tagged the N-terminus of PpIPD3 with eGFP and subsequently transformed the pavement cells of tobacco leaves with *Agrobacterium rhizogenes* (**Additional Data 1a**). Transformed cells consistently displayed nuclear localization of PpIPD3, confirming the conservation of localization between mosses and legumes.

Brood cells of *PpIPD3*^{DD}-transformed Physcomitrella contained large cytoplasmic lipid droplets.

A common trait of drought-stressed moss cells is the presence of large cytoplasmic lipid stores in the form of large droplets (Pressel & Duckett, 2010). To reaffirm that our previous phenotypes of PpIPD3^{DD} lines were those of *bona fide* brood cells, we tested the presence of lipid droplets in those cells by Nile red staining (**Additional Data 2**). Indeed, large cytoplasmic lipid droplets were observed in PpIPD3^{DD} brood cells but not the chloronema of wild-type Physcomitrella.

Constitutively active CCaMK in Lotus does not cause elevated levels of ABA

The direct influence of CCaMK or IPD3 on ABA levels has not been reported in angiosperms. We took advantage of a point-mutant of CCaMK in Lotus, T265I, which causes constitutive activation (Madsen *et al.*, 2010). Total ABA was extracted from roots and the T265I mutant was compared to wild-type (**Additional Data 3**). The levels of ABA in these roots did not differ from wild-type, suggesting the CCaMK/IPD3-regulating activity of ABA signaling is not a conserved trait in angiosperms.

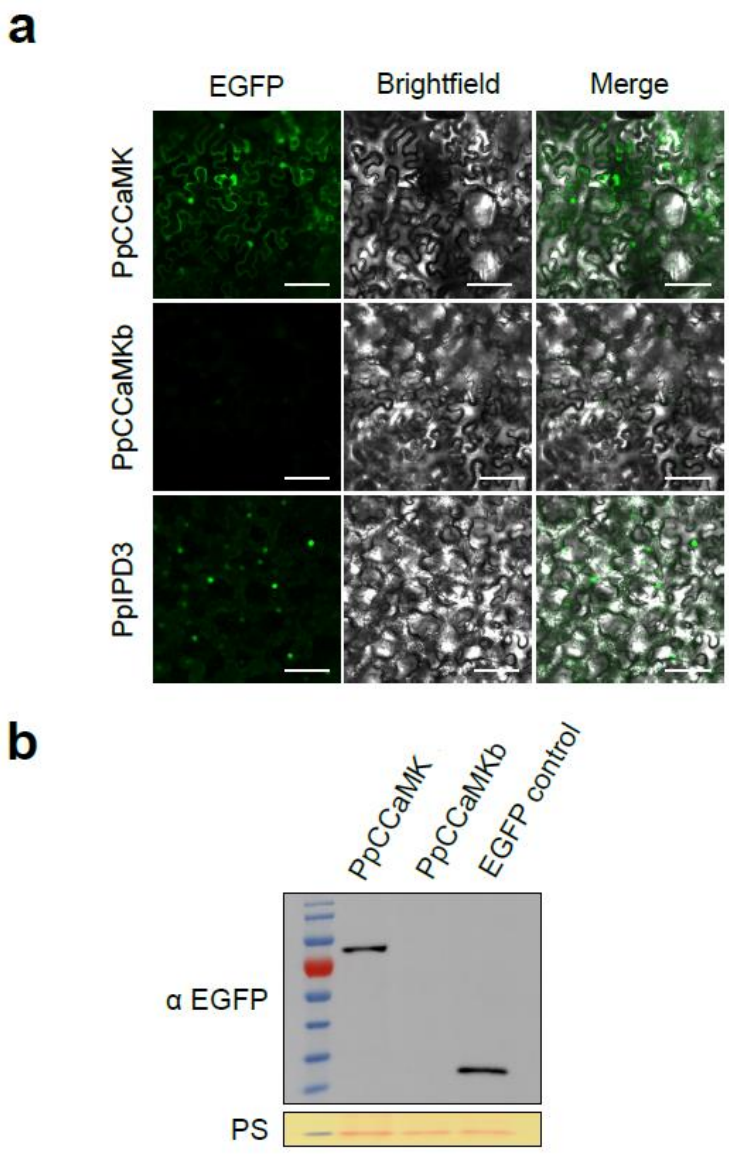

Additional Data 1: Subcellular localization of PpCCaMK, PpCCaMKb, and PpIPD3 in tobacco pavement cells.

a) EGFP was fused in frame with the N-terminus of the native coding sequences of either PpCCaMK, PpCCaMKb, or PpIPD3. Fusion-gene constructs were transformed into *Nicotiana benthemiana* leaves. Pavement cells were subsequently imaged using confocal laser scanning microscopy. Scale bar = 100 µm.
b) Western blot against EGFP of tobacco leaf protein extracts, post-transformation. PS: Ponceau S staining.

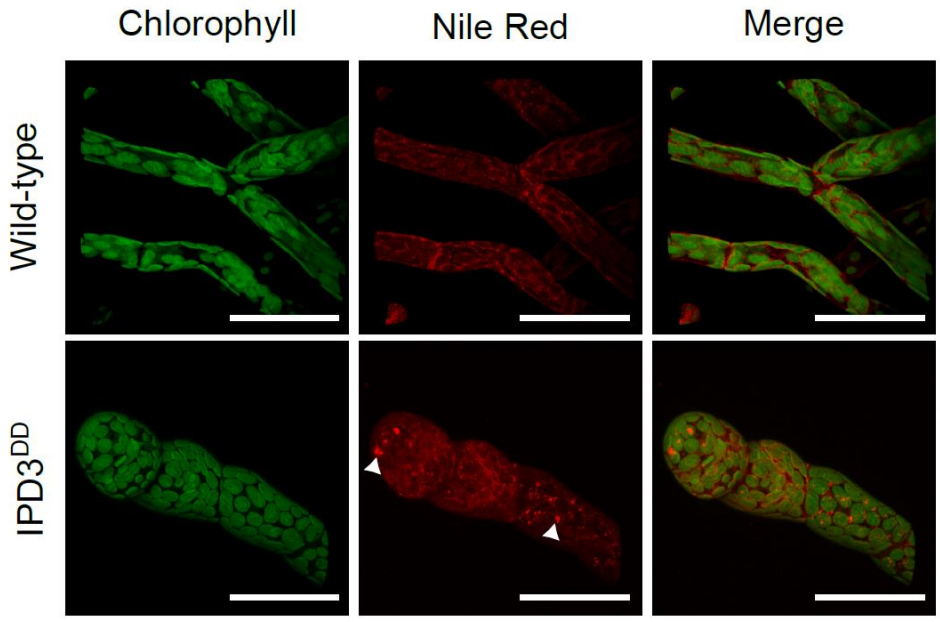

Additional Data 2: Presence of large lipid droplets in the cytoplasm of IPD3^{DD} lines. Three-week-old protonemal tissue was sampled from BCDAT medium plates. Neutral lipids were stained using the selective stain, nile red. Z-stacks of chlorophyll and nile red were subsequently imaged using confocal laser scanning microscopy. Arrowheads indicate the presence of large intracellular lipid droplets. Scale bar = 50 µm.

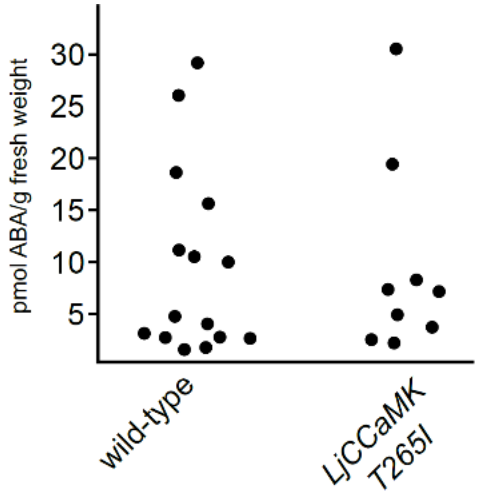

Additional Data 3: Constitutively active CCaMK does not cause elevated ABA levels in *Lotus japonicus* roots.
A *Lotus japonicus CCaMK* point-mutant, T265I causes constitutive kinase activity but does not cause elevated levels of ABA, suggesting the ABA-inducing activity of the Physcomitrella CCaMK/IPD3 module is not a conserved trait within angiosperms. Total ABA was extracted from roots of four-week-old plants and analyzed by ELISA assay.

2.10 - References

Ané J-M, Kiss GB, Riely BK, Penmetsa RV, Oldroyd GED, Ayax C, Lévy J, Debellé F, Baek J-M, Kalo P, *et al.* 2004. *Medicago truncatula DMI1* required for bacterial and fungal symbioses in legumes. *Science (New York, N.Y.)* **303**: 1364–7.

Le Bail A, Scholz S, Kost B. **2013**. Evaluation of reference genes for RT qPCR analyses of structure-specific and hormone regulated gene expression in *Physcomitrella patens* gametophytes. *PLoS One* **8**: e70998.

Bonfante P, Genre A. **2008**. Plants and arbuscular mycorrhizal fungi: an evolutionary-developmental perspective. *Trends in plant science* **13**: 492–498.

Bopp M. **2000**. 50 Years of the Moss Story. Progress in Botany. Springer, 3–34.

Bressendorff S, Azevedo R, Kenchappa CS, Ponce de Leon I, Olsen J V, Rasmussen MW, Erbs G, Newman M-A, Petersen M, Mundy J. **2016**. An innate immunity pathway in the moss *Physcomitrella patens*. *The Plant Cell* **28**: tpc.00774.2015.

Buendia L, Wang T, Girardin A, Lefebvre B. **2015**. The LysM receptor-like kinase SlLYK10 regulates the arbuscular mycorrhizal symbiosis in tomato. *New Phytologist* **210**: 184–195.

Capoen W, Sun J, Wysham D, Otegui MS, Venkateshwaran M, Hirsch S, Miwa H, Downie JA, Morris RJ, Ané J-M. **2011**. Nuclear membranes control symbiotic calcium signaling of legumes. *Proceedings of the National Academy of Sciences* **108**: 14348–14353.

Carleton TJ, Read DJ. **1991**. Ectomycorrhizas and nutrient transfer in conifer–feather moss ecosystems. *Canadian Journal of Botany* **69**: 778–785.

Chen C, Ané J, Zhu H. **2008**. OsIPD3, an ortholog of the Medicago truncatula DMI3 interacting protein IPD3, is required for mycorrhizal symbiosis in rice. *New Phytologist* **180**: 311–315.

Correns C. **1899**. *Untersuchungen über die Vermehrung der Laubmoose durch Brutorgane und Stecklinge*. G. Fischer.

Davey ML, Currah RS. **2006**. Interactions between mosses (Bryophyta) and fungi. *Botany* **84**: 1509–1519.

Delaux P. **2017**. Comparative phylogenomics of symbiotic associations. *New Phytologist* **213**: 89–94.

Delaux P-M, Radhakrishnan G V., Jayaraman D, Cheema J, Malbreil M, Volkening JD, Sekimoto H, Nishiyama T, Melkonian M, Pokorny L, *et al.* 2015a. Algal ancestor of land plants was preadapted for symbiosis. *Proceedings of the National Academy of Sciences* **112**: 201515426.

Delaux P-M, Séjalon-Delmas N, Bécard G, Ané J-M. **2013**. Evolution of the plant–microbe symbiotic 'toolkit'. *Trends in plant science* **18**: 298–304.

Delaux PM, Varala K, Edger PP, Coruzzi GM, Pires JC, Ané JM. **2014**. Comparative phylogenomics uncovers the impact of symbiotic associations on host genome evolution. *PLoS Genetics* **10**.

Doyle JJ. **2011**. Phylogenetic perspectives on the origins of nodulation. *Molecular Plant-Microbe Interactions* **24**: 1289–1295.

Duckett JG, Ligrone R. **1992**. A survey of diaspore liberation mechanisms and germination patterns in mosses. *Journal of Bryology* **17**: 335–354.

Frank MH, Scanlon MJ. **2015**. Cell-specific transcriptomic analyses of three-dimensional shoot development in the moss *Physcomitrella patens*. *The Plant Journal* **83**: 743–751.

Garcia K, Chasman D, Roy S, Ane J-M. **2017**. Physiological responses and gene co-expression network of mycorrhizal roots under K+ deprivation. *Plant Physiology* **173**: 1811–1823.

Garcia K, Delaux P, Cope KR, Ané J. **2015**. Molecular signals required for the establishment and maintenance of ectomycorrhizal symbioses. *New Phytologist* **208**: 79–87.

Genre A, Chabaud M, Faccio A, Barker DG, Bonfante P. **2008**. Prepenetration apparatus assembly precedes and predicts the colonization patterns of arbuscular

mycorrhizal fungi within the root cortex of both *Medicago truncatula* and *Daucus carota*. *The Plant Cell* **20**: 1407–1420.

Gleason C, Chaudhuri S, Yang T, Munoz A, Poovaiah BW, Oldroyd GED. **2006**. Nodulation independent of rhizobia induced by a calcium-activated kinase lacking autoinhibition. *Nature* **441**: 1149–1152.

Gobbato E, Marsh JF, Vernié T, Wang E, Maillet F, Kim J, Miller JB, Sun J, Bano SA, Ratet P. **2012**. A GRAS-type transcription factor with a specific function in mycorrhizal signaling. *Current Biology* **22**: 2236–2241.

Hohe A, Egener T, Lucht JM, Holtorf H, Reinhard C, Schween G, Reski R. **2004**. An improved and highly standardised transformation procedure allows efficient production of single and multiple targeted gene-knockouts in a moss, *Physcomitrella patens*. *Current Genetics* **44**: 339–347.

Horváth B, Yeun LH, Domonkos Á, Halász G, Gobbato E, Ayaydin F, Miró K, Hirsch S, Sun J, Tadege M, *et al.* 2011. *Medicago truncatula IPD3* is a member of the common symbiotic signaling pathway required for rhizobial and mycorrhizal symbioses. *Molecular Plant-Microbe Interactions* **24**: 1345–1358.

J. Levy, C. Bres, R. Geurts, B. Chalhoub, O. Kulikova, G. Duc, EP Journet, JM Ane, E. Lauber, T. Bisseling, J. Denarie, C. Rosenberg FD. **2004**. A putative Ca2+ and calmodulin-dependent protein kinase required for bacterial and fungal symbioses. *Science* **303**: 1361–1364.

Kamel L, Keller-Pearson M, Roux C, Ané JJ-M, Keller-pearson M, Roux C, Ané JJ-M. **2016**. Tansley insight Biology and evolution of arbuscular mycorrhizal symbiosis in the light of genomics. *New Phytologist* **213**: 531–536.

Kleist TJ, Cartwright HN, Perera AM, Christianson ML, Lemaux PG, Luan S. **2017**. Genetically encoded calcium indicators for fluorescence imaging in the moss *Physcomitrella* : GCaMP3 provides a bright new look. *Plant Biotechnology Journal* **15**: 1235–1237.

Kleist TJ, Spencley AL, Luan S. **2014**. Comparative phylogenomics of the CBL-CIPK

calcium-decoding network in the moss *Physcomitrella, Arabidopsis*, and other green lineages. *Abiotic Stress: Molecular Genetics and Genomics*: 74.

Komatsu K, Suzuki N, Kuwamura M, Nishikawa Y, Nakatani M, Ohtawa H, Takezawa D, Seki M, Tanaka M, Taji T. **2013**. Group A PP2Cs evolved in land plants as key regulators of intrinsic desiccation tolerance. *Nature communications* **4**.

Koske RE, Gemma JN. **1989**. A modified procedure for staining roots to detect VA mycorrhizas. *Mycological Research* **92**: 486–488.

Lang D, Ullrich KK, Murat F, Fuchs J, Jenkins J, Haas FB, Piednoel M, Gundlach H, Van Bel M, Meyberg R, *et al.* 2018. The *Physcomitrella patens* chromosome-scale assembly reveals moss genome structure and evolution. *Plant Journal* **93**: 515–533.

de León IP, Hamberg M, Castresana C. **2015**. Oxylipins in moss development and defense. *Frontiers in plant science* **6**: 483.

Ma F, Lu R, Liu H, Shi B, Zhang J, Tan M, Zhang A, Jiang M. **2012**. Nitric oxide-activated calcium/calmodulin-dependent protein kinase regulates the abscisic acid-induced antioxidant defence in maize. *Journal of Experimental Botany* **63**: 4835–4847.

Madsen LH, Tirichine L, Jurkiewicz A, Sullivan JT, Heckmann AB, Bek AS, Ronson CW, James EK, Stougaard J. **2010**. The molecular network governing nodule organogenesis and infection in the model legume *Lotus japonicus*. *Nature Communications* **1**.

Maillet F, Poinsot V, Andre O, Puech-Pagès V, Haouy A, Gueunier M, Cromer L, Giraudet D, Formey D, Niebel A. **2011**. Fungal lipochitooligosaccharide symbiotic signals in arbuscular mycorrhiza. *Nature* **469**: 58–63.

Mann DGJ, LaFayette PR, Abercrombie LL, King ZR, Mazarei M, Halter MC, Poovaiah CR, Baxter H, Shen H, Dixon RA. **2012**. Gateway-compatible vectors for high-throughput gene functional analysis in switchgrass (*Panicum virgatum L*.) and other monocot species. *Plant Biotechnology Journal* **10**: 226–236.

Messinese E, Mun J-H, Yeun LH, Jayaraman D, Rougé P, Barre A, Lougnon G, Schornack S, Bono J-J, Cook DR. **2007**. A novel nuclear protein interacts with the

symbiotic DMI3 calcium-and calmodulin-dependent protein kinase of Medicago truncatula. *Molecular Plant-Microbe Interactions* **20**: 912–921.

Miller JB, Pratap A, Miyahara A, Zhou L, Bornemann S, Morris RJ, Oldroyd GED. **2013**. Calcium/Calmodulin-dependent protein kinase is negatively and positively regulated by calcium, providing a mechanism for decoding calcium responses during symbiosis signaling. *The Plant Cell* **25**: 5053–5066.

Miyata K, Kozaki T, Kouzai Y, Ozawa K, Ishii K, Asamizu E, Okabe Y, Umehara Y, Miyamoto A, Kobae Y, *et al.* 2014. Bifunctional plant receptor, OsCERK1, regulates both chitin-triggered immunity and arbuscular mycorrhizal symbiosis in rice. *Plant & cell physiology* **55**: 1864–1872.

Mun T, Bachmann A, Gupta V, Stougaard J, Andersen SU. **2016**. Lotus Base: An integrated information portal for the model legume *Lotus japonicus*. *Scientific Reports* **6**: 1–18.

Oldroyd GED. **2013**. Speak, friend, and enter: signalling systems that promote beneficial symbiotic associations in plants. *Nature Reviews Microbiology* **11**: 252–263.

Oliver JP, Castro A, Gaggero C, Cascón T, Schmelz EA, Castresana C, De León IP. **2009**. Pythium infection activates conserved plant defense responses in mosses. *Planta* **230**: 569–579.

Ondzighi-Assoume CA, Chakraborty S, Harris JM. **2016**. Environmental nitrate stimulates abscisic acid accumulation in arabidopsis root tips by releasing it from inactive stores. *Plant Cell* **28**: 729–745.

Ortiz-Ramírez C, Hernandez-Coronado M, Thamm A, Catarino B, Wang M, Dolan L, Feijó JAA, Becker JDD. **2016**. A Transcriptome Atlas of *Physcomitrella patens* Provides Insights into the Evolution and Development of Land Plants. *Molecular Plant* **9**: 205–220.

Parniske M. **2008**. Arbuscular mycorrhiza: the mother of plant root endosymbioses. *Nature reviews. Microbiology* **6**: 763–75.

Pirozynski KA, Malloch DW. **1975**. The origin of land plants: a matter of mycotrophism. *Biosystems* **6**: 153–164.

Ponce de León I. **2011**. The moss *Physcomitrella patens* as a model system to study interactions between plants and phytopathogenic fungi and oomycetes. *Journal of pathogens* **2011**.

Pressel S, Bidartondo MI, Ligrone R, Duckett JG. **2010**. Fungal symbioses in bryophytes: New insights in the Twenty First Century. *Phytotaxa* **9**: 238.

Pressel S, Duckett JG. **2010**. Cytological insights into the desiccation biology of a model system: moss protonemata. *New Phytologist* **185**: 944–963.

Rabatin SC. **1980**. The occurrence of the vesicular-arbuscular-mycorrhizal fungus *Glomus tenuis* with moss. *Mycologia* **72**: 191–195.

Read DJ, Ducket JG, Francis R, Ligron R, Russell a. **2000**. Symbiotic fungal associations in 'lower' land plants. *Philosophical transactions of the Royal Society of London. Series B, Biological sciences* **355**: 815–830; discussion 830-831.

Redecker D, Kodner R, Graham LE. **2000**. Glomalean fungi from the Ordovician. *Science* **289**: 1920–1921.

Remy W, Taylor TN, Hass H, Kerp H. **1994**. Four hundred-million-year-old vesicular arbuscular mycorrhizae. *Proceedings of the National Academy of Sciences of the United States of America* **91**: 11841–11843.

Rensing SA, Lang D, Zimmer AD, Terry A, Salamov A, Shapiro H, Nishiyama T, Perroud P-F, Lindquist EA, Kamisugi Y. **2008**. The *Physcomitrella* genome reveals evolutionary insights into the conquest of land by plants. *Science* **319**: 64–69.

Routray P, Miller JB, Du L, Oldroyd G, Poovaiah BW. **2013**. Phosphorylation of S344 in the calmodulin-binding domain negatively affects CCaMK function during bacterial and fungal symbioses. *Plant Journal* **76**: 287–296.

Schnepf E, Reinhard C. **1997**. Brachycytes in *Funaria* protonemate: induction by abscisic acid and fine structure. *Journal of Plant Physiology* **151**: 166–175.

Shi B, Ni L, Liu Y, Zhang A, Tan M, Jiang M. **2014**. OsDMI3-mediated activation of OsMPK1 regulates the activities of antioxidant enzymes in abscisic acid signalling in rice.

Plant, cell & environment **37**: 341–352.

Shi B, Ni L, Zhang A, Cao J, Zhang H, Qin T, Tan M, Zhang J, Jiang M. **2012**. OsDMI3 is a novel component of abscisic acid signaling in the induction of antioxidant defense in leaves of rice. *Molecular Plant* **5**: 1359–1374.

Shinde S, Nurul Islam M, Ng CK. **2012**. Dehydration stress-induced oscillations in LEA protein transcripts involves abscisic acid in the moss, *Physcomitrella patens*. *New Phytologist* **195**: 321–328.

Shinde S, Shinde R, Downey F, Ng CK-Y. **2013**. Abiotic stress-induced oscillations in steady-state transcript levels of Group 3 LEA protein genes in the moss, *Physcomitrella patens*. *Plant signaling & behavior* **8**: e22535.

Singh S, Katzer K, Lambert J, Cerri M, Parniske M. **2014**. CYCLOPS, A DNA-binding transcriptional activator, orchestrates symbiotic root nodule development. *Cell Host and Microbe* **15**: 139–152.

Smith SE, Read DJ. **2010**. *Mycorrhizal symbiosis*. Academic press.

Spatafora JW, Chang Y, Benny GL, Lazarus K, Smith ME, Berbee ML, Bonito G, Corradi N, Grigoriev I, Gryganskyi A. **2016**. A phylum-level phylogenetic classification of zygomycete fungi based on genome-scale data. *Mycologia* **108**: 1028–1046.

Strullu-Derrien C, Kenrick P, Pressel S, Duckett JG, Rioult JP, Strullu DG. **2014**. Fungal associations in *Horneophyton ligneri* from the Rhynie Chert (c. 407 million year old) closely resemble those in extant lower land plants: Novel insights into ancestral plant-fungus symbioses. *New Phytologist* **203**: 964–979.

Strullu-Derrien C, Wawrzyniak Z, Goral T, Kenrick P. **2015**. Fungal colonization of the rooting system of the early land plant *Asteroxylon mackiei* from the 407-Myr-old Rhynie Chert (Scotland, UK). *Botanical Journal of the Linnean Society* **179**: 201–213.

Sun J, Miller JB, Granqvist E, Wiley-Kalil A, Gobbato E, Maillet F, Cottaz S, Samain E, Venkateshwaran M, Fort S. **2015**. Activation of symbiosis signaling by arbuscular mycorrhizal fungi in legumes and rice. *The Plant Cell* **27**: 823–838.

Takeda N, Maekawa T, Hayashi M. **2012**. Nuclear-localized and deregulated calcium- and calmodulin-dependent protein kinase activates rhizobial and mycorrhizal responses in *Lotus japonicus*. *The Plant cell* **24**: 810–22.

Takezawa D, Watanabe N, Ghosh TK, Saruhashi M, Suzuki A, Ishiyama K, Somemiya S, Kobayashi M, Sakata Y. **2015**. Epoxycarotenoid-mediated synthesis of abscisic acid in *Physcomitrella patens* implicating conserved mechanisms for acclimation to hyperosmosis in embryophytes. *New Phytologist* **206**: 209–219.

Tang H, Krishnakumar V, Bidwell S, Rosen B, Chan A, Zhou S, Gentzbittel L, Childs KL, Yandell M, Gundlach H, *et al.* 2014. An improved genome release (version Mt4.0) for the model legume *Medicago truncatula*. *BMC Genomics* **15**: 1–14.

Tirichine L, Imaizumi-Anraku H, Yoshida S, Murakami Y, Madsen LH, Miwa H, Nakagawa T, Sandal N, Albrektsen AS, Kawaguchi M, *et al.* 2006. Deregulation of a Ca2+/calmodulin-dependent kinase leads to spontaneous nodule development. *Nature* **441**: 1153–6.

Venkateshwaran M, Volkening JD, Sussman MR, Ané J-M, Michael R. **2013**. Symbiosis and the social network of higher plants. *Current opinion in plant biology* **16**: 118–127.

Vesty EF, Saidi Y, Moody LA, Holloway D, Whitbread A, Needs S, Choudhary A, Burns B, McLeod D, Bradshaw SJ. **2016**. The decision to germinate is regulated by divergent molecular networks in spores and seeds. *New Phytologist* **211**: 952–966.

Wang C, Liu Y, Li S-S, Han G-Z. **2015**. Insights into the origin and evolution of the plant hormone signaling machinery. *Plant physiology* **167**: 872–886.

Wang B, Qiu Y-LYL. **2006**. Phylogenetic distribution and evolution of mycorrhizas in land plants. *Mycorrhiza* **16**: 299–363.

Wang B, Yeun LH, Xue JY, Liu Y, Ané JM, Qiu YL. **2010**. Presence of three mycorrhizal genes in the common ancestor of land plants suggests a key role of mycorrhizas in the colonization of land by plants. *New Phytologist* **186**: 514–525.

Xue L, Cui H, Buer B, Vijayakumar V, Delaux P-M, Junkermann S, Bucher M. **2015**.

Network of GRAS transcription factors involved in the control of arbuscule development in *Lotus japonicus*. *Plant physiology* **167**: 854–871.

Yan J, Guan L, Sun Y, Zhu Y, Liu L, Lu R, Jiang M, Tan M, Zhang A. **2015**. Calcium and ZmCCaMK are involved in brassinosteroid-induced antioxidant defense in maize leaves. *Plant and Cell Physiology* **56**: 883–896.

Yang C, Li A, Zhao Y, Zhang Z, Zhu Y, Tan X, Geng S, Guo H, Zhang X, Kang Z. **2011**. Overexpression of a wheat *CCaMK* gene reduces ABA sensitivity of Arabidopsis thaliana during seed germination and seedling growth. *Plant Molecular Biology Reporter* **29**: 681–692.

Yano K, Yoshida S, Müller J, Singh S, Banba M, Vickers K, Markmann K, White C, Schuller B, Sato S, *et al.* 2008. CYCLOPS, a mediator of symbiotic intracellular accommodation. *Proceedings of the National Academy of Sciences of the United States of America* **105**: 20540–20545.

Yotsui I, Saruhashi M, Kawato T, Taji T, Hayashi T, Quatrano RS, Sakata Y. **2013**. *ABSCISIC ACID INSENSITIVE3* regulates abscisic acid-responsive gene expression with the nuclear factor Y complex through the ACTT-core element in *Physcomitrella patens*. *New Phytologist* **199**: 101–109.

Young ND, Debellé F, Oldroyd GED, Geurts R, Cannon SB, Udvardi MK, Benedito VA, Mayer KFX, Gouzy J, Schoof H, *et al.* 2011. The *Medicago* genome provides insight into the evolution of rhizobial symbioses. *Nature* **480**: 520–524.

Chapter 3 - (MANUSCRIPT IN PREPARATION FOR SUBMISSION)

IPD3 deletion causes 'wrong-way-response' in gravitropic caulonema in *Physcomitrella patens*.

Anthony Bortolazzo[1,2], Thomas B. Irving[2], C.J. Bascom[3], Ashley Henry[4], Thomas J. Kleist[5], Edgar Spalding[4], Magdalena Bezanilla[3] and Jean-Michel Ané[2,6,#]

[1] Laboratory of Genetics, University of Wisconsin-Madison, Madison, WI 53706, USA

[2] Department of Bacteriology, University of Wisconsin-Madison, Madison, WI 53706, USA

[3] Department of Biological Sciences, Dartmouth College, Hanover, NH 03755, USA

[4] Department of Botany, University of Wisconsin-Madison, Madison, WI 53706, USA

[5] Department of Biology, Heinrich Heine University, Düsseldorf 40225, Germany

[6] Department of Agronomy, University of Wisconsin-Madison, Madison, WI 53706, USA

[#] Corresponding authors: Jean-Michel Ané, Phone: 608-262-6457, Email: jeanmichel.ane@wisc.edu

A.Bortolazzo's contributions to manuscript/Ch. 3

AB identified the wrong-way-response in dark-grown caulonema. Aside from timescale imaging and root gravitropism experiments, AB carried out all experiments and observations. AB illustrated all figures and wrote the draft and final versions of the manuscript with regular input on writing from J.-M.A. and T.I.

3.1 - Abstract

The plant transcription factor Interacting Protein of DMI3 (IPD3) plays symbiotic signaling roles between angiosperms and arbuscular mycorrhizal fungi or rhizobia and is typically absent from the genomes of plants that do not form endosymbiotic interactions with these microbes. Despite this, IPD3 is present in the genomes of mosses even though mosses are not known to form symbiotic interactions with either arbuscular mycorrhizal fungi or rhizobia. Without a visually apparent phenotype in *Physcomitrella patens* (Physcomitrella) lines lacking the *IPD3* locus, we sought to characterize fine-scale growth patterns using a microfluidics-imaging technique. Long-term fine scale imaging revealed an atypical curling pattern of growth in caulonemal cells of *Ppipd3-1* moss relative to wild-type. Given that caulonema are specifically negatively gravitropic, we tested if the curling phenotype is a manifestation of abnormal gravitropism. In this work we describe a 'wrong-way-response' of *Ppipd3-1* mutant moss in which caulonema cells have switched from a preference of negative gravitropism to positive gravitropism, which has been previously reported in mutant mosses, however unmapped. We previously elucidated roles of IPD3 and its upstream kinase, the Calcium/Calmodulin-dependent protein Kinase (CCaMK) in ABA signaling activity. Neither deletion of the CCaMK locus in Physcomitrella nor the addition of ABA to *Ppipd3-1* mutant moss altered preferences of caulonema gravitropism, suggesting an uncoupling of IPD3 from CCaMK or ABA signaling in gravitropism in mosses.

3.2 - Introduction

Arbuscular mycorrhizal symbiosis (AM) and AM-like interactions are widespread in extant plants, from angiosperms to bryophytes (Wang & Qiu, 2006). Plant and fungal fossils indicate such interactions arose in some of the earliest land plants (Remy *et al.*, 1994b; Redecker *et al.*, 2000). The interaction between the plant host and AM fungi (AMF) is mediated through a conserved plant signal transduction pathway termed the common symbiosis pathway (CSP) (Maclean *et al.*, 2017). The CSP has acquired its name due to the fact that it also mediates plant signal transduction from exuded rhizobial signals in a mechanistically similar manner (Oldroyd, 2013). The CSP is activated in host plants by signaling molecules exuded from AMF, namely chitooligosaccharides (COs) and lipo-chitooligosaccharides (LCOs) (Maillet *et al.*, 2011b). These signals induce high amplitude, oscillatory calcium signals within the nucleus, termed ‘calcium spikes’ (Capoen *et al.*, 2011). Calcium spikes are decoded the Calcium/Calmodulin-dependent Protein Kinase (CCaMK) which subsequently phosphorylates and activates a transcription factor Interacting Protein of DMI3 (IPD3/CYCLOPS) (Singh *et al.*, 2014). IPD3 activation is then responsible for initiating a transcriptional cascade necessary for symbiotic association with AMF (Pimprikar *et al.*, 2016).

Comparative genomics of have found that numerous components of the CSP are conserved in early-diverging plant lineages, including liverworts and hornworts which form AMS-like interactions (Wang *et al.*, 2010b; Grosche *et al.*, 2018). Furthermore, genes of the CSP emerged in the algal progenitors of land plants as evidenced by their presence in advanced charophyte algae (Delaux *et al.*, 2015a). In land plants, the loss of AM and AM-like interaction is concomitant with gene loss of the CSP (Delaux *et al.*, 2014a).

CCaMK and *IPD3* are almost always present in host-plant species and absent in lineages that lost the ability to host AMF. A striking exception to this pattern is the conservation of *CCaMK* and *IPD3* in the genomes of mosses.

Unlike other bryophyte lineages, the vast majority of mosses do not form AM-like interactions, raising questions on the biological function(s) of such genes in mosses. Our previous studies in *Physcomitrella patens* (Physcomitrella) have elucidated signaling roles of CCaMK and IPD3 upstream of abscisic acid (ABA) signaling and associated moss stress-responses. However, the consequences of deletion of either the *CCaMK* or *IPD3* loci were still unknown **(Chapter 2, Kleist *et al*., in preparation for submission)**. As such, we sought to characterize the growth and development of the Physcomitrella *ccamk-1* and *ipd3-1* mutants in more detail.

Physcomitrella is a useful model for studying developmental genetics. As a gametophyte dominant plant, most tissues of Physcomitrella are haploid. Physcomitrella possesses a simple life cycle as well as organization of tissues, most only the thickness of one cell-layer (Prigge & Bezanilla, 2010). Given the small stature of Physcomitrella, long-term time scale imaging can be accomplished through recent advances in microfluidics. By inserting liquid medium and young tissue into tightly enclosed chambers constructed of polydimethylsiloxane bound to microscopy coverslips, growth patterns and developmental stages can be faithfully imaged while maintaining natural levels of gas exchange during the process (Bascom *et al.*, 2016). We used this tool to image the filamentous growth of the *Ppipd3-1* mutant previously described.

In this work, we discovered an unexpected gravitropic phenotype in the *Ppipd3-1* mutant in which gravitropic tip-growing cells displayed abnormal curling or, when grown

in the dark, showed an opposite directional growth response, a ‘wrong way response’ (wwr). In plants that host AMF, loss of *CCaMK* or *IPD3* is associated with symbiotic defects. In our previous work with Physcomitrella (Chapter 2, Kleist *et al.*, submitted for peer review), we found that CCaMK or IPD3 activation had shared drought-like phenotypes. Despite the mechanistic and phenotypic linkage of *CCaMK* and *IPD3*, ccamk mutants in Physcomitrella were not defective in gravitropic responses, indicating an uncoupling of *CCaMK* and *IPD3* concerning gravitropism in mosses.

3.3 - Results

Ppipd3-1 caulonema grow in an atypical spiral pattern.

At the start of the moss life-cycle, spores germinate into the filamentous chloroplast-dense ‘chloronema’. Over time, chloronema switch into the distinct filamentous stage known as ‘caulonema’. In standard growth conditions, caulonema grow in straight patterns and serve as a means of colony expansion and dispersion on growth substrates. In contrast, the caulonema of the *Ppipd3-1* mutant grew in spiral patterns (**Figure 1**). No directional preference was observed at the tips of the caulonemal filaments as both clockwise and counterclockwise examples of spiral growth were observed. Previous studies in *Ceratodon purpureus* (Ceratodon), a closely related species, demonstrated that protonema grown in zero-gravity and on clinostats defaulted to atypical spiral growth (Kern *et al.*, 2005). To assess if the spiral growth phenotype of *Ppipd3-1* moss was a manifestation of faulty gravitropism, we sought to test if *Ppipd3-1* moss displayed an abnormal phenotype using a widely established gravitropism assay for mosses.

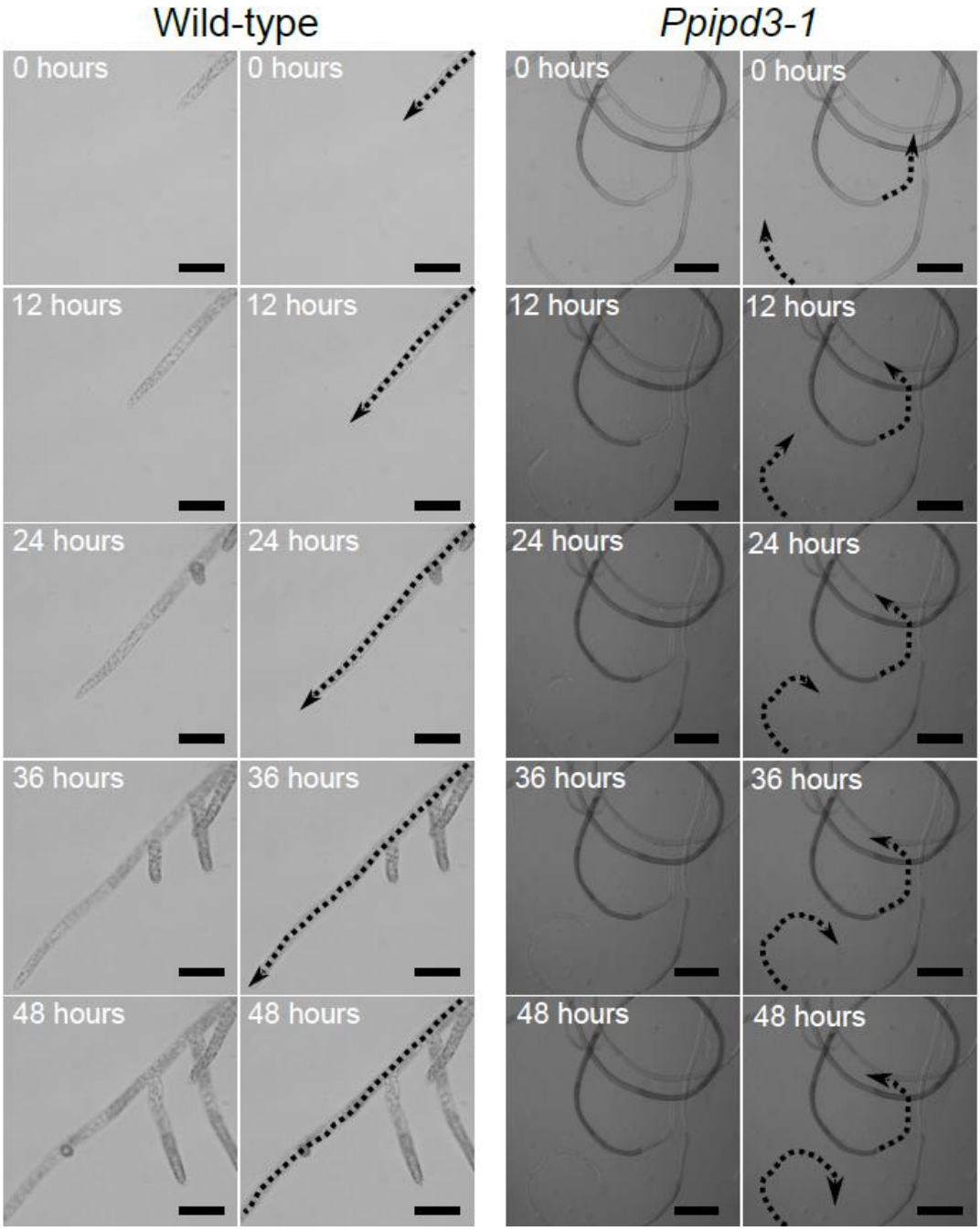

Figure 1: *Ppipd3-1* mutant moss caulonema display an atypical curling pattern.

Wild-type and *Ppipd3-1* mutant moss were blended and injected into microfluidics long-term imaging chamber. Caulonema growth was imaged for a total of 48 hours. The *Ppipd3-1* mutant displays an atypical curling pattern. No preference for clock-wise or counterclock-wise curling was observed. Each time panel is shown in duplicate, the right of which shows growth tracings. Arrowheads indicate the direction of the filament tip. Scale = 50 µm.

Ppipd3-1 caulonema display a 'wrong-way-response' when negative gravitropism is promoted.

A proportion of caulonema filaments regularly display negative gravitropism, however when the growth substrate is parallel to the gravity vector, a much larger proportion of these cells grow against the gravity vector (Wagner *et al.*, 1997). The negative gravitropism of caulonema is further enhanced when grown in darkness. To test if negative gravitropism was defective in *Ppipd3-1* moss, protonema was grown on medium placed upright, in the darkness, and supplemented with sucrose, all other conditions kept standard. After three weeks of growth, *Ppip3-1* filaments displayed a preference for positive gravitropism whereas wild-type displayed a preference for negative gravitropism (**Figure 2a**). Similar wwr phenotypes have been described in Physcomitrella and Ceratodon (Wagner *et al.*, 1997). In addition to the wwr phenotype of *Ppipd3-1*, the caulonemal tips of the mutant also displayed uncoordinated, wavy patterns of growth as compared to wild-type (**Supplementary Video 1**). Although gametophore development seldomly occurs in darkness, when etiolated gametophores were observed in *Ppipd3-1* Physcomitrella, they displayed negative gravitropism similarly to wild-type (**Supplementary Figure 1**).

Modulation of ABA levels did not alter the gravitropic preferences of wild-type or Ppipd3-1 Physcomitrella.

Our previous studies of CCaMK/IPD3-mediated signaling in Physcomitrella demonstrated a causal role of CCaMK and IPD3 in ABA synthesis and downstream drought-associated phenotypes. We sought to test if IPD3-mediated ABA signaling is mechanistically linked to the wwr phenotype of *Ppipd3-1* moss. The dark-gravitropism

assays were repeated with wild-type or *Ppipd3-1* moss grown on standard sucrose-supplemented medium or medium also supplemented with ABA or abamine, a pharmacological inhibitor of ABA synthesis. In all conditions tested, the gravitropic preferences of caulonema were unaltered in both wild-type and *Ppipd3-1* strains (**Figure 2b**).

Ppccamk-1 caulonema display typical response when negative gravitropism is promoted.

In symbiotic signaling, IPD3 phosphorylation and transcriptional activity lies immediately downstream of the kinase activity of CCaMK, as has been elucidated in legume and monocot genetic models (Singh *et al.*, 2014). Therefore, we hypothesized that *Ppccamk-1* mutant moss would similarly display atypical gravitropic activity of dark-grown caulonema. When grown on upright sugar-supplemented media in the darkness, *Ppccamk-1* caulonema displayed the typical preference for negative gravitropism as seen in wild-type (**Figure 2c**).

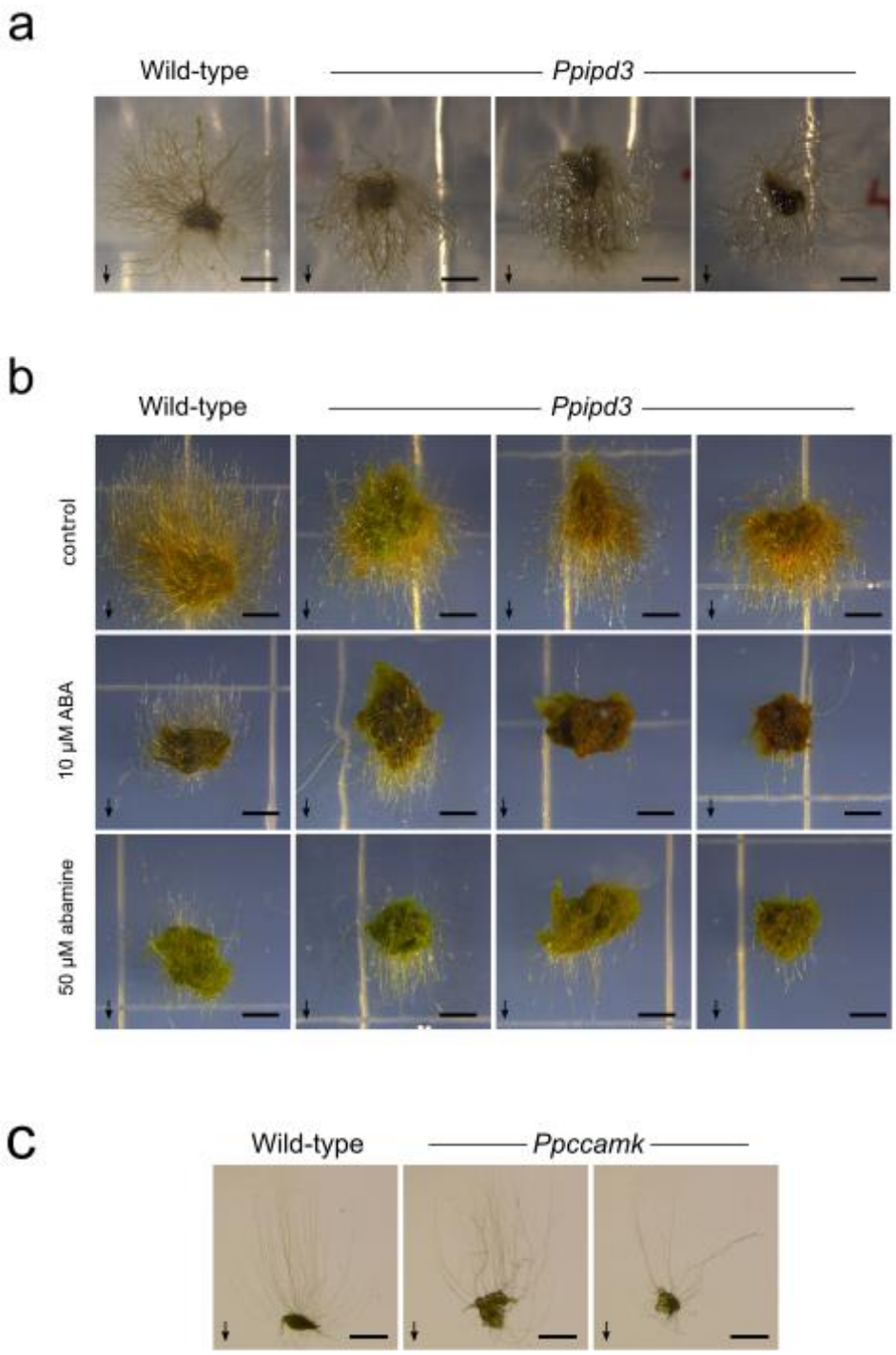

Figure 2: *Ppipd3-1* mutant caulonema display a 'wrong-way-response' and the phenotype is not rescued by modulating ABA signaling.

a) Wild-type and *Ppipd3* protonema was acclimated to sugar containing medium before being shielded from light to encourage negative gravitropism of caulonemal filaments. Arrows indicate the direction of the gravity vector. Scale bar = 2 mm. Three independent mutant lines were tested (**legend continued on next page**)

Ppipd3 mutant moss caulonema have a 'wrong-way-response' (wwr) phenotype where dark-grown caulonema grow in the direction of the gravity vector, whereas wild-type grows against the gravity vector. *Ppipd3-1* caulonema also showed a distinctive uncoordinated, waving pattern of growth, of which Supplementary Video 1 shows over long-term growth.
b) ABA or abamine, an ABA synthesis inhibitor, had no effects on the directionality of dark-grown caulonema. Higher concentrations of ABA supplementation also had no affects upon directionality (**Supplementary Figure 1**).
c) *Ppccamk* mutant caulonema grow against the gravity vector similar to wild-type. Arrows indicate the direction of the gravity vector. Scale bar = 2 mm. Two independent mutant lines were tested.

ccamk and ipd3 mutants of Medicago truncatula and rice do not display abnormal root gravitropism.

In angiosperms, CCaMK and IPD3 are expressed and active in root tissues (Levy *et al*., 2004; Messinese *et al.*, 2007; Chen *et al.*, 2008). As such, we sought to test if *CCaMK* or *IPD3* loss-of-function in angiosperms results in abnormal gravitropism of growing roots. Medicago seedlings of *ccamk-1* and *ipd3-1* and rice seedlings of *ccamk-1* were gravistimulated by rotating 90 degrees prior to growth and analyzing the angle of bending at root tips. Secondary and primary roots were analyzed in rice, however only secondary roots were analyzed for Medicago as primary roots were weakly or unresponsive to gravistimulation in all lines. No differences were observed in rice or Medicago between all lines tested **(Figure 3a,b)**.

3.4 - Discussion

The wwr phenotype of *Ppipd3-1* was certainly unexpected. Similar wwr mutant phenotypes have been described in Physcomitrella and Ceratodon, however the causal mutations are currently unmapped (Wagner *et al.*, 1997). Indicated by mutant complementation crosses, it is likely that the currently known wwr phenotype in

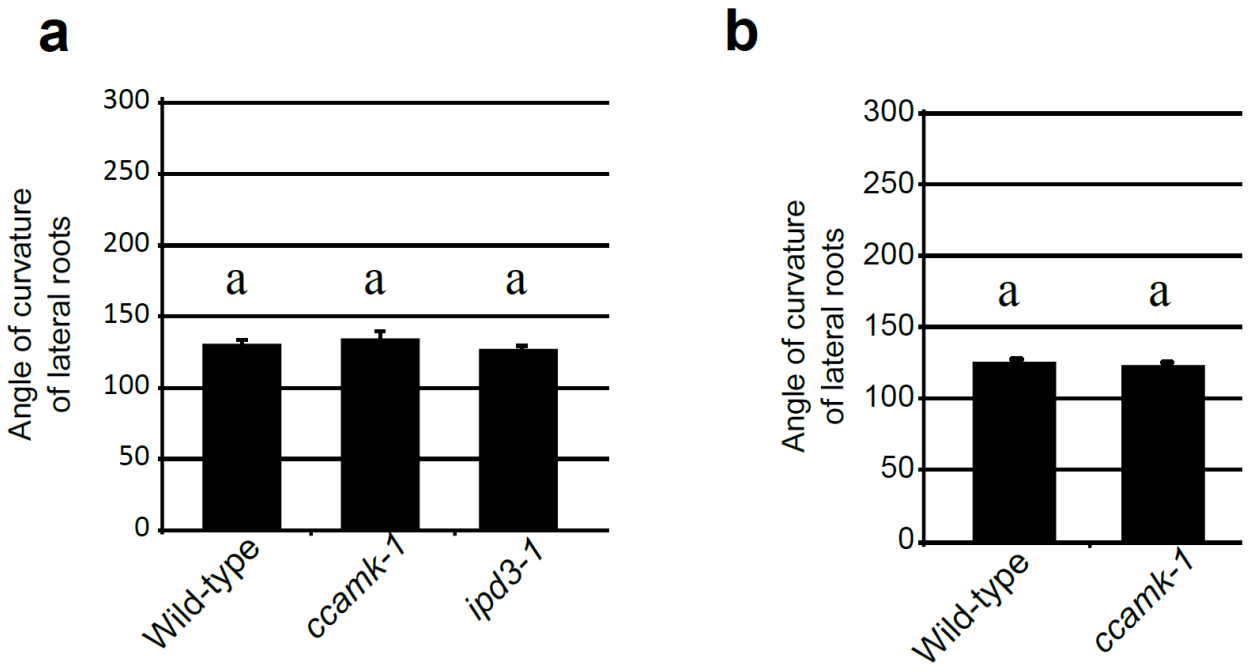

Figure 3: Symbiotic signaling mutants in Medicago and rice do not display abnormal gravitropic responses in roots.

Seedlings of wild-type/mutant Medicago (a) or rice (b) were plated onto modified Fahraeus medium. Plates were turned 90 degrees to encourage gravistimulation of lateral roots, prior to measurement of the angle of lateral root curvature. Neither *ccamk-1* or *ipd3-1* mutants in Medicago nor *ccamk-1* mutants in rice displayed abnormal gravitropism of roots.

Physcomitrella is due to the loss-of-function of one locus, however this hasn't been experimentally verified.

The role and effects of ABA in moss stress signaling have been of considerable interest to bryologists. Exogenous application of ABA to mosses faithfully triggers drought-like responses, including the development of brachycytes and expression of drought-associated genes (Duckett & Ligrone, 1992; Shinde *et al.*, 2012; Arif *et al.*, 2019). That we could not reverse or alter the polarity of dark-grown caulonema by supplementation of ABA or abamine suggests that IPD3's role in downstream ABA signaling is mechanistically uncoupled to its loss-of-function wwr phenotype and that IPD3

likely has a pleiotropic role in moss development. Furthermore, the absence of any gravitropic phenotype in *Ppccamk-1* moss suggests that the gravitropic defects of *Ppipd3-1* moss are mechanistically uncoupled to the calcium-regulated activity of CCaMK relative to IPD3.

Gravitropic mechanisms in moss tip-growing cells are likely similar to those of the tip growing cells of *Chara*, involving the sedimentation of organelles/particles upon the membrane and cell wall of actively curling filaments (Hodick, 1994). Our results suggest IPD3 has no involvement in root gravitropism of angiosperms. It should be noted that root gravitropisms are governed by the activity of amyloplasts in columella cells, which is mechanistically distinct from the tip growth mechanisms of *Chara* or mosses. Furthermore, to our knowledge, there are no descriptions of gravitropic phenotypes or mechanisms reported in any tip growing cells of angiosperms, including root hairs or pollen tubes. However, the Medicago *dmi2-1* mutant, which is defective in a critical signaling component upstream of CCaMK and IPD3, has a non-symbiotic defect upon the tip growth of root hairs. When *dmi2-1* root hairs were mechanically stressed, changes occurred in the cytoplasmic architecture near the tip that are distinct from wild-type (Esseling *et al.*, 2004). Mechanical stimulation of epidermal root cells by microneedle or AMF is associated with cytoplasmic aggregation of organelles. The Medicago *ccamk-1* mutant lost this aggregation response to mechanical stress (Genre *et al.*, 2009). It remains unexplored if similar tip growth or mechanical stress phenotypes are also observed in *ipd3* mutant legumes. One might hypothesize that the CSP between mosses and angiosperms share mechanistic roles in tip growth despite that root hairs are not gravitropic. In Medicago, the LCO receptor mutant, *nod factor perception,* is deficient in

inducing a rapid calcium flux in the tips of root hairs in response to LCOs (Amor *et al.*, 2003). Calcium signaling at the tips of growing filaments of Physcomitrella is strongly correlated to directional growth (Bascom *et al.*, 2018). Overall, it appears in angiosperms that various CSP signaling components are involved in calcium signaling, cytoplasmic organization, and mechanical stress response in root hairs. Although root hairs themselves are not gravitropic, it is interesting to note that all of these cellular processes are mechanistically related to tip growth, gravitropism, or effecting the direction of gravitropism, in moss caulonema. There are characteristic organizations of dense organelles/particles in the tips of moss caulonemal cells with gravitropic phenotypes. An agravitropic Physcomitrella mutant showed an absence of the regularly dense set of organelles at the tips of caulonema (Jenkins *et al.*, 1986). Likewise, in a wwr mutant of Ceratodon, positively gravitropic caulonema had an unusually dense packing of these organelles in caulonemal tips (Wagner *et al.*, 1997). As such, it appears the Physcomitrella *Ppipd3-1* mutant is defective in a process that is governed by calcium signaling, the activity of organellular movement, and the mechanical stimulation of those movements in caulonemal tips. This suggests there may be a connection between angiosperms and mosses in tip growth regulation by the CSP, although it doesn't appear to be gravitropism.

The mechanism by which IPD3 loss-of-function causes the wwr phenotype is still enigmatic. Despite that gravitropic mechanisms vary greatly, especially between complex tissues and filamentous tissues, they are typically separated into similar stages: gravity sensing, signal transduction, and subsequent gravitropic growth response. The main distinction in filamentous tissues like moss caulonema is that these processes are likely

confined to apical cells. As such, the morphology, behavior, and molecular biology of apical caulonema cells would provide a simplistic model for elucidating the effects of IPD3 upon gravitropism in mosses.

3.5 - Methods and Materials

Plant material

All Physcomitrella strains used in this study are derived from the common type strain, wild-type Gransden isolate. The *Ppccamk-1* and *Ppipd3-1* mutants used were described previously **(Ch. 2, Kleist *et al.*, in preparation).** For *Medicago truncatula* experiments, the Jemalong, A17 was used including the *ccamk-1* and *ipd3-1* mutants. For *Oryza sativa* experiments, the cultivar Nipponbare was used including the *ccamk-1* and *ipd3-1* Tos17 mutants.

Long-term imaging of Physcomitrella caulonema

One-week-old protonemata of wild-type or *ipd3-1* moss was gently homogenized in water prior to injection in into polydimethylsiloxane microfluidic chambers described previously (Bascom *et al.*, 2016). The polydimethylsiloxane chambers were subsequently filled with liquid Hoagland's medium and incubated on a microscope stage for imaging. For long-term brightfield imaging, images were acquired with a TIE body with an automated stage. Imaging was performed with a 20X objective and images were acquired with a Ds-Fi1 camera. Samples were continuously illuminated from above with an external 60-watt fluorescent bulb positioned above the microscope stage.

Growth conditions for Physcomitrella gravitropism experiments

Moss lines were maintained and bulked on standard BCDAT pH 6.0 medium, at 20° C, under 40 μmol/m^2/s of light intensity of cool white light, using a 16 hour/8 hour light/dark cycle. For gravitropism experiments, two-week-old moss protonemata was transferred to standard BCD pH 6.5 medium supplemented with 0.5% sucrose. To promote negative gravitropism of caulonema, culture plates were covered with aluminum foil and placed upright during the growth period. To minimize plate to plate effects, all lines were grown in each culture plate used. Media supplementation with abscisic acid (ABA) or abamine during gravitropism experiments was carried out at the concentrations indicated.

Infrared imaging of Physcomitrella caulonema during dark-growth gravitropism experiments

Wild-type or *Ppipd3-1* moss was grown on standard BCD pH 6.5 plates supplemented with 0.5% sucrose, as was done for end-point gravitropism experiments. Time-lapse digital images were acquired in a dark-room at 10-minute intervals for 21 days by CCD Marlin F-146B cameras using infrared light.

Growth conditions for Medicago truncatula and Oryza sativa gravitropism experiments

Prior to plating on growth medium, *Medicago truncatula* seeds were scarified in neat sulfuric acid for 8 minutes, rinsed 5 times with sterile water, sterilized in commercial bleach for 2 minutes, then rinsed another 5 times in sterile water and imbibed on 1% agar

plates with 1 μM gibberellic acid for 2 days at 4° C, followed another day at room temperature in darkness to germinate.

Rice seeds had the seedcoat removed, and were gently shaken for 15 minutes in commercial bleach, rinsed 5 times in sterile water and shaken overnight in water to imbibe. They were germinated via a 3 day incubation at room temperature in the dark on 1% agar plates with 1 μM gibberellic acid.

Seedlings were placed on large plates (modified Fahraeus medium with 1 mM ammonium nitrate) overlayed with germination paper to allow growth (Catoira *et al.*, 2000). Plants were grown for 18 days at 25° C, with 16 hour days of 100 μM/m^2/s cool white light. Plates were rotated 90 degrees in order to gravistimulate seedling roots. After 5 more days of growth, the bending angle of primary and secondary roots was measured. Primary roots were not assessed as most plants of both wild-type and mutant lines responded to gravistimulation by cessation of primary root growth.

Author Contributions

A.B., T.B.I., C.J.B., A.H., E.S., M.B., and J.-M.A. designed the research. A.B., T.B.I., C.J.B., A.H., M.B performed the experiments. A.B., T.B.I., C.J.B., M.B, and J.-M.A analyzed the data. A.B. and J.M.A. wrote the paper with assistance and input from all authors.

3.6 - Acknowledgements

A.B. was funded through an NIH Training Grant to the Laboratory of Genetics (grant # 5T32GM007133-40) and by the NSF Graduate Research Fellowship Program (grant # DGE-1256259. T.J.K. was funded in part by the NSF Graduate Research Fellowship

Program (grant # DGE-1106400). This work was supported in part by the Vilas Faculty Young/Mid-Career Award to J.M.A.

3.7 - Supplementary Figures

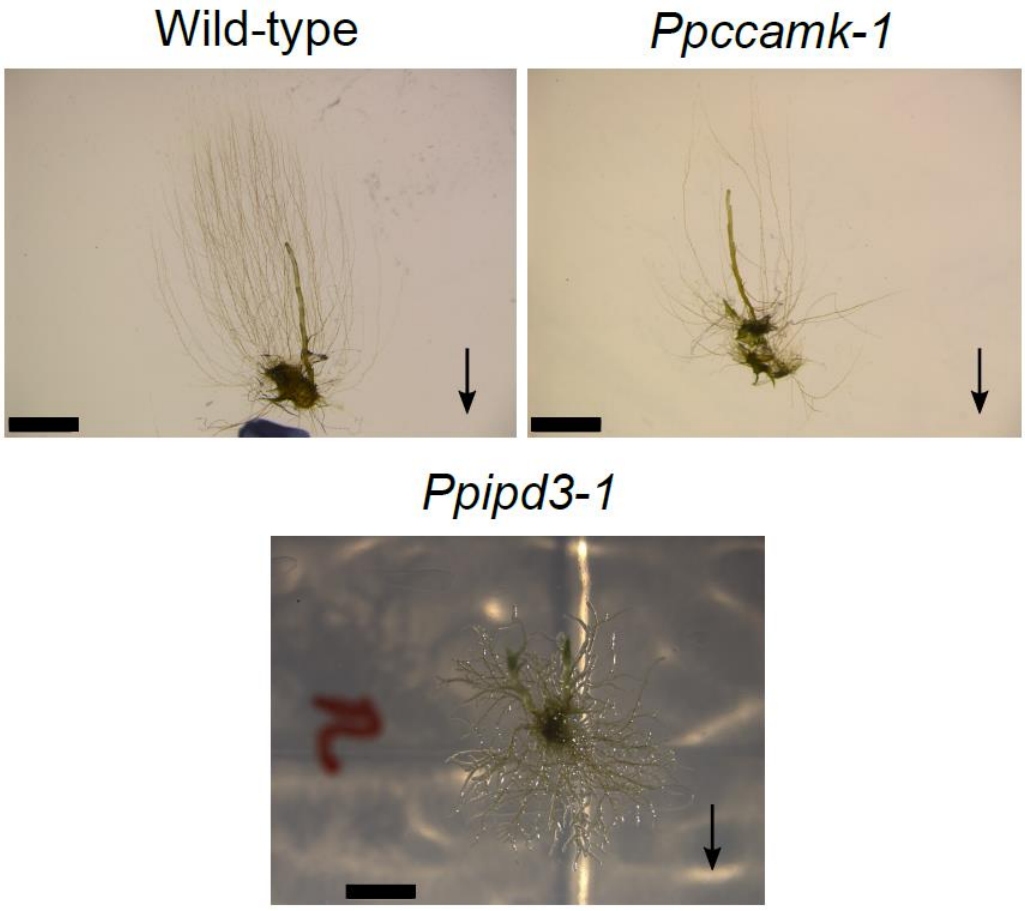

Supplementary Figure 1: Gametophores of wild-type, *Ppccamk-1,* and *Ppipd3-1* all display typical negative gravitropism of etiolated gametophores.

Gametophores in wild-type normally grow against the gravity vector. The same is true for *Ppccamk-1* and *Ppipd3-1*. This suggests the IPD3-related gravitropisms are specific to caulonemal cells. Arrows indicate the direction of the gravity vector. Scale bars = 2 mm.

3.8 - Supplementary Video Figure Legends

Supplementary Video 1. Time-scale growth of Physcomitrella wild-type compared to *Ppipd3-1.*

Small pieces of wild-type of Ppipd3-1 tissue from one-week-old cultures were incubated on sugar-supplemented media placed upright, and imaged in darkness for three weeks. Ppipd3-1 caulonemal growth is reversed and uncoordinated compared to wild-type. Scale bar = 2 mm.

3.9 - References

Hodick D. **1994**. Negative gravitropism in *Chara* protonemata : A model integrating the opposite gravitropic responses of protonemata and rhizoids. **195**: 43–49.

Amor B Ben, Shaw SL, Oldroyd GED, Maillet F, Penmetsa RV, Cook D, Long SR, Dénarié J, Gough C. **2003**. The *NFP* locus of *Medicago truncatula* controls an early step of Nod factor signal transduction upstream of a rapid calcium flux and root hair deformation. *Plant Journal* **34**: 495–506.

Arif MA, Hiss M, Tomek M, Busch H, Meyberg R, Tintelnot S, Reski R, Rensing SA, Frank W. **2019**. ABA-induced vegetative diaspore formation in *Physcomitrella patens*. *Frontiers in Plant Science* **10**: 1–18.

Bascom CS, Winship LJ, Bezanilla M. **2018**. Simultaneous imaging and functional studies reveal a tight correlation between calcium and actin networks. *Proceedings of the National Academy of Sciences of the United States of America* **115**: E2869–E2878.

Bascom CS, Wu SZ, Nelson K, Oakey J, Bezanilla M. **2016**. Long-term growth of moss in microfluidic devices enables subcellular studies in development. *Plant Physiology* **172**: 28–37.

Capoen W, Sun J, Wysham D, Otegui MS, Venkateshwaran M, Hirsch S, Miwa H, Downie JA, Morris RJ, Ané J-M. **2011**. Nuclear membranes control symbiotic calcium signaling of legumes. *Proceedings of the National Academy of Sciences* **108**: 14348–

14353.

Catoira R, Galera C, De Billy F, Penmetsa R V., Journet EP, Maillet F, Rosenberg C, Cook D, Gough C, Denarie J. **2000**. Four genes of *Medicago truncatula* controlling components of a Nod factor transduction pathway. *Plant Cell* **12**: 1647–1665.

Chen C, Ané J, Zhu H. **2008**. OsIPD3, an ortholog of the *Medicago truncatula* DMI3 interacting protein IPD3, is required for mycorrhizal symbiosis in rice. *New Phytologist* **180**: 311–315.

Delaux P-M, Radhakrishnan G V., Jayaraman D, Cheema J, Malbreil M, Volkening JD, Sekimoto H, Nishiyama T, Melkonian M, Pokorny L, *et al.* 2015. Algal ancestor of land plants was preadapted for symbiosis. *Proceedings of the National Academy of Sciences* **112**: 201515426.

Delaux PM, Varala K, Edger PP, Coruzzi GM, Pires JC, Ané JM. **2014**. Comparative phylogenomics uncovers the impact of symbiotic associations on host genome evolution. *PLoS Genetics* **10**.

Duckett JG, Ligrone R. **1992**. A survey of diaspore liberation mechanisms and germination patterns in mosses. *Journal of Bryology* **17**: 335–354.

Esseling JJ, Lhuissier FGP, Emons AMC. **2004**. A nonsymbiotic root hair tip growth phenotype in *NORK*-mutated legumes: Implications for modulation factor-induced signaling and formation of a multifaceted root hair pocket for bacteria. *Plant Cell* **16**: 933–944.

Genre A, Ortu G, Bertoldo C, Martino E, Genre A, Ortu G, Bertoldo C, Martino E, Bonfante P, Vegetale B, *et al.* 2009. Biotic and abiotic stimulation of root epidermal cells reveals common and specific responses to arbuscular mycorrhizal fungi. **149**: 1424–1434.

Grosche C, Genau AC, Rensing SA. **2018**. Evolution of the symbiosis-specific gras regulatory network in bryophytes. *Frontiers in Plant Science* **871**: 1–13.

J. Levy, C. Bres, R. Geurts, B. Chalhoub, O. Kulikova, G. Duc, EP Journet, JM Ane, E. Lauber, T. Bisseling, J. Denarie, C. Rosenberg FD. **2004**. A putative Ca2+

and calmodulin-dependent protein kinase required for bacterial and fungal symbioses. *Science* **303**: 1361–1364.

JENKINS GI, COURTICE GRM, COVE DJ. **1986**. Gravitropic responses of wild-type and mutant strains of the moss *Physcomitrella patens*. *Plant, Cell & Environment* **9**: 637–644.

Kern VD, Schwuchow JM, Reed DW, Nadeau JA, Lucas J, Skripnikov A, Sack FD. **2005**. Gravitropic moss cells default to spiral growth on the clinostat and in microgravity during spaceflight. *Planta* **221**: 149–157.

Maclean AM, Bravo A, Harrison MJ. **2017**. Plant signaling and metabolic pathways enabling arbuscular mycorrhizal symbiosis. *Plant Cell* **29**: 2319–2335.

Maillet F, Poinsot V, André O, Puech-Pagés V, Haouy A, Gueunier M, Cromer L, Giraudet D, Formey D, Niebel A, *et al.* 2011. Fungal lipochitooligosaccharide symbiotic signals in arbuscular mycorrhiza. *Nature* **469**: 58–64.

Messinese E, Mun J-H, Yeun LH, Jayaraman D, Rougé P, Barre A, Lougnon G, Schornack S, Bono J-J, Cook DR. **2007**. A novel nuclear protein interacts with the symbiotic DMI3 calcium-and calmodulin-dependent protein kinase of *Medicago truncatula*. *Molecular Plant-Microbe Interactions* **20**: 912–921.

Oldroyd GED. **2013**. Speak, friend, and enter: signalling systems that promote beneficial symbiotic associations in plants. *Nature Reviews Microbiology* **11**: 252–263.

Pimprikar P, Carbonnel S, Paries M, Katzer K, Klingl V, Bohmer MJ, Karl L, Floss DS, Harrison MJ, Parniske M. **2016**. A CCaMK-CYCLOPS-DELLA complex activates transcription of *RAM1* to regulate arbuscule branching. *Current Biology* **26**: 987–998.

Prigge MJ, Bezanilla M. **2010**. Evolutionary crossroads in developmental biology: *Physcomitrella patens*. *Development* **137**: 3535–3543.

Redecker D, Kodner R, Graham LE. **2000**. Glomalean fungi from the Ordovician. *Science* **289**: 1920–1921.

Remy W, Taylor TN, Hass H, Kerp H. **1994**. Four hundred-million-year-old vesicular

arbuscular mycorrhizae. *Proceedings of the National Academy of Sciences of the United States of America* **91**: 11841–11843.

Shinde S, Nurul Islam M, Ng CK. **2012**. Dehydration stress-induced oscillations in LEA protein transcripts involves abscisic acid in the moss, *Physcomitrella patens*. *New Phytologist* **195**: 321–328.

Singh S, Katzer K, Lambert J, Cerri M, Parniske M. **2014**. CYCLOPS, A DNA-binding transcriptional activator, orchestrates symbiotic root nodule development. *Cell Host and Microbe* **15**: 139–152.

Toyota M, Gilroy S. **2013**. Gravitropism and mechanical signaling in plants. *American Journal of Botany* **100**: 111–125.

Wagner TA, Cove DJ, Sack FD, Wagner TA, Cove DJ, Sack FD. **1997**. A positively gravitropic mutant mirrors the wild-type protonemal response in the moss *Ceratodon purpureus*. *Planta* **202**: 149–154.

Wang B, Qiu Y-LYL. **2006**. Phylogenetic distribution and evolution of mycorrhizas in land plants. *Mycorrhiza* **16**: 299–363.

Wang B, Yeun LH, Xue JY, Liu Y, Ané JM, Qiu YL. **2010**. Presence of three mycorrhizal genes in the common ancestor of land plants suggests a key role of mycorrhizas in the colonization of land by plants. *New Phytologist* **186**: 514–525.

Chapter 4 - Development of tools for genetic transformation of zygnematalean algae

4.1 – Introduction

The colonization of land by plants roughly 500 million years ago (MYA) had far-reaching effects upon the Earth's biota and environment. Studying the genetics and molecular biology of streptophytes is necessary to understand the critical innovations that allowed plants colonized land and dominate the landscape. The streptophytes are a monophyletic clade, and encompass a large diversity of green plants that can be mainly split into two subgroups: the embryophytes, colloquially referred to as "land plants", and the charophyte algae.

Like land plants, charophytes are diverse in morphology, behavior, and habitat. In the vegetative growth state, the various clades of charophytes show examples of unicellular, filamentous, and filamentous-branched species (**Figure 1**). The charophytes also consist of both microalgae, such as unicellular desmids, and macrophyte algae, such as the large "stoneworts" of the Charales. Charophytes are generally associated with oligotrophic freshwater environments, however they can often be found in areas with fluctuating water availability, soil, or even aeroterrestrial habitats. Like land plants and other algae, charophytes are known to form many and diverse epiphytic interactions with bacteria and fungi (Knack *et al.*, 2015).

Given that land plants emerged from a charophyte ancestor, investigating the contrasts between extant land plants and charophytes is key to elucidating critical evolutionary innovations that permitted plant terrestrial colonization (Kenrick & Crane, 1997). Determining the presence and absence of genes such as regulators, transcription

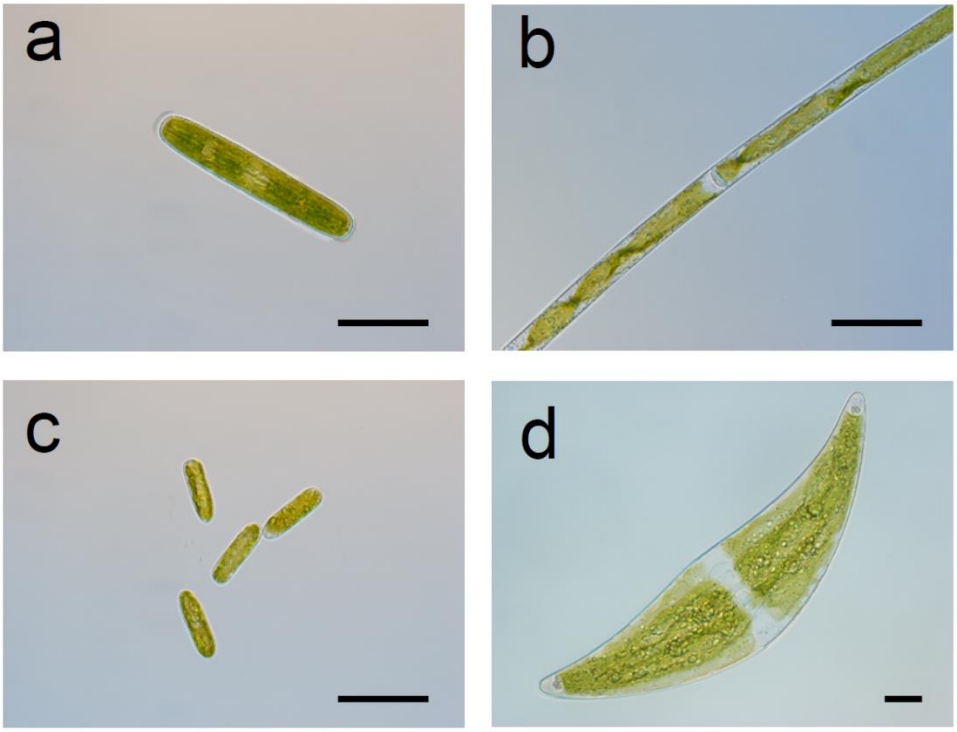

Figure 1: Examples of zygnematalean algae used in these transformation studies.

a) *Penium margaritaceum*, previously transformed via *Agrobacterium tumefaciens* (Sorensen, *et al.* 2014)
b) *Mougeotia transeaui*.
c) *Mesotaenium caldariorum*.
d) *Closterium sp.*
These four algal species all belong to the Zygnematophyceae, known to undergo cell-to-cell conjugation to form diploid zygospores under stressful conditions. All scale bars = 50 μm.

factors or assemblies of signaling pathways is a key component of such comparative studies.

Interest in the genomics of green algae has increased substantially in the last decade. The recent 1,000 Plant Genomes project (1KP) has included 171 green algal transcriptomes, including the transcriptomes of 38 Zygnematalean species (Wickett *et al.*, 2014). One genome of the Charophyceae and two genomes of the Zygnematales, close to the branching point of land plants, have been published (Nishiyama *et al.*, 2018; Cheng

et al., 2019). Recent phylogenomic and transcriptomics analysis of the 1KP data has demonstrated the conspicuous presence of common symbiosis signaling pathway genes in later diverging lineages of charophytes, sometimes referred to as ‘advanced charophytes’ (Delaux *et al.*, 2015b). These revelations were surprising considering that to date, the function of the common symbiosis signaling pathway has been understood to be specific to mediating the interactions of land plants to arbuscular mycorrhizal fungi or root-nodulating bacteria, neither of which have been described in algae. Even the latest-diverging charophytes emerged prior to the estimated emergence of arbuscular mycorrhizal interactions. This has raised considerable questions about the cellular function(s) and the biological relevance of these homologs in late-diverging charophytes. Understanding the activity of such genes and the consequence of their activity or mutation would provide valuable insight into the evolutionary history of this conserved plant signaling pathway and how it shaped the evolution of these lineages.

Unfortunately, the lack of reliable and scalable genetic transformation techniques of charophytes is a major hindrance to studying the conserved and divergent nature of these taxa, and thus the understanding of critical innovations of land plant colonization. A few examples of transformation have been reported in two unicellular and one filamentous zygnematalean species, all by microparticle bombardment, however only the example of *Closterium* was verified as stable (Vannerum *et al.*, 2010; Abe *et al.*, 2011; Regensdorff *et al.*, 2018). Stable transformation of *Penium margaritaceum* has been reported using *Agrobacterium tumefaciens*, sidestepping the need for expensive reagents and equipment, however to our knowledge has not been replicated since (Sørensen *et al.*, 2014). We sought to cast a wide net with regards to species and transformation

techniques in order to develop a more reliable system to study the genetics of CSP homologs in these algae.

4.2 – General Materials and Methods

Plasmid construction

The G-GECO1.2 visual reporter plasmid TB70 and the ZsGREEN visual reporter plasmids TB4, TB5, and TB6 were constructed using in-house designed, synthesized DNA parts (SynBiotech) and DNA parts previously described according to the MoClo Golden Gate construction rules (Matz *et al.*, 1999; Weber *et al.*, 2011; Engler *et al.*, 2014). More detailed descriptions of the DNA parts used and their origins can be found in **Supplemental Table 1**.

Unialgal strains

Penium margaritaceum was isolated from a creek in Saratoga Springs, New York and provided by David Domozych. *Closterium sp.* was isolated from Bright Lake in Packwaukee, Wisconsin. The following strains were purchased from the Culture Collection of Algae and The University of Texas at Austin (UTEX): *Zygnema sp.* (UTEX LB 923), *Mougeotia transeaui* (UTEX LB 2496), *Mesotaenium caldariorum* (UTEX 41).

Algal culture conditions

All algal strains were grown and maintained in Woods Hole Medium (WHM) supplemented with thiamine, biotin, and cyanocobalamin, and soil extract water (Carolina Biological Supply). For the nutrient starvation step in *Agrobacterium*-mediated transformations, Mating Induction (MI) medium was used. Detailed descriptions of the formulation of these media can be found in **Supplemental Table 2**. Slight modifications

to the formulation of WHM are indicated in the body of the Results section. When indicated, WHM and MI were used with the addition of 1% High Gel Strength Agar (Sigma) in petri plates. All strains were grown at 20° Celsius, under 40 µmol/m^2/s of cool white light, using a 16/8-hour light/dark cycle. For routine strain maintenance, strains were grown for four weeks at a time in WHM prior to being diluted 1,000-fold into fresh WHM. For all transformation methods described, two-week-old cultures were used.

4.3 – *Agrobacterium*-mediated transformation

For decades, *Agrobacterium tumifaciens* and *Agrobacterium rhizogenes*, the causative pathogens of crown galls and root galls, have been used for genetic engineering of plants through the horizontal transfer of transgene-containing Ti/Ri plasmids or T-DNA-containing engineered plasmids (Zambryski *et al.*, 1989; Zambryski, 1992; Zupan *et al.*, 2000). Horizontal transfer occurs through a bacterial conjugation-like mechanism involving the bridging of the bacterial and plant cytoplasm. These horizontal T-DNA transfer methods have been used with success in many model plant systems from *Arabidopsis thaliana*, to the liverwort *Marchantia polymorpha*, to the chlorophyte alga *Chlamydomonas reinhardtii* (Clough & Bent, 1998; Kumar *et al.*, 2004; Ishizaki *et al.*, 2008).

The *Agrobacterium*-mediated transformation of the model desmid *P. margaritaceum* has been reported more recently (Sørensen *et al.*, 2014). This method held two main advantages over the previous reports of particle bombardment in *Closterium peracerosum–strigosum–littorale complex* (*C. psl complex*) and *Micrasterias denticulata*; first, *Agrobacterium*-mediated transformation does not require expensive equipment and reagents such as the Biolistic PDS-1000/He Particle Delivery System or

gold microparticles, and second, *Agrobacterium*-mediated transformation is more associated with single-copy transgene integration in order to produce more easily characterized genetic lines (Vannerum *et al.*, 2010; Abe *et al.*, 2011; Jackson *et al.*, 2013). The proposed mechanism of transformation relied on the induction of cell-to-cell conjugation by incubation of cultures in low-nutrient 'mating induction' (MI) medium, where allegedly such conjugating pairs of cells were more susceptible to conjugation with transgene-carrying *A. tumefaciens* at the site of the conjugation papillae. However, it is worth noting that no evidence of cell-to-cell conjugation was actually reported (Tsuchikane *et al.*, 2011; Sørensen *et al.*, 2014).

Given its simplicity, we aimed to repeat this method of transformation. We used a panel of *Agrobacterium* strains and a panel of fluorescent protein-expressing plasmids. To help ensure faithful replication of the established method, we used the identical strains of *P. margaritaceum* and *A. tumefaciens* GV2260 as well as the in-house-developed pART27 visual reporter plasmid, coding for an endoplasmic reticulum-localized Red Fluorescent Protein (ER-RFP), reported by the authors (Gleave, 1992; Sørensen *et al.*, 2014). The base protocol from the original authors is described below; after which modifications to the base protocol that were tested are further discussed.

Base protocol for Agrobacterium-mediated transformation of Penium margaritaceum (Sørensen et al., 2014)

Reagents and Biological Materials. Full descriptions of media and expression plasmids used can be found in the supplemental sections at the end of this chapter.

- *P. margaritaceum*, isolated by David Domozych, Saratoga Springs, NY, USA
- *A. tumefaciens* GV2260, electrocompetent
- pART27, ER-RFP
- 2 mm electroporation cuvettes
- GenePulser 2 (BioRad) or equivalent electroporation device
- Lysogeny broth (LB), sterilized
- Woods Hole Medium (WHM), both liquid, and 1% agar plates, sterilized
- Mating induction medium (MI), liquid, sterilized
- 50 mg/mL spectinomycin stock dissolved in sterile water
- 50 mg/mL kanamycin stock dissolved in sterile water
- 500 mg/mL cefotaxime stock dissolved in sterile water
- 500 mM acetosyringone stock dissolved in dimethylsulfoxide

Transformation of Agrobacterium tumefaciens

1. Thaw 100 µL aliquot of electrocompetent GV2260 on ice for 10 minutes.
2. Add 200uL of miniprep-quality pART27-ER-RFP plasmid and incubate on ice for 10 minutes.
3. Add cell/plasmid mixture to pre-chilled 2 mm electroporation cuvette and electroporate at 2.5 kV.
4. Plate on LB supplemented with 50 µg/mL spectinomycin and incubate for 48 hours at 28° Celsius to recover individual colonies.
5. Genotype colonies for the presence of the ER-RFP coding sequence by colony-PCR prior to liquid culture for algal transformation.

Transformation of Penium margaritaceum

1. Seventy-two hours prior to co-culture, to prepare algal cells, pellet a 50 mL liquid culture that is in the logarithmic phase of growth* at 1620 relative centrifugal force (rcf) for 1 minute. (*It is best to harvest a culture that is at 2 weeks of age after 1,000-fold dilution from a previous culture).
2. Wash the algal pellet twice in sterile MI medium, using the same centrifugation conditions.
3. Resuspend washed algal pellet in 50 mL MI medium and incubate on orbital shaker at 60 rpm using general algal growth conditions.
4. Twenty-four hours prior to co-culture with algae, inoculate bacterial colony into 5 mL LB broth supplemented with 50 µg/mL spectinomycin, and incubate at 28° Celsius shaking at 230 rpm.
5. On the day of co-culture, pellet bacteria at 1620 rcf for 15 minutes and resuspend in MI medium supplemented with 500 µM acetosyringone to OD_{600} = 1.0.
6. Incubate cell suspension at room temperature, on an orbital platform at 300 rpm, in darkness, for 3 hours.

7. After 3 hour bacterial incubation, pellet cells using previous centrifugation conditions and resuspend cells to OD_{600} = 2.5 in fresh MI supplemented with 500 µM acetosyringone. Keep this cell suspension ready to mix with algae.
8. After the 72 hour algal MI medium incubation, pellet cells using previous centrifugation conditions and resuspend cells in 250 µL fresh MI medium supplemented with 500 µM acetosyringone.
9. Gently mix 250 µL of bacterial suspension with the 250 µL algal suspension and plate onto the middle of an MI 1% agar medium plate. (Note: there is no need to spread this suspension around the plate, simply plate and leave as a large droplet to dry in the center of the plate.
10. Parafilm the plate and incubate at general algal growth conditions for 24 hours.

Agrobacterium negative selection

1. Wash algal cells off of MI medium plate into 15 mL of WHM medium supplemented with 500 µg/mL cefotaxime and incubate this cell suspension on orbital shaker at 60 rpm at room temperature for 15 minutes.
2. Centrifuge algal suspension at 1620 rcf for 15 seconds and resuspend algal pellet in fresh WHM medium supplemented with 500 µM acetosyringone.
3. Incubate algal suspension under general algal growth conditions, on an orbital shaker at 60 rpm for 5 days to select against *Agrobacterium*.

Antibiotic selection of transgene-expressing algae

1. After the initial negative selection against *Agrobacterium*, pellet algae at 1,620 rcf for 1 minute. Resuspend algal pellet in fresh WHM supplemented with 500 µg/mL cefotaxime and 50 µg/mL kanamycin* (*kanamycin was used for the pART27-ER-RFP expression plasmid, and this reagent should be adjusted accordingly depending on the binary vector used).

Notes on base protocol conveyed personally from the original authors

- Steps where gentle pipetting of cell suspensions is needed, single-use plastic bulb pipettes are useful.
- The authors have not witnessed cell-to-cell conjugation upon incubation in MI medium with this New York-derived strain of *P. margaritaceum*.
- In assessing individual cells post-transformation, when observing chlorophyll autofluorescence (which is seen as two red lobes directly flanking the nucleus and run the length of the two semi-cells), bright red puncta are indicative of compromised chloroplasts and a dying cell.
- If the starting algal cells appear unhealthy, partly indicated by shrunken chloroplasts, do not bother proceeding with MI medium incubation or transformation protocol. Make a very dilute fresh culture and start from scratch.
- Antibiotic selection after the negative selection of *Agrobacterium* is not necessary when expressing visual reporters. Visual selection can be performed after the 5-day *Agrobacterium* negative selection step.

Summary of *Agrobacterium*-mediated transformation trials and results

In numerous trials, using identical algal and bacterial strains, including the visual reporter plasmid published in the original methods article, we have not been able to replicate transformation of *P. margaritaceum*. After these unsuccessful trials, we attempted multiple modifications to the original protocol (summarized below) including the use of a panel of *Agrobacterium* species on *P. margaritaceum*, the use of *A. tumefaciens* GV2260 on a panel of algal species, culture conditions to reduce mucilage secretion in *P. margaritaceum*, and a method to potentially reduce physical disruption of conjugating pairs of *P. margaritaceum* cells.

Table 1. Summary of Agrobacterium-mediated transformation trials of P. margaritaceum.

Overall, five species of algae and *Agrobacterium* were used in accordance to the published method (Sørensen *et al.*, 2014). In all cases, a vector verified to have functioned in *P. margaritaceum* was used, expressing an ER-localized RFP derived from the authors of the original protocol. No instances of transformation were observed.

Alga	Volume (mL)	Agrobacterium	Modifications	trials
P. margaritaceum	50	*A. rhizogenes* MSU440	none	2
	100	*A. tumefaciens* GV2260	none	5
	50	*A. rhizogenes* ARQUA1, *A. rhizogenes* 18r12v	none	1
	100	*A. tumefaciens* GV2260	10x $CaCl_2$ in all media	1
M. caldariorum, Closterium sp., Zygnema sp., M. transeaui	50	*A. tumefaciens* GV2260	none	1

4.4 – Protoplast generation and PEG/Ca^{2+} transformation

The cell walls of plant, fungal, and bacterial cells present an extra physical boundary that must be bypassed in order to successfully transform these organisms (Ortiz-Matamoros *et al.*, 2018). Numerous transformation methods have been used to address the cell wall barrier, including the use of cell wall-deficient mutants in *Chlamydomonas reinhardtii*, or the use of high-velocity microparticle projectile-based methods (further expanded on in section 4.7) (Rochaix & Van Dillewijn, 1982). Digesting the cell wall completely with various cellulases to release plant protoplasts is another way to bypass the cell wall as a physical barrier for transformation (Yoo *et al.*, 2007). Reliable release of intact protoplasts could be achieved with four species in total (**Figure 2**). Protoplasts themselves can be transformed by various means, including electroporation or the use of DNA-containing liposomes, however the most common method of transformation is the use of polyethylene glycol (PEG).

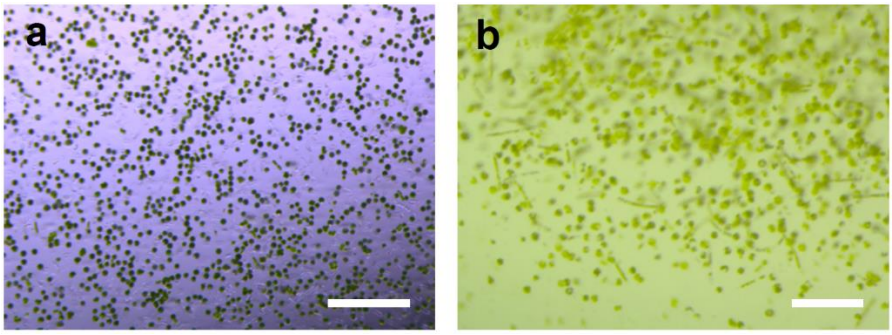

Figure 2: Released protoplasts from *P. margaritaceum* and *M. caldariorum*.

Treatment of *P. margaritaceum* or *M. caldariorum* for two hours with 2% driselase reliably produces many intact protoplasts. Healthy, intact, cell wall-less protoplasts of unialgal cultures may be useful in performing transient molecular or genetic experiments with charophytes.
a) *P. margaritaceum*, scale = 500 µm.
b) *M. caldariorum*, scale = 200 µm.

Importantly, since protoplasts are lacking the cell wall, they are especially sensitive to osmotic changes in their surrounding medium. As such, media must be supplemented with osmotic agents, such as mannitol, and care must be taken to not expose protoplasts to air to prevent their bursting or desiccation. For protoplast transformation, we tested a panel of algae that could be reliably generated with driselase digestion. For transformation parameters, we tested a range of DNA concentrations and a range of PEG transformations. Summary results can be found in **Table 2**.

Base protocol for protoplast generation and PEG/CA^{2+} transformation of algae (based upon and modified from Yoo et al., 2007).

Reagents and Biological Materials. Full descriptions of media and expression plasmids used can be found in the supplemental sections at the end of this chapter.

- *P. margaritaceum*, isolated by David Domozych, Saratoga Springs, NY, USA
- *Closterium sp*., in-house isolate, Bight Lake, Packwaukee, WI, USA
- *M. caldariorum*, UTEX41
- Plasmid DNA
- 200 mM M 4-morpholineethanesulfonic acid (MES) stock, filter sterilized
- 8.5% mannitol, sterilized
- 1 M $CaCl_2$, sterilized
- 2 M $MgCl_2$, sterilized
- 2 M KCl, sterilized
- 10% fetal bovine serum, filter sterilized
- PEG4000
- WI solution
- W5 solution
- MMG solution
- 100 mg/mL ampicillin stock dissolved in sterile water
- 2% driselase solution

Generation and isolation of algal protoplasts

1. Starting with 0.5 L algal cultures, 4 weeks of age, cells were centrifuged at 3,000 rcf for 10 minutes.
2. Cell pellets were washed twice in 15 mL of 8.5% mannitol solution, using previous centrifugation conditions.
3. Cell pellets were resuspended in driselase solution and agitated in sterile 90 mm petri plate on orbital shaker at 60 rpm for 3 hours.

4. Released protoplasts were mixed with 15 mL of W5 solution (an equal volume) and centrifuged at 200 rcf for 2 minutes.
5. Protoplast pellets were washed twice with 15 mL W5 solution and resuspended in a 2 mL of W5 solution prior to protoplast counting.
6. Protoplasts were adjusted to a concentration of 200,000/mL by addition of W5 solution.
7. Let protoplasts chill on ice for 15 minutes until they form a loose pellet in the tube. Remove as much W5 supernatant as possible without disturbing the protoplasts and replace with an equal volume of MMG solution. At this point, protoplasts were incubated on ice while transformation tubes were prepared.

PEG-Ca2+-transformation of protoplasts

1. For each transformation, indicated amounts of DNA was added to a sterile 1.5 mL tube.
2. 100 µL of previously counted protoplasts (~20,000 protoplasts) were added to tube containing plasmid DNA.
3. 110 µL of PEG solution was added to each tube and gently inverted to mix and initiate the transformation.
4. After 10 minutes of incubation at room temperature, 400 µL of W5 solution was added to each tube to terminate the transformation.
5. Protoplasts were centrifuged at 200 rcf for 2 minutes to pellet.
6. Protoplasts were gently resuspended in 0.5 mL of WI solution supplemented with 100 µg/mL ampicillin and transferred to the wells of a 12-well plate* (*Note: during the 10 minute transformation step, each well was treated with 10% fetal bovine serum which was promptly removed).
7. Culture well-plates were incubated in standard algal conditions overnight prior to imaging for expression of the fluorescent visual reporter. Culture wells that didn't contain GFP-expressing cells were screened again ~48 hours after transformation.

Table 2. Summary of PEG/Ca^{2+} protoplast transformation trials and results

Four species of algae, for whom protoplast generation was reliable and repeatable, were tested for PEG/Ca^{2+} protoplast transformation, using *pGlycine max SUB1:ZsGREEN*. Different concentrations of plasmid DNA and PEG were tested. No instances of transformation were observed.

Alga	PEG (%)	DNA tested (µg)
M. kramstaii	10, 15, 20	control
		10
		30
M. caldariorum	10, 15, 20	control
		10
		30
P. margaritaceum	10, 15, 20	control
		10
		30
Closterium sp.	10, 15, 20	control
		10
		30

4.5 – Cell-penetrating peptide transformation

Cell-penetrating peptides (CPPs) have been used with success for intracellular delivery of drugs, proteins, and transgenes in a variety of model systems (Guidotti *et al.*, 2017). CPPs cross the cell membrane by virtue of their interactions with the lipid bilayer; CPPs can have been elucidated as poly-anion, hydrophobic, and amphiphilic types. In the case of poly-anionic CPPs, translocation across the cell membrane is mechanistically due to the development of multilamellar structures in the membrane followed by the self-fusion of those structures to the membrane in order so form pores through which macromolecules may pass (Allolio *et al.*, 2018). CPPs have also been shown to internalize by inducing endocytic pathways (Richard *et al.*, 2005; Jiao *et al.*, 2009; Futaki & Nakase, 2017).

Commonly used variants of CPPs are various basic truncated peptides derived from the HIV-1 protein, Tat, the “Trans activator of transcription” of HIV-1 promoters (Laspia *et al.*, 1989; Vivès *et al.*, 1997). Numerous truncated Tat peptides have been used with success in animal, bacterial, and plant systems including the model alga Chlamydomonas reinhardtii (Ignatovich *et al.*, 2003; Lakshmanan *et al.*, 2013; Suresh & Kim, 2013; Numata *et al.*, 2018; Islam *et al.*, 2019). Conveniently, short CPPs such as Tat peptides may also be covalently modified with the addition of fluorescent reporters, side chain “stapling”, or the addition of reactive chemical groups for easy labeling of other macromolecules (Shen *et al.*, 2007; Nischan *et al.*, 2015; Klein *et al.*, 2017).

Given the successful use of Tat peptides in numerous cell-walled plant models, we aimed first to test the internalization of a Tat peptide in charophyte algae. To test internalization visually, we used Tat (47-57) (the sequence of which is YGRKKRRQRRR, heretofore referred to as “Tat”) labelled with the fluorescent dye, 5-carboxytetramethylrhodamine (TAMRA) at its N-terminus (**Figure 3**). Subsequently, we tested the ability of Tat-TAMRA to transform a panel of Zygnematalean algae by co-incubation with plasmid DNA carrying a GFP-expressing transgene. Given the highly positively charged nature of Tat-TAMRA and the highly negatively charged nature of DNA, these molecules readily form complexes. A commonly used parameter for testing the relative levels of Tat peptide to DNA is the “N/P” ratio, which is the ratio of positively charged amine groups to the negatively charges phosphate groups (Lakshmanan *et al.*, 2013). Using a standard amount of plasmid DNA for each transformation, we tested a panel of different N/P ratios by varying the levels of Tat-TAMRA in co-incubation. Summary results can be found in **Table 3**.

Protocol for testing Tat-TAMRA internalization in algae

Reagents and Biological Materials. Full descriptions of media and expression plasmids used can be found in the supplemental sections at the end of this chapter.

- *M. kramstaii*
- 2 mg/mL Tat-TAMRA stock in 30% glycerol, filter sterilized
- WHM, liquid, sterilized

Protocol

1. Starting from a roughly two-week-old liquid culture, 1.5 mL of cells were transferred to a 1.5 mL tube.
2. Cells were centrifuged at 3,000 rcf for 2 minutes to pellet.
3. Cells were resuspended in fresh WHM supplemented with 2 µg/mL Tat-TAMRA.
4. Cell-Tat-TAMRA-suspension was incubated at room temperature in darkness for 10 minutes with occasional agitation.

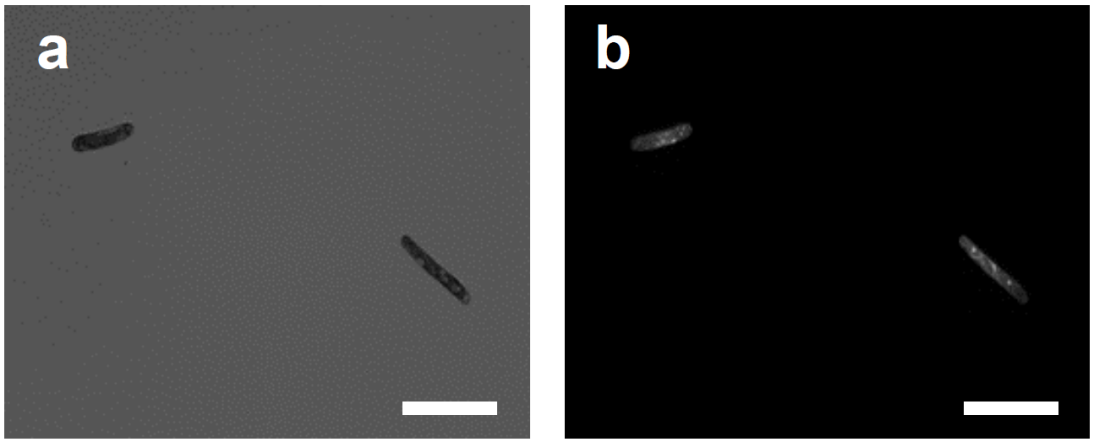

Figure 3: *Mesotaenium kramstaii* readily internalizes TAMRA-labelled Tat cell-penetrating peptide.

Treatment of *M. kramstaii* with algae medium supplemented Tat-TAMRA for 10 minutes display internalized TAMRA signal. Similar results were obtained with 5 minute incubation or 2 minute incubation. a) Brightfield. b) Fluorescent TAMRA signal. Scale = 100 µm.

Protocol for testing Tat-mediated transformation of algae

Reagents and Biological Materials. Full descriptions of media and expression plasmids used can be found in the supplemental sections at the end of this chapter.

- *M. kramstaii*
- *M. caldariorum*, UTEX 41
- *P. margaritaceum*, isolated by David Domozych, Saratoga Springs, NY, USA
- *Closterium sp*., in-house isolate, Bight Lake, Packwaukee, WI, USA
- 2 mg/mL Tat-TAMRA stock in 30% glycerol, sterile
- 2 µg/µL TB4 plasmid DNA, *2x35S:ZsGREEN*
- 24-well culture plate
- WHM, liquid, sterilized

Protocol

1. Starting with 2-week-old cultures, 10 mL of culture was spun down at 3,000 rcf for 5 minutes to pellet.
2. Supernatant medium was discarded and cells were resuspended in 1 mL fresh WHM.
3. In each transformation well of a 24-well plate, 100 µL of cell suspension was added.
4. For the combinations of Tat-TAMRA-DNA loading, the indicated volumes of plasmid DNA and Tat-TAMRA were pre-incubated for 15 minutes before being added to the respective transformation wells.

Table 3. Summary results of Tat-mediated transformations

Four species of algae were tested for transformation of *pGlycine max SUB1:ZsGREEN.* Combinations of various concentrations of plasmid DNA and Tat-peptide (indicated by N/P ratio) were used. No instances of transformation were observed.

Alga	N/P ratio	DNA tested (µg)
M. kramstaii	0.5, 1, 2	control
		5
		15
		45
M. caldariorum	0.5, 1, 2	control
		5
		15
		45
P. margaritaceum	0.5, 1, 2	control
		5
		15
		45
Closterium sp.	0.5, 1, 2	control
		5
		15
		45

4.6 – Silicon carbide whisker transformation

Silicon carbide whiskers (SiCW) are microscopic rod-shaped particles that have been used with some success in direct transformation of multiple species of plants, including algae (TG Dunahay, 1993; Frame *et al.*, 1994; Serik *et al.*, 1996; Dalton *et al.*, 1998). Silicon carbide, the principle mineral of the mineral moissanite, has similar chemical makeup and physical properties as diamond. SiCWs are principally used to create physical lesions in a cell's surface by rough agitation, allowing the internalization of transgenes. SiCWs of various lengths and diameters can be used, but are typically short, 50 µm or less in length, and thin, 0.5 µm in diameter. When agitated with plant cells, SiCWs are shown to impale plant cells without compromising the overall shape or integrity of the cell (Kaeppler *et al.*, 1992). We tested a panel of algal species for transformation, using varying amounts of DNA and two methods of agitation. Summary results can be found in **Table 4**.

Protocol for silicon carbide whisker transformation in algae

Reagents and Biological Materials. Full descriptions of media and expression plasmids used can be found in the supplemental sections at the end of this chapter.

Materials:

- *M. caldariorum*
- *M. kramstaii*
- *Penium margaritaceum*
- *Closterium sp.*
- WHM, liquid
- WHM, 1% agar plates
- pTEX(H)-GFP, *35S:GFP*
- Silicon carbide whiskers (SiCWs), 0.65 µm x 20 µm (SI-TUFF, Haydale)
- Sterile water
- 70% ethanol

Preparation of silicon carbide whiskers

1. For each transformation, 50 mg of SiCWs were weighed out into 1.5 mL tubes.
2. 1 mL of 70% ethanol was added to each tube and vortexed to sterilize SiCWs.

3. Ethanol was removed from SiCWs and each tube was washed three times with sterile water prior to transformation.

Transformation

1. For each transformation, 50 mL of 2-week-old culture was centrifuged at 3,000 rcf to pellet cells.
2. 250 µL of WHM was added to algal pellet, resuspended, and transferred to transformation tube containing pre-sterilized SiCWs.
3. Indicated amounts of TB4, 2x35S:ZsGREEN plasmid DNA was added to transformation tube.
4. Transformation tubes were vortexed on high (‘10’ on Vortex Genie) for 1 minute.
5. Suspension was plated onto WHM, 1% agar plate, and incubated overnight in darkness in otherwise standard algal culture conditions.
6. After overnight recovery period, cells were screened for GFP expression.

Table 4. Summary results of silicon carbide whisker transformations.

Five species of algae were tested for transformation of *pGlycine max SUB1:ZsGREEN.* Concentrations of plasmid DNA were varied. Also varied were the methods of mechanical agitation, using either a table-top vortex or bead mill. No instances of transformation were observed.

Alga	Agitation	DNA tested (µg)
P. margaritaceum	Vortex Genie	control
		23
		46
		92
	Bead mill 30/sec	control
		23
		46
		92
M. caldariorum	Vortex Genie	control
		23
		46
		92
Closterium sp.	Vortex Genie	control
		23
		46
		92
	Bead mill 30/sec	control
		23
		46
		92
M. transeaui	Bead mill 30/sec	control
		23
		46
		92

4.7 – Particle bombardment transformation

Particle bombardment, often referred to “gene-gun transformation” or “biolistics”, is a direct transformation process involving the coating of microscopic inert metal particles with the transgene(s) of interest, followed by high-velocity projection of the particles into the tissue of interest. Microparticles of tungsten or gold are typically used for the delivery of nucleic acids which are precipitated onto such microparticles with the use of ethanol, salts, and nucleic acid-compacting reagents such as spermidine. Originally, propulsion of microparticles relied on the gas pressure created by ignition of black powder, however the current standard relies on the regulated release of gas pressure of helium (T.M. Klein, E.D. Wolf, R. Wu, 1987; Klein & Fitzpatrick-Mcelligott, 1993). Aside from genetic transformation, particle bombardment-based delivery systems have also been used for intracellular delivery of proteins, fluorescent reporter dyes, or pharmacological compounds for example (Kettunen *et al.*, 2002; Martin-Ortigosa & Wang, 2014). Particle bombardment has been used with much success in a variety of tissue systems in animals, plants and fungi. Importantly, gold particle bombardment has been previously used with success in transformation of *Micrasterias* and *Closterium* (Vannerum *et al.*, 2010; Abe *et al.*, 2011). We aimed to test similar microparticle bombardment transformation on a panel of algal strains using multiple parameters, including three promoters driving the same visual reporter, different sizes of gold microparticles, different shooting distances, and different air pressures applied to the microparticles. Using ZsGREEN as a visual reporter, successful transient transformation of Zygnema sp., M. caldariorum, or M. transeaui was achieved with either the *Glycine max SUPERUBIQUITIN1*, *CaMV 35S*, or *M. scalaris TUBULIN1A* promoters (**Figure 4, Table 5**). Transformed cells were checked every two

days post-bombardment for the appearance of newly divided sister cells expressed ZsGREEN. No such sister cells were observed post-bombardment.

Base protocol for particle bombardment transformation of algae

Reagents and Biological Materials. Full descriptions of media and expression plasmids used can be found in the supplemental sections at the end of this chapter.

- *P. margaritaceum*, isolated by David Domozych, Saratoga Springs, NY, USA
- *Closterium sp*., in-house isolate, Bight Lake, Packwaukee, WI, USA
- *M. caldariorum*, UTEX41
- *Zygnema sp.,* UTEX LB 923
- *M. transeaui*, UTEX LB 2496
- Plasmid DNA
- Biolistic PDS-1000/He Particle Delivery System (BioRad)
- Gold microparticles, 0.6 µm, 1.0 µm, and 1.6 µm sizes (BioRad)
- Rupture disks, 600 psi, 900 psi, and 1100 psi varieties (BioRad)
- Macrocarrier disks (BioRad)
- Steel macrocarrier holders
- Metal stopping screens, sterilized
- 100% ethanol
- 70% ethanol
- 100% isopropanol
- 50% glycerol
- Sterile petri plates
- Drierite
- WHM 1% agar plates

Preparation of algae on plates prior to particle bombardment

1. Starting with a roughly 2-week-old culture grown under standard conditions, 5 mL of algal culture was spread equally on WHM 1% agar plates.
2. Algal plates were grown under standard conditions for 1 week, after which point cultures were roughly confluent on the plate. At this point, DNA-coated gold microparticles were prepared for transformation.

DNA coating of gold microparticles

1. Gold microparticles were ethanol-sterilized and suspended in 50% glycerol as per the standard BioRad protocol for the Biolistic PDS-1000/He Particle Delivery System.
2. Individual macrocarriers for each instance of bombardment were prepared using standard concentrations of spermidine and $CaCl_2$ as recommended by BioRad with the following amounts of gold and circular plasmid DNA:
    a. 0.3 mg gold particles per bombardment
    b. 15 µg plasmid DNA per bombardment

3. Until immediately before use, prepared macrocarriers overlaid with gold/DNA were kept in a sealed container containing Drierite to discourage any moisture from affecting the DNA coating.

Gold microparticle bombardment and post-transformation treatment

1. Indicated rupture disks were pre-sterilized by submerging in 100% isopropanol, air dried over Drierite, and assembled into the 'gene-gun' along with the macrocarrier with DNA-coated gold particles.
2. Each algal culture plate was placed in the gene-gun at the indicated shelf position.
3. At all times, the gene-gun chamber was put under a vacuum at 27.5 mm Hg prior to firing.
4. After firing, algal plates were immediately removed from the chamber, sealed, and incubated in darkness, overnight, at room temperature.
5. After overnight incubation, algal plates were visually screened for the expression of the fluorescent visual reporter.

Table 5. Summary of parameters of particle bombardment trials

Each column represents a transformation trial. Five species of algae were tested. The varied parameters were air pressure (using specific rupture disks), distance from the gene-gun to the target, the size of gold particles used, and the expression vector used. The number of plates shot is also indicated. Bolded rows indicate trials that yielded transformed cells. A fuller explanation of expression vectors can be found in **Supplemental Table 1**.

Alga	Pressure (psi)	Distance (in)	Gold (μm)	Transgene(s)	Plates
Zygnema sp.	900, 1100	3, 6, 9	1	TB4 TB5 TB6	2
M. caldariorum	**900, 1100**	**6**	**1**	**TB61**	**1**
M. caldariorum	**1100, 1350**	**3**	**0.6**	**TB4 TB5 TB6**	**3**
Zygnema sp.	**900, 1100**	**3**	**1**	**TB50**	**4**
Zygnema sp., M. caldariorum, P. margaritaceum, Closterium sp.	900	3	1 for *Zygnema/Mesotaenium* 1.6 for *Penium/Closterium*	TB53	1
M. transeaui	**1100**	**3**	**1.6**	**TB70**	**15**

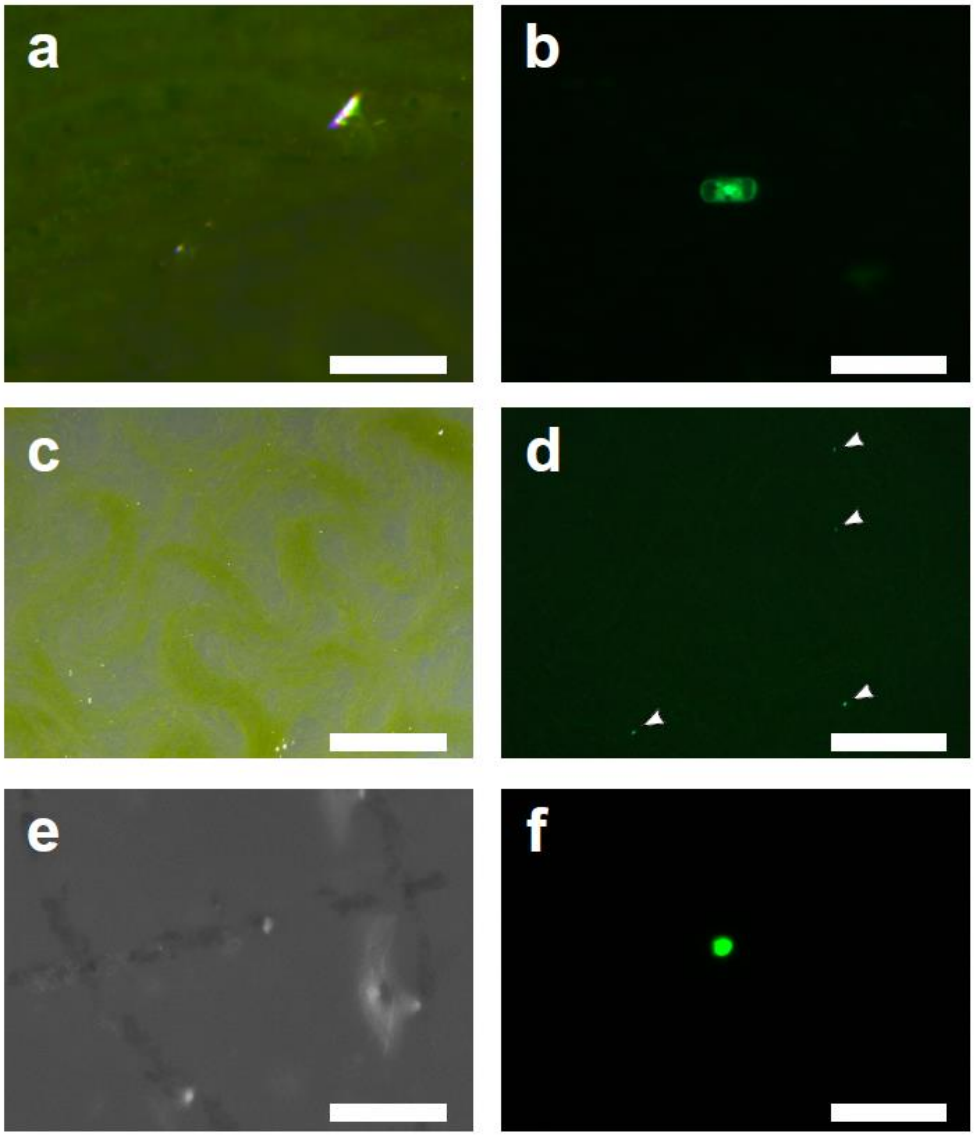

Figure 4: Zygnematalean algae genetically transformed by microparticle bombardment.

A generalizable microparticle bombardment protocol can be used to transform multiple species of charophytes, including *Zygnema sp*., *M. transeaui,* and *M. caldariorum*. Left panels, brightfield. Right panels, GFP signal.

(a-b) *Zygnema sp.*, expressing ZsGREEN tagged at the N-terminus with an ER-localization signal, under the control of the *Glycine max SUPERUBIQUITIN1* promoter. Scale = 150 µm.

(c-d) *Zygnema sp*., transformed with same construct as (a-b), showing expression 21 days after microparticle bombardment. Arrowheads indicate transformed cells. Scale = 2 mm. **(legend continued on next page)**

(e-f) *M. transeaui*, expressing the calcium-sensitive fluorescent reporter G-GECO1.2 tagged at the N-terminus with a nuclear localization signal, under the control of the *M. scalaris TUBULIN1A* promoter. Scale = 100 µm.

4.8 - Fluorescence activated cell sorting of clonal Mesotaenium transformants

The ability to perform faithful genetic experiments requires the analysis of numerous individuals, and often multiple genetic lines or allelic variants. Furthermore, by microparticle bombardment transformation, transgenes are prone to integrate randomly within the genome, but also in high copy number which may cause transgene silencing (Kohli *et al.*, 2003). As such, when using microparticle bombardment to generate stable genetic lines, care must be taken to genetically characterize transformants and isolate clonal lines. Clonal transformants of charophytes have been isolated by hand, with the use of a micropipette, however this may be slow and cumbersome (Sørensen *et al.*, 2014). We sought to test if single transformants could be isolated through the use of fluorescence activated cell sorting (FACS). FACS, through the use of a flow cytometer, relies on the emission signal of a fluorophore to pick cells for isolation out of a large population of cells. Cells are passed through a fluidics system such that individual cells become enveloped within buffered water droplets, which subsequently are passed through a fluorescence excitation/emission apparatus, one by one. Droplets containing labelled cells or cells expressing fluorescent protein(s) are applied a charge which causes the separation of the individual from the population through interaction with a cathode or anode. With more advanced FACS machines, not only can fluorescent cells be separated from non-fluorescent cells, but they can also be isolated from one another solving the issue of isolating clonal transformants. Such sorting methods have been used to analyze

transformants or large populations of cells, including microalgae (Terashima *et al.*, 2015; Seed *et al.*, 2016).

Some microalgal species are incompatible with FACS and flow cytometry. *Zygnema sp*. and *M. transeaui* are filamentous species and thus cells cannot be separated from one another by microfluidics. *Closterium sp*. is by far too large of a cell to be passed through the excitation/emission detection apparatus of typical flow cytometers. Species of the genus *Mesotaenium* are conveniently small, less than 50 μm in length, and unicellular, and thus a good model system with which to test FACS.

With *M. caldariorum*, we compared a cell population transformed with a Cauliflower Mosaic Virus 35S (CaMV-35S) driven *ZsGREEN* to a mock-transformed cell population which was bombarded without plasmid DNA (**Figure 5**). A gated region of green fluorescent signal was chosen for differentiating between transformed and non-transformed cells. With this determined signal cutoff, cells of a wide range of brightness were detected. Cells with green fluorescent signal as high as 10^5x that of an average non-transformed cell were detected and sorted. In total, 33 transformed cells of a total population of 5,000 were sorted, indicating a 0.621% transformation method with our microparticle bombardment protocol. The GFP signal range from dim to bright cells varied by five orders of magnitude in signal, the cells within the GFP gated region themselves covering a region roughly three orders of magnitude. With this method of cell sorting, future genetic studies with *Mesotaenium* can be enhanced by the isolation of different genetic lines and quick separation negating the need of cumbersome manual manipulations of cells.

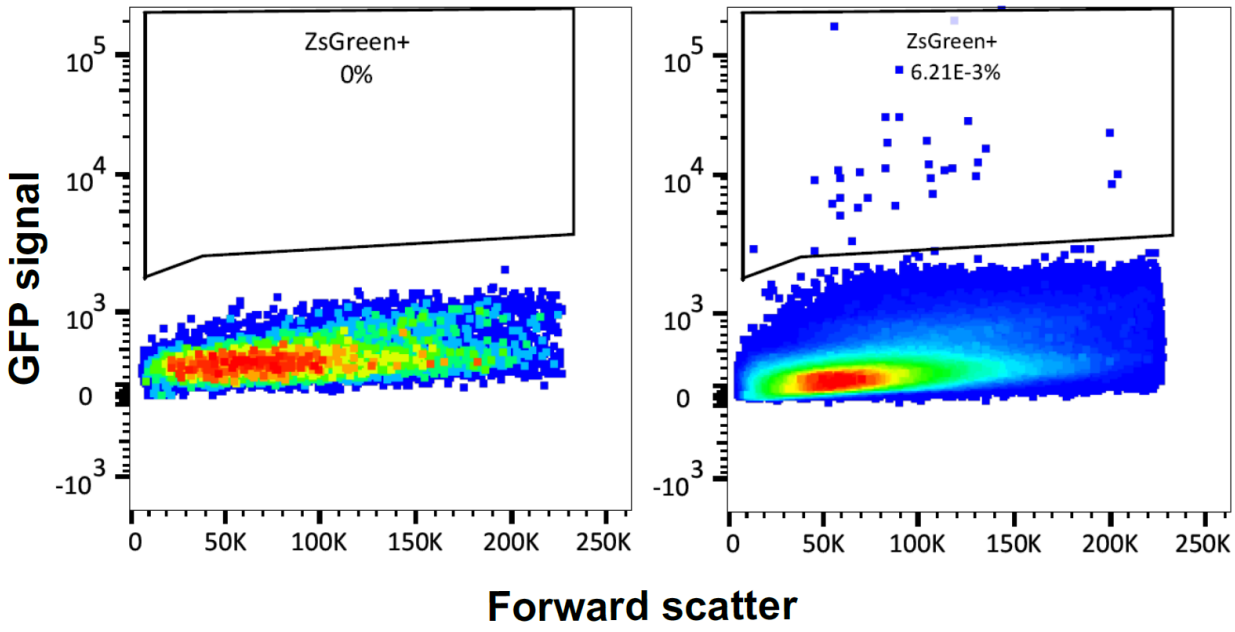

Figure 5: Fluorescence activated cell sorting of *M. caldariorum* transformed with *CaMV 35S:ZsGREEN*

M. caldariorum cells are small enough to be reliably sorted into transformed and non-transformed populations using GFP signal as the criteria. The left panel is a sorted population of cells that were mock-transformed without an expression vector. The right panel is a sorted population transformed with *CaMV 35S:ZsGREEN* by microparticle bombardment. GFP fluorescence signal is measured on the y-axis and forward scatter, a proxy measurement for cell-size, is measured on the x-axis. Both panels show 10,000 sorting events and *ZsGREEN*-expressing cells are determined based upon the upper gated region compared between mock and transformed samples.

4.9 - Discussion and future prospects for charophyte transformation

The only successful method of transformation in this work was microparticle bombardment, which to date is the more commonly used method for charophyte algae in the literature (Vannerum *et al.*, 2010; Abe *et al.*, 2011; Regensdorff *et al.*, 2018). To our knowledge, there has been no published replication of *Agrobacterium*-mediated transformation since the original method (Sørensen *et al.*, 2014). From this work, we show that the viral 35S promoter is functional in a newly tested species, *M. caldariorum*.

Additionally, we show that a newly tested promoter, the *SUPER UBIQUITIN1 (SUBI1*) promoter of *Glycine max* is functional in both *M. caldariorum* and *Zygnema sp*. Lastly, we have shown that the recently published TUBULINA1 promoter from *Mougeotia scalaris* is functional in another species of the same genus, *M. transeaui* (Regensdorff *et al.*, 2018). All instances of transformation were transient, the longest example of which *G. max SUBI1* drove *ZsGREEN* expression for three weeks in *Zygnema sp.* Although stable transformation allows for the generation of many genetic tools, there are advantages to transient transformation. Transient expression of Cas9 and small guide RNAs can be sufficient for generating mutants of interest, or facilitating the integration of DNA parts (Mallett *et al.*, 2019).

Stable transformation by microparticle bombardment has been reported in *C. psl complex*, however this was not the same species we tested in this panel. Although this study elucidated the *G.max SUPBI1* promoter as active numerous zygnematalean species, the transformation efficiency needs significant improvement in order to generate sufficient transgenic cells for future studies. A study in *M. scalaris* demonstrated that promoter choice not only determines strength of expression, as would be expected, but also transformation efficiency (Regensdorff *et al.*, 2018). To improve transformation efficiency, a larger variety of promoters, gold sizes, and DNA loading conditions should be tested. Mitosis-blocking chemicals, such as colchicine, may also be helpful in increasing efficiency by unifying the growth stage of cells that are transformed. By unifying a population of cells in their growth stages, the time at which the nuclear envelope disassembles can be controlled, creating a larger population of cells lacking the nuclear envelope as an extra physical barrier to transgene integration. To reliably use this

method, however, one would want to know the doubling times of individual species and also the time from colchicine removal to the dissolution of the nuclear envelope.

The inability to observe cell division and subsequent expression of ZsGREEN in sister cells may suggest a few things. It is possible that the retention and/or expression of our selected transgenes, in their circular-vector form or otherwise, is not stable past a round of mitosis. On the other hand, the bombardment procedure used may have been lethal in all the instances that cell division was checked for. It may be worthwhile to cytologically assess individual transformed cells in order to determine if they have apparently entered the process of “dying” or that their regular cell-division machinery has been perturbed. Cell-sorting using FACS may be useful is separating “dying” transformants from candidates that may be expanded into clonal lines; living, stable transformed lines have been isolated from bombarded cultures in many plant models.

Overall, this study, in conjunction with published literature, strongly suggests that direct means of transformation are most replicable, namely by microparticle bombardment. *Agrobacterium*-mediated transformations are known to integrate fewer transgene copies, tandem or otherwise, as compared to microparticle bombardment and as such may be advantageous in generating more easily characterized genetic lines or genetic lines less prone to endogenous gene silencing (Jackson *et al.*, 2013). Given the additional simplicity of *Agrobacterium*-mediated methods, with no need for expensive equipment, reagents, or highly concentrated purified plasmid DNA, we eagerly sought to reproduce methods described previously (Sørensen *et al.*, 2014). When these efforts failed, we tested other species of algae, and also various strains of *A. rhizogenes* and *A. tumefaciens*, unsuccessfully. Given that *Agrobacterium* has been used with success even

in chlorophyte algae, such as *Chlamydomonas reinhardtii*, it is still worth exploring a wider range of charophyte algae in conjunction with a wider range of *A. rhizogenes* and *A. tumefaciens* strains (Kumar *et al.*, 2004; Pratheesh *et al.*, 2014). The combination of *Agrobacterium* and electroporation has also been demonstrated in *C. reinhardtii*, suggesting a means of improving *Agrobacterium*-mediated transformation in *P. margaritaceum.*

Surprisingly PEG-mediated protoplast transformation, using the already confirmed CaMV35S promoter and a range of DNA and PEG concentration conditions yielded no observable expression. To our knowledge this technique hasn't been reported in any charophyte algae, although as is the case with *Agrobacterium*, it has been used successfully in a range of both chlorophyte algae and land plants. In addition to expanding the range of conditions tested in this work, it may also be worthwhile testing amphiphilic, membrane-disrupting compounds other than PEG. The caveat of this methodology, though, is utility of protoplasts in one's research. Without the cell wall, protoplasts are generally considered highly atypical compared to their walled counterparts. Depending on the scientific questions being asked, researchers should consider if the lack of a cell wall would impact their process of interest.

With the rise of synthetic biology, there has been growing interest in the use of nanoparticles and nanomaterials, such as CPPs, in genetic engineering or cell manipulation (Guidotti *et al.*, 2017; Sanzari *et al.*, 2019; Wang *et al.*, 2019b). We demonstrate that Tat-TAMRA, for example, is readily internalized into *M. kramstaii*, as it has been shown to do in numerous plant models (Numata *et al.*, 2018). Currently, there are many characterized CPPs of different chemical subtypes and even a published

repository for them (Agrawal *et al.*, 2016). The Tat-based method tested in this work relied upon non-covalent interactions between Tat-peptide and DNA. Other options with CPPs make use of the strong covalent interaction of biotinylation and streptavidin, the latter of which can be fused in frame with Cas9 or functional reporter proteins like G-GECO1.2, for example (Sun *et al.*, 2012). Synthetic CPPs can also potentially be used in conjunction with self-labeling protein tags such as the HALO tag or SNAP tag to generate CPP-derivative reporter proteins or Cas9 (England *et al.*, 2015; Hussain *et al.*, 2019).

The experiments reported here all rely upon transgene expression within the nucleus. Genetic transformation of chloroplasts presents another opportunity with which to study charophytes, however with caveats. Chloroplast transformation, although most common in land plants, has been used in microalgae (Bateman & Purton, 2000; Zedler *et al.*, 2016; Lapidot *et al.*, 2017). There are numerous benefits to chloroplast transformation over nuclear transformation. Expression systems of chloroplasts are immune from nuclear silencing mechanisms such as small RNA-mediated mechanisms (Adem *et al.*, 2017). High levels of protein expression can be achieved. Chloroplast-expressed protein in *Chlamydomonas* has been reported as high as 5% of total cell protein (Tran *et al.*, 2013). The utility of chloroplast-expressed proteins is limited however. To our knowledge, although there are mechanisms to import nuclear-expressed proteins into the chloroplast, there are no known methods to export chloroplast-expressed proteins from the chloroplasts.

4.10 – Supplemental tables

Supplemental Table 1. Expression vectors used in this study

pART24	pART27 – ER-RFP (provided by Jocelyn Rose)
TB4	pCANNON-*Glycine max UBI3:ZsGREEN:OCS*
TB5	pCANNON- *Oryza sativa UBI2:intron:ZsGREEN:OCS*
TB6	pCANNON- *2x35S:ZsGREEN:OCS*
TB70	pCANNON- *M. scalaris TUBULIN1A:ZsGEEN:OCS*

Supplemental Table 2. Media formulations used to grow zygnematalean algae.

Woods Hole Medium, as outlined in (Sorensen *et al.,* 2014). Carbon-free Woods Hole Medium was used for routine maintenance and bulking of algal cultures.

Salt/Vitamin	**Mol weight (g/mol)**	**Stock (add to liter)**	**Stock concentration**	**Each liter WHM**	**Final concentration**
$CaCl_2.2H_2O$	147.0	36.76g	0.25M	1 mL	0.25mM
$MgSO_4.7H_2O$	246.5	36.97g	0.15M	1 mL	0.15mM
$NaHCO_3$	84.0	12.60g	0.15M	1 mL	0.15mM
K_2HPO_4	174.2	8.71g	0.05M	1 mL	0.05mM
$NaNO_3$	85.00	85.01g	1M	1 mL	1mM
Na_2EDTA	372.2	4.36g	0.012M	1 mL	0.012mM
$FeCl_3.6H_2O$	270.3	3.15g	0.012M	1 mL	0.012mM
Metals: $CuSO_4.5H_2O$ $ZnSO_4.7H_2O$ $CoCl_2.6H_2O$ $MnCl_2.4H_2O$ $Na_2MoO_4.2H_2O$	 249.7 287.6 237.9 197.9 242.0	 10mg 22mg 10mg 180mg 6mg	 0.04mM 0.08mM 0.04mM 0.91mM 0.025mM	 1 mL	 0.04µM 0.08µM 0.04µM 0.91µM 0.025µM
Tris base	121.1	250.0 g	2M	1 mL	2mM
Vitamin stock: Vitamin B_{12} Vitamin B_1 Biotin	 1355.4 337.3 244.3	 0.55mg 100mg 0.5mg	 0.4µM 300µM 2µM	 1 mL	 0.4pM 0.3µM 2pM

Mating Induction (MI) medium, as outlined in (Sorensen *et al.,* 2014), originally described by Ichimura, 1971. Carbon-free Woods Hole Medium was used for routine maintenance and bulking of algal cultures.

Salt/Vitamin	**Mol. Weight (g/mol)**	**Stock**	**Each liter MI**	**Final concentration**
$CaCl2.2H_2O$	147.0		200 mg	1.36mM
KCl	74.6		140 mg	1.88mM
Na_2-β-glycerophosphate.$5H_2O$	216.0		100 mg	4.63M
$MgSO_4.7H_2O$	246.5		80 mg	0.32mM
Tris base	121.1		500 mg	4.13mM
Metals: $ZnCl_2$ $CoCl_2.6H_20$ $MnCl_2.4H_2O$ Na_2MoO_4 Na_2EDTA $FeCl_3.6H_2O$	 136.3 237.9 197.9 205.9 372.2 270.3	In 500 mL H_2O 5mg 2mg 41mg 4mg 500mg 97mg	6 mL	
Vitamin stock: Vitamin B_{12} Biotin Vitamin B_1	 1355.4 244.3 337.3	In 10 mL H_2O 1mg 1mg 100mg	10 µL	 0.74pM 4.1pM 0.3µM

4.11 - References cited

Abe J, Hori S, Tsuchikane Y, Kitao N, Kato M, Sekimoto H. **2011**. Stable nuclear transformation of the *Closterium peracerosum-strigosum- littorale* complex. *Plant and Cell Physiology* **52**: 1676–1685.

Adem M, Beyene D, Feyissa T. **2017**. Recent achievements obtained by chloroplast transformation. *Plant Methods* **13**: 1–11.

Agrawal P, Bhalla S, Usmani SS, Singh S, Chaudhary K, Raghava GPS, Gautam A. **2016**. CPPsite 2.0: A repository of experimentally validated cell-penetrating peptides. *Nucleic Acids Research* **44**: D1098–D1103.

Allolio C, Magarkar A, Jurkiewicz P, Baxová K, Javanainen M, Mason PE, Šachl R, Cebecauer M, Hof M, Horinek D, *et al.* 2018. Arginine-rich cell-penetrating peptides induce membrane multilamellarity and subsequently enter via formation of a fusion pore. *Proceedings of the National Academy of Sciences of the United States of America* **115**: 11923–11928.

Bateman JM, Purton S. **2000**. Tools for chloroplast transformation in *Chlamydomonas*: Expression vectors and a new dominant selectable marker. *Molecular and General Genetics* **263**: 404–410.

Cheng S, Xian W, Fu Y, Marin B, Keller J, Wu T, Sun W, Li X, Xu Y, Zhang Y, *et al.* 2019. Genomes of subaerial zygnematophyceae provide insights into land plant evolution. *Cell* **179**: 1057-1067.e14.

Clough SJ, Bent AF. **1998**. Floral dip: A simplified method for *Agrobacterium*-mediated transformation of *Arabidopsis thaliana*. *Plant Journal* **16**: 735–743.

Dalton SJ, Bettany AJE, Timms E, Morris P. **1998**. Transgenic plants of *Lolium multiflorum, Lolium perenne, Festuca arundinacea* and *Agrostis stolonifera* by silicon carbide fibre-mediated transformation of cell suspension cultures. *Plant Science* **132**: 31–43.

Delaux P-M, Radhakrishnan G V, Jayaraman D, Cheema J, Malbreil M, Volkening JD, Sekimoto H, Nishiyama T, Melkonian M, Pokorny L. **2015**. Algal ancestor of land plants was preadapted for symbiosis. *Proceedings of the National Academy of Sciences* **112**: 13390–13395.

England CG, Luo H, Cai W. **2015**. HaloTag technology: A versatile platform for biomedical applications. *Bioconjugate Chemistry* **26**: 975–986.

Engler C, Youles M, Gruetzner R, Ehnert TM, Werner S, Jones JDG, Patron NJ, Marillonnet S. **2014**. A Golden Gate modular cloning toolbox for plants. *ACS Synthetic Biology* **3**: 839–843.

Frame BR, Drayton PR, Bagnall S V., Lewnau CJ, Bullock WP, Wilson HM, Dunwell JM, Thompson JA, Wang K. **1994**. Production of fertile transgenic maize plants by

silicon carbide whisker-mediated transformation. *The Plant Journal* **6**: 941–948.

Futaki S, Nakase I. **2017**. Cell-surface interactions on arginine-rich cell-penetrating peptides allow for multiplex modes of internalization. *Accounts of Chemical Research* **50**: 2449–2456.

Gleave AP. **1992**. A versatile binary vector system with a T-DNA organisational structure conducive to efficient integration of cloned DNA into the plant genome. *Plant Molecular Biology* **20**: 1203–1207.

Guidotti G, Brambilla L, Rossi D. **2017**. Cell-penetrating peptides: From basic research to clinics. *Trends in Pharmacological Sciences* **38**: 406–424.

Hussain AF, Heppenstall PA, Kampmeier F, Meinhold-Heerlein I, Barth S. **2019**. One-step site-specific antibody fragment auto-conjugation using SNAP-tag technology. *Nature Protocols* **14**: 3101–3125.

Ignatovich IA, Dizhe EB, Pavlotskaya A V., Akifiev BN, Burov S V., Orlov S V., Perevozchikov AP. **2003**. Complexes of plasmid DNA with basic domain 47-57 of the HIV-1 Tat protein are transferred to mammalian cells by endocytosis-mediated pathways. *Journal of Biological Chemistry* **278**: 42625–42636.

Ishizaki K, Chiyoda S, Yamato KT, Kohchi T. **2008**. *Agrobacterium*-mediated transformation of the haploid liverwort *Marchantia polymorpha* L., an emerging model for plant biology. *Plant and Cell Physiology* **49**: 1084–1091.

Islam MM, Odahara M, Yoshizumi T, Oikawa K, Kimura M, Su'Etsugu M, Numata K. **2019**. Cell-penetrating peptide-mediated transformation of large plasmid DNA into *Escherichia coli*. *ACS Synthetic Biology* **8**: 1215–1218.

Jackson MA, Anderson DJ, Birch RG. **2013**. Comparison of *Agrobacterium* and particle bombardment using whole plasmid or minimal cassette for production of high-expressing, low-copy transgenic plants. *Transgenic Research* **22**: 143–151.

Jiao CY, Delaroche D, Burlina F, Alves ID, Chassaing G, Sagan S. **2009**. Translocation and endocytosis for cell-penetrating peptide internalization. *Journal of Biological Chemistry* **284**: 33957–33965.

Kaeppler HF, Somers DA, Rines HW, Cockburn AF. **1992**. Silicon carbide fiber-mediated stable transformation of plant cells. *Theoretical and Applied Genetics* **84**: 560–566.

Kenrick P, Crane PR. **1997**. The origin and early evolution of plants on land. *Nature* **389**: 33–39.

Kettunen P, Demas J, Lohmann C, Kasthuri N, Gong Y, Wong ROL, Gan WB. **2002**. Imaging calcium dynamics in the nervous system by means of ballistic delivery of indicators. *Journal of Neuroscience Methods* **119**: 37–43.

Klein TM, Fitzpatrick-Mcelligott S. **1993**. Particle bombardment: A universal approach for gene transfer to cells and tissues. *Current Opinion in Biotechnology* **4**: 583–590.

Klein MJ, Schmidt S, Wadhwani P, Bürck J, Reichert J, Afonin S, Berditsch M, Schober T, Brock R, Kansy M, *et al.* 2017. Lactam-stapled cell-penetrating peptides: cell uptake and membrane binding properties. *Journal of Medicinal Chemistry* **60**: 8071–8082.

Knack JJ, Wilcox LW, Delaux P-M, Ané J-M, Piotrowski MJ, Cook ME, Graham JM, Graham LE, Knoll AH. **2015**. Microbiomes of stephtophyte algae and bryophytes suggest that a functional suite of microbiota fostered plant colonization of land. *Int. J. Plant Sci.* **176**: 405–420.

Kohli A, Twyman RM, Abranches R, Wegel E, Stoger E, Christou P. **2003**. Transgene integration, organization and interaction in plants. *Plant Molecular Biology* **52**: 247–258.

Kumar SV, Misquitta RW, Reddy VS, Rao BJ, Rajam MV. **2004**. Genetic transformation of the green alga - *Chlamydomonas reinhardtii* by *Agrobacterium tumefaciens*. *Plant Science* **166**: 731–738.

Lakshmanan M, Kodama Y, Yoshizumi T, Sudesh K, Numata K. **2013**. Rapid and efficient gene delivery into plant cells using designed peptide carriers. *Biomacromolecules* **14**: 10–16.

Lapidot M, Raveh D, Sivan A, Arad SM, Shapira M, Lapidot M, Raveh D, Sivan A, Arad SM, Shapira M. **2017**. Stable chloroplast transformation of the unicellular red alga

porphyridium species. *American Society of Plant Biologists*. **129**: 7–12.

Laspia MF, Rice AP, Mathews MB. **1989**. HIV-1 Tat protein increases transcriptional initiation and stabilizes elongation. *Cell* **59**: 283–292.

Mallett DR, Chang M, Cheng X, Bezanilla M. **2019**. Efficient and modular CRISPR-Cas9 vector system for *Physcomitrella patens*. *Plant Direct* **3**: 1–15.

Martin-Ortigosa S, Wang K. **2014**. Proteolistics: a biolistic method for intracellular delivery of proteins. *Transgenic Research* **23**: 743–756.

Matz M V., Fradkov AF, Labas YA, Savitsky AP, Zaraisky AG, Markelov ML, Lukyanov SA. **1999**. Fluorescent proteins from nonbioluminescent *Anthozoa species*. *Nature Biotechnology* **17**: 969–973.

Nischan N, Herce HD, Natale F, Bohlke N, Budisa N, Cardoso MC, Hackenberger CPR. **2015**. Covalent attachment of cyclic TAT peptides to GFP results in protein delivery into live cells with immediate bioavailability. *Angewandte Chemie - International Edition* **54**: 1950–1953.

Nishiyama T, Sakayama H, de Vries J, Buschmann H, Saint-Marcoux D, Ullrich KK, Haas FB, Vanderstraeten L, Becker D, Lang D, *et al.* 2018. The *Chara* Genome: Secondary complexity and implications for plant terrestrialization. *Cell* **174**: 448-464.e24.

Numata K, Horii Y, Oikawa K, Miyagi Y, Demura T, Ohtani M. **2018**. Library screening of cell-penetrating peptide for BY-2 cells, leaves of *Arabidopsis*, tobacco, tomato, poplar, and rice callus. *Scientific Reports* **8**: 1–17.

Ortiz-Matamoros MF, Villanueva MA, Islas-Flores T. **2018**. Genetic transformation of cell-walled plant and algae cells: Delivering DNA through the cell wall. *Briefings in Functional Genomics* **17**: 26–33.

Pratheesh PT, Vineetha M, Kurup GM. **2014**. An efficient protocol for the *Agrobacterium*-mediated genetic transformation of microalga *Chlamydomonas reinhardtii*. *Molecular Biotechnology* **56**: 507–515.

Regensdorff M, Deckena M, Stein M, Borchers A, Scherer G, Lammers M, Hänsch

R, Zachgo S, Buschmann H. **2018**. Transient genetic transformation of *Mougeotia scalaris* (Zygnematophyceae) mediated by the endogenous *α-TUBULIN1* promoter. *Journal of Phycology* **54**: 840–849.

Richard JP, Melikov K, Brooks H, Prevot P, Lebleu B, Chernomordik L V. 2005. Cellular uptake of unconjugated TAT peptide involves clathrin-dependent endocytosis and heparan sulfate receptors. *Journal of Biological Chemistry* **280**: 15300–15306.

Rochaix JD, Van Dillewijn J. **1982**. Transformation of the green alga *Chlamydomonas reinhardii* with yeast DNA. *Nature* **296**: 70–72.

Sanzari I, Leone A, Ambrosone A. **2019**. Nanotechnology in plant science: to make a long story short. *Frontiers in Bioengineering and Biotechnology* **7**: 1–12.

Seed CE, Larma I, Tomkins JL. **2016**. Cell size selection in *Chlamydomonas reinhardtii* gametes using fluorescence activated cell sorting. *Algal Research* **16**: 93–101.

Serik O, Ainur I, Murat K, Tetsuo M, Masaki I. **1996**. Silicon carbide fiber-mediated DNA delivery into cells of wheat (*Triticum aestivum L*.) mature embryos. *Plant Cell Reports* **16**: 133–136.

Shen D, Liang K, Ye Y, Tetteh E, Achilefu S. **2007**. Modulation of nuclear internalization of Tat peptides by fluorescent dyes and receptor-avid peptides. *FEBS Letters* **581**: 1793–1799.

Sørensen I, Fei Z, Andreas A, Willats WGT, Domozych DS, Rose JKC. **2014**. Stable transformation and reverse genetic analysis of *Penium margaritaceum*: A platform for studies of charophyte green algae, the immediate ancestors of land plants. *Plant Journal* **77**: 339–351.

Sun W, Fletcher D, Van Heeckeren RC, Davis PB. **2012**. Non-covalent ligand conjugation to biotinylated DNA nanoparticles using TAT peptide genetically fused to monovalent streptavidin. *Journal of Drug Targeting* **20**: 678–690.

Suresh A, Kim YC. **2013**. Translocation of cell penetrating peptides on *Chlamydomonas reinhardtii*. *Biotechnology and Bioengineering* **110**: 2795–2801.

T.M. Klein, E.D. Wolf, R. Wu JCS. **1987**. High-velocity microprojectiles for delivering nucleic acids into living cells. *Nature* **327**: 70–73.

Terashima M, Freeman ES, Jinkerson RE, Jonikas MC. **2015**. A fluorescence-activated cell sorting-based strategy for rapid isolation of high-lipid *Chlamydomonas* mutants. *Plant Journal* **81**: 147–159.

TG, Dunahay. **1993**. Transformation of *Chlamydomonas reinhardtii* with silicon carbide whiskers. *Biotechniques* **3**: 4452–455.

Tran M, Henry RE, Siefker D, Van C, Newkirk G, Kim J, Bui J, Mayfield SP. **2013**. Production of anti-cancer immunotoxins in algae: Ribosome inactivating proteins as fusion partners. *Biotechnology and Bioengineering* **110**: 2826–2835.

Tsuchikane Y, Tsuchiya M, Kokubun Y, Abe J, Sekimoto H. **2011**. Conjugation processes of *Penium margaritaceum* (Zygnemophyceae, Charophyta). *Phycological Research* **59**: 74–82.

Vannerum K, Abe J, Sekimoto H, Inzé D, Vyverman W. **2010**. Intracellular localization of an endogenous cellulose synthase of *Micrasterias denticulata* (Desmidiales, Chlorophyta) by means of transient genetic transformation. *Journal of Phycology* **46**: 839–845.

Vivès E, Brodin P, Lebleu B. **1997**. A truncated HIV-1 Tat protein basic domain rapidly translocates through the plasma membrane and accumulates in the cell nucleus. *Journal of Biological Chemistry* **272**: 16010–16017.

Wang Y, Ye M, Xie R, Gong S. **2019**. Enhancing the in vitro and in vivo stabilities of polymeric nucleic acid delivery nanosystems. *Bioconjugate Chemistry* **30**: 325–337.

Weber E, Engler C, Gruetzner R, Werner S, Marillonnet S. **2011**. A modular cloning system for standardized assembly of multigene constructs. *PLoS ONE* **6**.

Wickett NJ, Mirarab S, Nguyen N, Warnow T, Carpenter E, Matasci N, Ayyampalayam S, Barker MS, Burleigh JG, Gitzendanner MA. **2014**. Phylotranscriptomic analysis of the origin and early diversification of land plants. *Proceedings of the National Academy of Sciences* **111**: E4859–E4868.

Yoo SD, Cho YH, Sheen J. **2007**. *Arabidopsis* mesophyll protoplasts: A versatile cell system for transient gene expression analysis. *Nature Protocols* **2**: 1565–1572.

Zambryski PC. **1992**. Chronicles from the *Agrobacterium*-plant cell DNA transfer story. *Annual Review of Plant Physiology and Plant Molecular Biology* **43**: 465–490.

Zambryski P, Tempe J, Schell J. **1989**. Transfer and function of T-DNA genes from *Agrobacterium* Ti and Ri plasmids in plants. *Cell* **56**: 193–201.

Zedler JAZ, Mullineaux CW, Robinson C. **2016**. Efficient targeting of recombinant proteins to the thylakoid lumen in *Chlamydomonas reinhardtii* using a bacterial Tat signal peptide. *Algal Research* **19**: 57–62.

Zupan J, Muth TR, Draper O, Zambryski P. **2000**. The transfer of DNA from *Agrobacterium tumefaciens* into plants: A feast of fundamental insights. *Plant Journal* **23**: 11–28.

5.1 - Summary

We sought to characterize the role of *CCaMK* and *IPD3* in *Physcomitrella patens* (Physcomitrella) given their conspicuous presence in mosses, the vast majority of which are non-mycorrhizal. This work presents the first rigorous study of the endogenous roles of CCaMK and IPD3 in mosses. CCaMK and IPD3 have been very well characterized in legumes, revealing strategies to force the activation of these two proteins, specifically by truncation of CCaMK or phosphomimetic mutation in IPD3 (Gleason *et al.*, 2006a; Tirichine *et al.*, 2006; Miller *et al.*, 2013; Singh *et al.*, 2014). We leveraged these mutagenic strategies to elucidate the physiological consequence of their activity in Physcomitrella. Constitutive activation of CCaMK and IPD3 uncovered a direct roles in downstream drought-like development, through abscisic acid (ABA) signaling. However, CCaMK and IPD3 were not required for ABA signaling. This suggests that the CCaMK/IPD3 signaling module constitute a stress-signaling role outside of drought-stress signaling. ABA signaling is known to be required for proper AM development (Herrera-Medina *et al.*, 2007; Charpentier *et al.*, 2014). Despite this, there are no known links between CCaMK/IPD3 activity directly upon ABA synthesis/signaling; transcriptomic analysis of constitutively active CCaMK in *Lotus japonicus* did not reveal any drought-stress patterning (Takeda *et al.*, 2012). There is still the curious link between CSP signaling and drought-response in both mosses and angiosperms. One might hypothesize that the overall relevance of the CSP in green plants concerns drought-response, however it would be clear the mechanistic linkages are quite different. Finding a true biological role for CCaMK and IPD3 in Physcomitrella, such as what stimuli lie upstream of CCaMK/IPD3 activation, would inform this hypothesis.

There is growing interest in the role of fungi in growth and development of other bryophytes, such as liverworts, including the contribution of host-plant genetics (Carella *et al.*, 2018; Nelson & Shaw, 2019). The mycorrhizal liverwort *Marchantia paleacea* possesses the CCaMK/IPD3 signaling module and may prove to be a useful genetic model to extend similar studies into liverworts with the extra context that many liverworts are mycorrhizal.

Our initial observations of *ccamk* and *ipd3* mutants Physcomitrella were enigmatic as they were not apparently different than wild-type. We used a microfluidics strategy in order to observe fine-scale temporal growth of individual filaments, which unexpectedly led us to a directional growth phenotype, a “wrong way response”, of gravitropic filaments unique to the *ipd3* mutant The lack of a similar phenotype in the *ccamk* mutant suggests a mechanistic uncoupling of CCaMK and IPD3 concerning this phenotype. Modulating ABA signaling did not affect the *ipd3* phenotype, suggesting an uncoupling of IPD3-mediated ABA signaling and IPD3-mediated gravitropism. This was also enigmatic because pleiotropic effects of IPD3 are not well studied in angiosperms. To our knowledge, there are no known report of CSP involvement in root gravitropisms, nor did we observe any gravitropic phenotypes in analogous mutants of rice and *Medicago truncatula*. Similarly, *Marchantia paleacea* would prove useful to determine if the *ipd3* phenotype is moss-specific.

The larger community studying the CSP still has not tackled the question of biological function in charophyte algae. In this work, we tested numerous methods of direct and indirect genetic transformation on a panel of zygnematalean species. We were successful in producing a microparticle bombardment strategy that is generalizable to

three species: *Mesotaenium caldariorum*, *Mougeotia transeaui*, and *Zygnema sp.* Furthermore, we found that the *SUPERUBIQUITIN1* promoter of *Glycine max* is functional in *M. caldariorum* and *Zygnema sp.* Upon further development of this method, it is our hope that genetic transformation of diverse charophyte species becomes more common, as they are central to so many evolutionary questions of green plants.

5.2 - Future directions in the study of Physcomitrella

Elucidating the relevance of CCaMK/IPD3 in ABA signaling may prove difficult without a known upstream stimulus. There are still decent candidate moss-fungal interactions worth testing for phenotypes in the *ccamk* and *ipd3* mutants. Liverworts and numerous vascular plants are known to form endophytic interactions with fungal species of the Mucoromycotina, the sister clade to the Glomeromycotina containing many AMF (Humphreys *et al.*, 2010; Bidartondo *et al.*, 2011; Hoysted *et al.*, 2019). The genus *Endogone* of the Mucoromycotina has been shown to interact with moss (Berch & Fortin, 1983). These appear to be the closest fungal relatives of AMF that form known associations with mosses.

Transcriptomic studies of the *ccamk* and *ipd3* mutants may prove useful in multiple ways. One can hypothesize that mosses have retained the ability to perceive AMF-like signaling molecules, despite their inability to form mycorrhizal interactions. Treatments of COs and LCOs against the *ccamk* and *ipd3* mutants followed by transcriptional analysis could help answer this question. Furthermore, transcriptomic analyses would provide valuable insight into the downstream regulated genes of IPD3. An intimate knowledge of the genes activated by IPD3 might provide clues into the biological relevance of the CSP

in mosses, perhaps a vantage point from which to test upstream stimuli or interactions for phenotypes in the mutants we describe here.

5.3 - Future directions in the study of charophyte algae

Enhancement of the transformation efficiency of charophytes is still of utmost importance to facilitate their usefulness as genetic models. Cell sorting strategies utilizing fluorescence activated cell sorting may help to quickly isolate genetic mutants in certain species, especially small species, however such methods would likely not work with filamentous species which are also of considerable interest. Considering the transient nature of our transformations, the testing of CRISPR-based strategies would also be useful, as CRISPR can be used with success in gene knock-outs and knock-ins when expressed transiently (Mallett *et al.*, 2019).

Charophyte algae possess a relatively intact ABA signaling pathway and are known to form land plant-like responses to water-stress or desiccation (Holzinger *et al.*, 2014; Wang *et al.*, 2015, 2019a). Due to scalability, using currently available transformation methods may prove difficult in the way of performing metabolomics with transformed lines. However, there are visual reporters of ABA that may be useful. Two genetically encoded FRET sensors for ABA have been independently produced, providing the opportunity to visualize ABA levels in single cells (Jones *et al.*, 2014; Waadt *et al.*, 2014). On the other hand, advancements in single-cell transcriptomics may partially mitigate the issues of low transformation efficiency, if gene regulation was sought. Interestingly, some charophyte species produce structures that are functionally similar to brachycytes/brood cells of mosses. For example, species of the genus *Zygnema* are known to develop akinetes from normal vegetative cells. In *Zygnema*, akinetes are found

in old cultures or cultures under stress and are considered dormant survival structures, similar to moss brachycytes/brood cells (Holzinger *et al.*, 2018; Trumhová *et al.*, 2019). Importantly, these cells can be visually discriminated against “healthy” cells, as they display cell wall thickenings and a very high vesicular content. As such, akinetes or pre-akinetes may serve as a useful visual marker to determine if CCaMK has similar stress response-like effects in charophyte algae.

5.4 – References

Berch SM, Fortin JA. **1983**. Endogone pisiformis: axenic culture and associations with Sphagnum, Pinus sylvestris, Allium cepa, and Allium porrum. *Canadian Journal of Botany* **61**: 899–905.

Bidartondo MI, Read DJ, Trappe JM, Merckx V, Ligrone R, Duckett JG. **2011**. The dawn of symbiosis between plants and fungi. *Biology letters* **7**: 574–7.

Carella P, Gogleva A, Tomaselli M, Alfs C, Schornack S. **2018**. Phytophthora palmivora establishes tissue-specific intracellular infection structures in the earliest divergent land plant lineage. *Proceedings of the National Academy of Sciences of the United States of America* **115**: E3846–E3855.

Charpentier M, Sun J, Wen J, Mysore KS, Oldroyd GED. **2014**. Abscisic acid promotion of arbuscular mycorrhizal colonization requires a component of the PROTEIN PHOSPHATASE 2A complex. *Plant physiology* **166**: 2077–2090.

Gleason C, Chaudhuri S, Yang T, Mun A, Muñoz A, Poovaiah BW, Oldroyd GED. **2006**. Nodulation independent of rhizobia induced by a calcium-activated kinase lacking autoinhibition. *Nature* **441**: 1149–1152.

Herrera-Medina MJ, Steinkellner S, Vierheilig H, Ocampo Bote JA, García Garrido JM. **2007**. Abscisic acid determines arbuscule development and functionality in the

tomato arbuscular mycorrhiza. *New Phytologist* **175**: 554–564.

Holzinger A, Albert A, Aigner S, Uhl J, Schmitt-Kopplin P, Trumhová K, Pichrtová M. **2018**. Arctic, Antarctic, and temperate green algae Zygnema spp. under UV-B stress: vegetative cells perform better than pre-akinetes. *Protoplasma* **255**: 1239–1252.

Holzinger A, Kaplan F, Blaas K, Zechmann B, Komsic-Buchmann K, Becker B. **2014**. Transcriptomics of desiccation tolerance in the streptophyte green alga Klebsormidium reveal a land plant-like defense reaction. *PLoS ONE* **9**.

Hoysted GA, Jacob AS, Kowal J, Giesemann P, Bidartondo MI, Duckett JG, Gebauer G, Rimington WR, Schornack S, Pressel S, *et al.* 2019. Mucoromycotina Fine Root Endophyte Fungi Form Nutritional Mutualisms with Vascular Plants. *Plant physiology* **181**: 565–577.

Humphreys CP, Franks PJ, Rees M, Bidartondo MI, Leake JR, Beerling DJ. **2010**. Mutualistic mycorrhiza-like symbiosis in the most ancient group of land plants. *Nature Communications* **1**.

Jones AM, Danielson JÅ, ManojKumar SN, Lanquar V, Grossmann G, Frommer WB. **2014**. Abscisic acid dynamics in roots detected with genetically encoded FRET sensors. *eLife* **3**: 1–30.

Mallett DR, Chang M, Cheng X, Bezanilla M. **2019**. Efficient and modular CRISPR-Cas9 vector system for *Physcomitrella patens*. *Plant Direct* **3**: 1–15.

Miller JB, Pratap A, Miyahara A, Zhou L, Bornemann S, Morris RJ, Oldroyd GED. **2013**. Calcium/Calmodulin-dependent protein kinase is negatively and positively regulated by calcium, providing a mechanism for decoding calcium responses during symbiosis signaling. *The Plant Cell* **25**: 5053–5066.

Nelson J, Shaw AJ. **2019**. Exploring the natural microbiome of the model liverwort: fungal endophyte diversity in Marchantia polymorpha L. *Symbiosis* **78**: 45–59.

Singh S, Katzer K, Lambert J, Cerri M, Parniske M. **2014**. CYCLOPS, A DNA-binding transcriptional activator, orchestrates symbiotic root nodule development. *Cell Host and Microbe* **15**: 139–152.

Takeda N, Maekawa T, Hayashi M. **2012**. Nuclear-localized and deregulated calcium- and calmodulin-dependent protein kinase activates rhizobial and mycorrhizal responses in Lotus japonicus. *The Plant cell* **24**: 810–22.

Tirichine L, Imaizumi-Anraku H, Yoshida S, Murakami Y, Madsen LH, Miwa H, Nakagawa T, Sandal N, Albrektsen AS, Kawaguchi M, *et al.* 2006. Deregulation of a Ca2+/calmodulin-dependent kinase leads to spontaneous nodule development. *Nature* **441**: 1153–6.

Trumhová K, Holzinger A, Obwegeser S, Neuner G, Pichrtová M. **2019**. The conjugating green alga Zygnema sp. (Zygnematophyceae) from the Arctic shows high frost tolerance in mature cells (pre-akinetes). *Protoplasma* **256**: 1681–1694.

Waadt R, Hitomi K, Nishimura N, Hitomi C, Adams SR, Getzoff ED, Schroeder JI. **2014**. FRET-based reporters for the direct visualization of abscisic acid concentration changes and distribution in Arabidopsis. *eLife* **3**: 1–28.

Wang S, Li L, Li H, Sahu SK, Wang H, Xu Y, Xian W, Song B, Liang H, Cheng S, *et al.* 2019. Genomes of early-diverging streptophyte algae shed light on plant terrestrialization. *Nature Plants*.

Wang C, Liu Y, Li S-S, Han G-Z. **2015**. Insights into the origin and evolution of the plant hormone signaling machinery. *Plant physiology* **167**: 872–886.